ICOEST

SARAJEVO

5TH INTERNATIONAL CONFERENCE ON ENVIRONMENTAL SCIENCE AND TECHNOLOGY

BOOK OF PROCEEDINGS

OCTOBER 09-13, 2019

www.icoest.eu

Organized by

Partners

5th INTERNATIONAL CONFERENCE ON ENVIRONMENTAL SCIENCE AND TECHNOLOGY (ICOEST)

ISBN 978-605-81426-2-6

ISSN – 2687-2439

PROCEEDINGS OF THE

5th INTERNATIONAL CONFERENCE ON ENVIRONMENTAL SCIENCE AND TECHNOLOGY

(ICOEST)

09-13 October 2019, Sarajevo, Bosnia-Herzegovina

Edited by

Prof. Dr. Özer Çınar

Published by:

info@icoest.eu
www.icoest.eu
www.cnrgroup.eu

CNR Group Laboratuvar ve Arge Hizmetleri Sanayi Ticaret Limited Şirketi Çifte Havuzlar Mah., Eski Londra Asfaltı Cad., Kuluçka Mrk., A1 Blok, 151/1C, Iç Kapı No:1 B-20, Esenler / Istanbul, 34220

ISBN 978-605-81426-2-6

ISSN - 2687-2439

SCIENTIFIC COMMITTEE

1. Prof.Dr. Adisa Parić – University of Sarajevo - Bosnia and Herzegovina
2. Prof.Dr. Ana Vovk-Korže - University of Maribor - Slovenia
3. Prof.Dr. Arslan Saral – Yıldız Technical University - Turkey
4. Prof.Dr. Ayşegül Pala – Dokuz Eylül University - Turkey
5. Prof.Dr. Cumali Kınacı - İstanbul Technical University - Turkey
6. Prof.Dr. Dragan Vinterhalter - University of Belgrade - Serbia
7. Prof.Dr. Dragutin T. Mihailović - University of Novi Sad - Serbia
8. Prof.Dr. Edina Muratović – University of Sarajevo - Bosnia and Herzegovina
9. Prof.Dr. Esad Prohic - University of Zagreb - Croatia
10. Prof.Dr. Hasan Merdun - Akdeniz University - Turkey
11. Prof.Dr. Jasna Huremović – University of Sarajevo - Bosnia and Herzegovina
12. Prof.Dr. Lada Lukić Bilela – University of Sarajevo - Bosnia and Herzegovina
13. Prof.Dr. Lukman Thalib - Qatar University - Qatar
14. Prof.Dr. M. Asghar Fazel - University of Environment - Iran
15. Prof.Dr. Mehmet Kitiş - Süleyman Demirel University - Turkey
16. Prof.Dr. Muhammad Arshad Javed - Universiti Teknologi Malaysia - Malaysia
17. Prof.Dr. Noureddine Djebli - Mostaganeml University - Algeria
18. Prof.Dr. Nuri Azbar - Ege University - Turkey
19. Prof.Dr. Özer Çınar - Yıldız Technical University - Turkey
20. Prof.Dr. Rifat Skrijelj - University of Sarajevo - Bosnia and Herzegovina
21. Prof.Dr. Samir Đug - University of Sarajevo - Bosnia and Herzegovina
22. Prof.Dr. Suad Bećirović - International University of Novi Pazar - Serbia
23. Prof.Dr. Tanju Karanfil - Clemson University - USA
24. Prof.Dr. Vladyslav Sukhenko - National University of Life and Environmental Sciences of Ukraine (Kyiv) - Ukraine
25. Assoc. Prof.Dr. Alaa Al Hawari - Qatar University - Qatar
26. Assoc. Prof.Dr. Cevat Yaman - Gebze Technical University - Turkey
27. Assoc. Prof. Dr. Kateryna Syera - National University of Life and Environmental Sciences of Ukraine (Kyiv) - Ukraine
28. Assoc. Prof.Dr. Mostafa Jafari - Research Institute of Forests and Rangelands - Iran
29. Assoc. Prof.Dr. Nusret Drešković - University of Sarajevo - Bosnia and Herzegovina
30. Assoc. Prof.Dr. Yuriy Kravchenko - National University of Life and Environmental Sciences of Ukraine (Kyiv) - Ukraine
31. Assist. Prof.Dr. Ahmad Talebi - University of Environment - Iran
32. Assist. Prof.Dr. Ahmet Aygün - Bursa Technical University - Turkey
33. Assist. Prof.Dr. Mostafa Panahi - Islamic Azad University - Iran
34. Assist. Prof.Dr. Rishee K. Kalaria - Navsari Agricultural University - India
35. Assist. Prof.Dr. Sasan Rabieh - Shahid Beheshti University - Iran
36. Assist. Prof.Dr. Ševkija Okerić - University of Sarajevo - Bosnia and Herzegovina
37. Dr. Hasan Bora Usluer - Galatasaray University - Turkey
38. Dr. Zsolt Hetesi - National University of Public Service, Budapest - Hungary
39. Dr. Zsolt T. Németh - National University of Public Service, Budapest - Hungary

ORGANIZATION COMMITTEE

Chairman(s) of the Conference

Prof. Dr. Özer Çınar – Yıldız Technical University

Members of the Committee

Prof. Dr. M. Asghar Fazel (Co-Chairman) – University of Environment

Dr. Gábor Baranyai (Co-Chairman) – National University of Public Service, Budapest

Prof. Dr. Samir Đug, University of Sarajevo

Assist. Prof. Dr. Sasan Rabieh Shahid Beheshti University

Assist. Prof. Dr. Ševkija Okerić - University of Sarajevo

Assist. Prof. Dr. Nusret Drešković - University of Sarajevo

Assist. Prof. Dr. Ranko Mirić - University of Sarejevo

Musa Kose - Zenith Group Sarajevo

Ismet Uzun - Zenith Group Sarajevo

Alma Ligata - Zenith Group Sarajevo

Ajdin Perco - Faktor.ba

WELCOME TO ICOEST 2019

On behalf of the organizing committee, we are pleased to announce that the 5th International Conference on Environmental Science and Technology (ICOEST-2019) is held from October 09 to 13, 2019 in Sarajevo. ICOEST 2019 provides an ideal academic platform for researchers to present the latest research findings and describe emerging technologies, and directions in Environmental Science and Technology. The conference seeks to contribute to presenting novel research results in all aspects of Environmental Science and Technology. The conference aims to bring together leading academic scientists, researchers and research scholars to exchange and share their experiences and research results about all aspects of Environmental Science and Technology. It also provides the premier interdisciplinary forum for scientists, engineers, and practitioners to present their latest research results, ideas, developments, and applications in al lareas of Environmental Science and Technology. The conference will bring together leading academic scientists, researchers and scholars in the domain of interest from around the world.

ICOEST 2019 is the oncoming event of the successful conference series focusing on Environmental Science and Technology. The scientific program focuses on current advances in th eresearch, production and use of Environmental Engineering and Sciences with particular focus on their role in maintaining academic level in Science and Technology and elevating the science level such as: Water and waste water treatment, sludge handling and management, Solid waste and management, Surface water quality monitoring, Noise pollution and control, Air pollution and control, Ecology and ecosystem management, Environmental data analysis and modeling, Environmental education, Environmental planning, management and policies for cities and regions, Green energy and sustainability, Water resources and river basin management. The conference's goals are to provide a scientific forum for all international prestige scholars around the world and enable the interactive exchange of state-of-the-art knowledge. The conference will focus on evidence-based benefits proven in environmental science and engineering experiments.

Best regards,

Prof. Dr.Özer ÇINAR

ICOEST
SARAJEVO
5TH INTERNATIONAL CONFERENCE ON ENVIRONMENTAL SCIENCE AND TECHNOLOGY
October 09-13 2019

CONTENT

ICOEST SARAJEVO
5TH INTERNATIONAL CONFERENCE ON ENVIRONMENTAL SCIENCE AND TECHNOLOGY
October 09-13 2019

Industry 4.0 and Autonomous Ships Effects on Marine Environment

Tayfun Acarer [1], Hasan Bora Usluer[2]

Abstract

The Economic flows and Financial resource flows are of great importance in the world trade economy. Developments that develop as the common denominator of these trends and which affect the world economies are known as "Industrial Revolutions". These Indsutrial Processes which have been increasingly influential since the early 18 centuries and reshaped the economies of the whole countries, have reached a new stage today and are defined as Industry 4.0. As a result of the effects of industry 4.0, autonomous ships which are developing technology products, are also preparing to serve in maritime transportation and maritime trade sector. It is clear that all these developments will continue to be implemented within the framework of unchanging maritime and environmental rules. In this study trying to explain all comments and observations on how the Industry 4.0 and autonomous ships could be integrated into the marine environment during the maritime transportation on maritime trade sector.

Keywords: Industry 4.0, Autonomous Ship, Marine Environment

1. INDUSTRY 4.0

Economic Flows and Financial Resource Flows are of great importance in the world economy. Developments that have developed as a common denominator of these currents and which affect the world economies are known as Industrial Revolutions. Especially since the early 1800s, these Industrial Processes, which have an increasing impact and reshaping the economies of all countries, have reached a new stage today and this process is defined as Industry 4.0.

1.1. Definition of Industry 4.0

Industry 4.0 is a project developed in Germany to equip traditional technology, such as manufacturing, with computerization and technology. The goal in this new industry is compliance, resource efficiency and ergonomics, which characterize the integration of both customers and business partners. Accordingly, Industry 4.0, or the 4th Industrial Revolution, is a collective term that includes many contemporary automation systems, data exchange and production technologies. Industry 4.0; communicating with each other, detect the environment with Sensors, identify the needs by analyzing data, Robots take over the production of autonomous infrastructures of higher quality, cheaper, faster and time-saving. [1]

[1] *Corresponding author: Bilgi University/Istanbul, Turkey.* tacarer@hotmail.com

[2] *Galatasaray University, Istanbul, Turkey,* hbusluer@gsu.edu.tr

Figure 1.Small view of the Industrial circle

Industry 4.0 aims to bring together information technologies and industry. Industry 4.0; In the production process, the automation process provides a working process which is integrated autonomously with all software and hardware and wireless information integration.

Figure 2.An Integration of Industry 4.0

At the beginning of Industry 4.0 Impact Areas; Productivity, Growth, Investment and Employment. [1] With efficiency; It is aimed to reduce labor need and costs. With growth; It is aimed to get more shares from the global value chain. Through the competitive advantage to be gained and the economy to be created around Industry 4.0, industrial production is expected to increase up to approximately 3% per year. This growth means an additional growth of 1% or more in GDP. With investment; In order to include the Industry 4.0 technologies in the production process, producers are expected to invest approximately 1-1.5% of their revenues in the next 10 years. With employment; It is foreseen that the labor need in the total industry will increase and, more importantly, a more qualified workforce structure with a high level of education and income will be formed. In this context, it is expected that in the next decade, the labor force will decrease in jobs with low level of competence, whereas industrial production will increase and employment will increase in total. At the same time, it is considered that the income pyramid and the know-how infrastructure will be developed with its highly qualified workforce structure. Therefore, Industry 4.0 will change the competencies required by employees and also Robot Repair, Personal Data Operator, Virtual Reality Architect, Dron Operator, Genetic Consultant, Astroid Miner, Organ Designer, Digital Style Consultant, Remote Control Operator of Transportation Vehicles, etc. also new professions will be emerged.

2. INDUSTRY 4.0 EFFECTS ON MARITIME INDUSTRY

Based on these explanations, it is possible to define End 4.0 as the general name of the development computerization stages in different sectors. End. 4.0 has Training 4.0, Health 4.0, Port 4.0, Logistics 4.0, Maritime 4.0, etc. many "Sub-Sectors and Breakdowns". [2] Although it is possible to expand the sub-sectors of 4.0, this article will focus on Maritime 4.0 and in particular the components of Ship Management 4.0, developments and requirements related to them. In addition, attention will be paid to the changes that will be caused by developments in Ship Management 4.0 in the conventional Maritime Sector.Especially today, the developments in the fields of Digitalization, Internet of Things (IoT), Machine to Machine (M2M), Artificial

Intelligence and Position Detection are combined with new opportunities in the Communication Sector. It is inevitable that in the near future, Ind. 4.0 will emerge as a very different Transport sector stakeholder.

Maritime Management Ind. 4.0 is focus on especially; Port Management, Logistics Management, Ship Management. It is possible to evaluate the lower fractures such as. In fact, all of these are issues that need to be examined separately, but this article aims to examine all components of "Ship Management 4.0" their synchronized working conditions, their possible effects and the changes that will result in the conventional Maritime sector. Components of Ship Management 4.0 is focus on; Navigation and machinery equipment,M2M IoT, Artificial intelligence, Management and Remote Control Equipment and Software and Communication Systems.

2.1. Electronic Navigation Systems at Bridge

Also it could be group. Although it is inevitable to add different components to them over time, only the sub-components listed above are considered at this stage. Among these, "Navigation and Machine equipments" is one of the most positively affected components from technological developments. As it is known, technological developments have made a very positive contribution to all machine systems and their remote controlled operation. Although these developments are still continuing, it has become possible to operate the machine systems of the new generation ships over the bridge or other spaces, be to control, to monitor their alarms from different places and to remedy the problems other than mechanical failures by remote control. This provides great opportunities for autonomous ship systems. Again, as a result of technological developments in recent years, the positive developments in the Navigation and Navigation Aids systems of ships have been even more than machine systems. Especially Radar, Ecdis (Electronic Chart Display), Barley Radar, Depth and Speed Measurement Devices, AIS (Autamatic Identification System), Marine Communication Equipment, Navtex (Navigational Telex) and so on. The use of devices on ships has increased significantly. However, within these systems, a separate parenthesis to AIS is required. Because the AIS equipment detects other AIS devices within range (about 25 miles between ships and ships), including their position, speed, course and so on. while receiving the navigation information, it also sends this information to the surrounding ships and to the Coast Radio Stations, if any. Although the query time of AIS devices depends on the movement speed of the ship, the query above a certain speed is automatically performed every 6 seconds.

Information received through AIS; Static, dynamic and course infirmations. [3]

Static Information; MMSI (Sea Passenger Service Identification Number),IMO Number,Call Sign And Name,Length and Beam,Type of Ship,Location of GPS Antenna [3]

Dynamic Information; Ship's Position, Time (UTC),Route by Land (COG),Speed over land (SOG),Bow, Time of Return [3] **Course Information**; Drafty of the ship,Dangerous Goods Information,Destination and Estimated Time of Arrival (ETA),Route Plan (turning points), Speed [3]

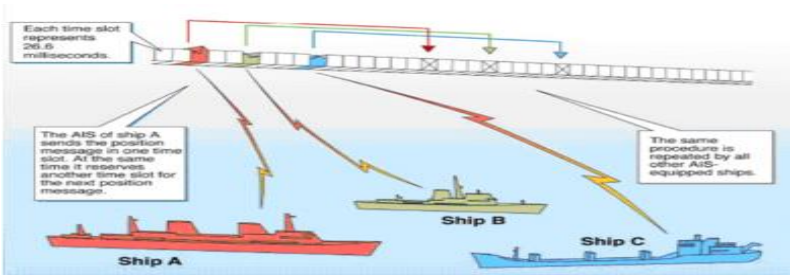

Figure 3.AIS Time Slot explain diagram

Different types of AIS devices are used in ships according to their tonnage and voyage areas. It is of great benefit to make this device compulsory for all vessels in order to increase the safety of navigation and to make new arrangements regarding the operating conditions. In addition, if the navigation information (route, speed, location, etc.) obtained from the surrounding ships in the AIS system is evaluated on a computer and the ship's route / speed is checked accordingly, the first unmanned autonomous driving of the ship will be realized.

It is also possible to broadcast navigation information via broadcasts via AIS devices at coast stations. At present, such publications are made especially in Northern European countries, Virtual (imaginary) buoy information and so on. Information on systems that are not physically available is transmitted to AIS devices. For this purpose, special codes for MMSI (Maritime Mobile Service Identity) numbers for Virtual AISs have been determined and assigned to countries by International Telecommunication Union (ITU).

It is possible to compare the Virtual AIS ”information, which will provide the necessary data for the production of safe navigation information in remote water channels and in areas with heavy ship traffic and to manage the ships remotely controlled, to the Way Smart Way” management in land transportation. While Smart Road Data in Road Transportation is provided with Sensors to be installed for these road routes, it is possible to provide such warning information (sharp turns, shallows, heels, rocky areas, etc.) in Virtual Transportation by Virtual Ais. Today, it is possible to obtain sufficient data for the ships' own shipments and administrations as a result of the evaluation of the navigational information to be received from the vessels in the vicinity via AIS devices and the navigational information to be sent via Virtual AIS. It is possible to evaluate this structure as Intelligent Auto Pilot. Especially on the high seas, these data provide sufficient data source for the autonomous safe navigation of the ship. Therefore, in Ship Management 4.0, the AIS systems should be evaluated separately and the capabilities and capabilities of this system should be maximized. Another important component in Ship Management 4.0 is M2M. This component, which is also defined as communication between machines, has become one of the most important elements of the IT Sector. The communication between the machines allows the machines to work synchronously with each other, and on the other hand, it is possible to detect the problem in a machine and to stimulate the necessary units to solve this problem. Nowadays, with the development of Artificial Intelligence applications, M2M facilities, which have become a different structure, will be one of the most important components in remote controlled and autonomous operation of ships. Another component of Ship Management 4.0 is IoT. This component, also called the Internet of Things, is still one of the most popular topics in the Information Technonologies sector. The economic dimension of IoT, whose application field is increasing day by day, is developing exponentially. While approximately 9 billion devices are connected to the internet in the world, it is estimated that this number will reach 50 billion devices in 2025 and the IoT market will reach 3 trillion dollars. [1] It is inevitable that the Internet of Things will find great application in Ship Management End.4.0. The fact that Ship Machines and Navigation Systems become more remote controlled with the developing technology will increase the possibilities of kullanim Internet of Things kullanim on ships. In addition to the increasing use of IoT in many systems, its compliance with IP (Internet Protocol) infrastructure, and the positive effects of improvements in the IPV6 (Internet Protocol Version 6) process on IoT applications, a very serious data flow between the system. It is possible to collect this big data to be produced firstly in Computer Systems and software related to Ship Management and to process the data warehouse to be produced and to produce the necessary information for Ship Management from this data warehouse. This data is one of the basic data required for Vessel Management 4.0 and will provide the information necessary for the remote control of vessels in particular. Part of the software and hardware systems to be developed for this purpose shall be on board ships and other complementary elements shall be on land.Artificial Intelligence, which is also defined as the technology to guide the future, will be a component of Ship Management 4.0 that will gradually increase in importance in the future. With Machine Learning, the artificial intelligence component will be the basic element of Autonomous Ships. Because, as a result of the evaluation of the data to be collected by AIS equipment, Sensors, M2M applications and IoT from different systems in Machine Learning and processing with artificial intelligence in Computer System which will take place in the management unit, a serious automation data will be provided for Ship Management. The experience to be provided by the big data to be produced in the ship systems during the process will lead to a significant accumulation of knowledge in the analysis systems. This information, coupled with the artificial intelligence component, will be a very important resource for the computer systems that will take place in Ship Management. This information to be collected in the pool; it is inevitable that it depends on the systems on board and the amount of data to be received from M2M and IoT applications. In other words, the more data collected in the repository, the more data will be processed and evaluated with artificial intelligence and the development of autonomous ship systems will be easy and quick. It is possible to define ship movement controlled by computer system supported by artificial intelligence as ship navigation system managed by Smart Auto Pilot. It is inevitable that this application will create very successful applications for Unmanned Ships in the high seas. One of the most important components of Ship Management 4.0 will undoubtedly be Communication Systems. Communication systems; It shall be used for the transmission of the information related to the Machinery and Navigation Systems located at different locations within the ship to the computers to be used in ship management, to access the information collected on this computer from the ship from the complementary systems on land and to operate the Ship Management systems remotely. For this reason,

different communication systems should be used in the data transmission between the ship and the ship / land and the data transfers should be examined separately. It is possible to collect data communication for the ship in two main groups as wire / wireless communication systems. Wire communication is mainly based on coaxial cable and will be used for the transmission of data from Main Machine, Auxiliary Machine, Radar, etc. to the Management Computer. For this reason, it is necessary to establish a serious cable infrastructure between the different equipments in the ship and the computer related to the management systems. In addition, it is possible to use the radio infrastructure for the data to be transferred to the Management computer by M2M systems and IoT equipment in the ship. However, if radio systems are used in the communication infrastructure of the ship, it is necessary to establish a communication infrastructure for this purpose and to form a freestanding network, especially in large hulled ships. In other words, an internal radio anet intranet ”structure should be established within the ship and it should be associated with the Ship Management 4.0 system. The structure I recommend is the hybrid model. In other words, if necessary, the wire infrastructure is a Communication Structure model in the form of a combination of radio infrastructure in suitable systems. In the wire / wireless communication system to be installed within the ship, the connection of the Ship Management system with the land unit should also be ensured. For this purpose, it is obligatory to establish a separate radio communication infrastructure between the ship and the land in order to be able to evaluate the data collected on board at the relevant unit on land and to intervene in the Ship Management system when necessary. It is possible to use different systems in the remote control of the ships depending on whether the ship is close or far away. For this purpose, mobile phone technologies (3 G, 4 G, 5 G systems) or VHF systems can be used in short distance communication. The common use of mobile telephony and VHF systems relative to the shore distance of ships, ie where there is mobile telephony coverage, a combination structure to ensure the use of the VHF system where this coverage is not considered as the best solution for short distance radio communication between ships / land.

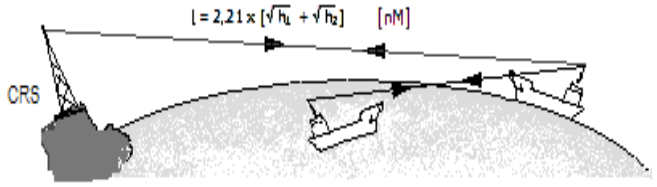

Figure 4.VHF communication working flow.

If the distance between the ship and the land is long (25 miles or more), long distance systems will have to be used. For this purpose it is technically possible to use either Inmarsat satellite system or Long distance (HF) terrestrial systems. In addition to the close seas such as the Mediterranean Sea and the Black Sea, both systems have the possibility of contacting the ships in the Ocean regions. The following figure shows the general operating principles of VHF (Short Distance), HF (Long Distance) and Inmarsat Satellite systems. Access is provided according to the principle of seeing the antennas of the devices in the VHF system (optical vision), while the access between the devices in the HF system is provided on the basis of the reflection of the electromagnetic wave from the ionesphere. In the Inmarsat system, the principle of reflection of the electromagnetic wave from the satellite is used in the access between the devices. [4]

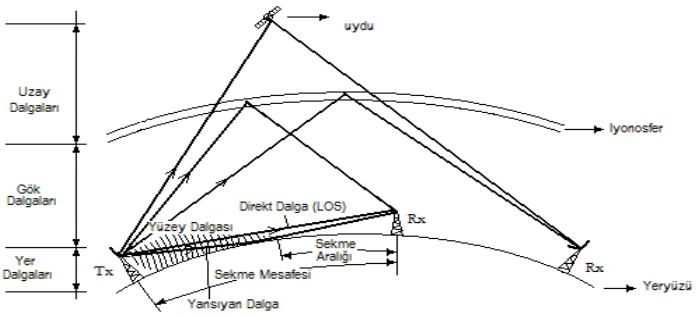

Figure 5.Terrestrial, Space and Satellite Waves

While it is possible to use both Inmarsat system and HF system technically in long distance access, Inmarsat system has more access advantages due to its ease of searching and higher accessibility.

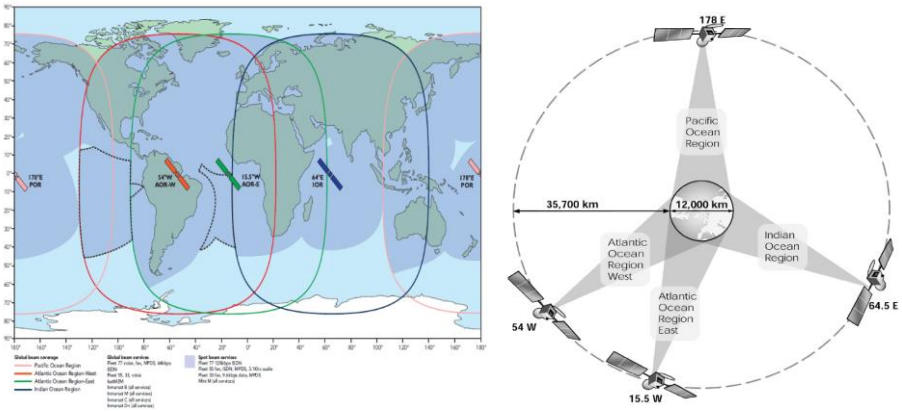

Figure 6.Coverage of Inmarsat Satellites of the world.

The services provided through Inmarsat are used in land, sea and air communications. Main services are Broadband Data access, Sound, M2M (Machine to Machine) and Emergency communication access.

2.2. Broadband Services - BGAN (Broadband Global Area Network)

IP based voice and broadband data communication services up to 512kbps are provided with BGAN link service. This system is operated on I-4 satellites with 99.9% uninterrupted rate. Simultaneous voice communication, Internet access or e-mail can be performed. Many BGAN terminals also support mobile ISDN services of 64 Kbps. It is compatible with VPN and encryption devices of military and public standards. Various quotas are available. Due to the use of L-Band frequencies, the satellite detection tolerance is high. It is therefore suitable for use in areas with seismic activity and strong winds. BGAN link has low energy requirements. Through BGAN Systems; FTP, SMS, Voip, Broadband Internet Access, E-Mail, VPN, Telephone, Video Conferencing, Wireless and Tracking services are provided. [6]

Figure 7.BGAN Terminal

Unlike other satellite internet access systems, it allows communication without the need for a large and heavy satellite antenna. It is also possible to use Inmarsat systems in M2M functions. Although it is possible to use wire / wireless systems especially in M2M communication within the ship, it is possible to use Inmarsat systems in the communication between the ship / land. Main M2M (Machine to Machine) Inmarsat Terminals to be used for this purpose and their main features.

2.3. BGAN M2M

It is a service offered for automation and scada applications via BGAN infrastructure. Supports up to 448 kbps connection speed. With its 800 ms delay time, it addresses different industries such as power lines and pipelines where delay and data losses are critical. Main Features; ECDIS is GPS tracking and IP SCADA.

2.4. ISATDATA PRO

It is a two way messaging service used for vehicle tracking systems. Inmarsat uses I-4 series satellites. It is capable of sending 6400 bytes of data and receiving 10000 bytes of data. Message transmission time varies between 15-60 seconds depending on message size. Main features; GPS tracking, SCADA, Telemetry, Weather reporting and Short message e-mail.

2.4.1. IsatData Pro Terminal (ISATM2M)

Isatm2m; is a low data rate messaging service that works with store and send logic. With these terminals, 100-byte messages can be received in the download direction. Main features; GPS tracking, SCADA and Short message e-mail.

2.4.2. Inmarsat Fleet Services

Inmarsat-Fleet77, Inmarsat-Fleet55 and Inmarsat-Fleet33 are serviced with three sub-services. GMDSS conditions are also provided with Fleet77 terminals. As the reason why Fleet service is preferred; low cost of space segment, e-mail communication, 64 kbps Mobile data packet service (MPDS), lighter and more useful.

2.5. INMARSAT Global Xpress (Ka Band)

Satellites will operate in Ka frequency band (20-30 GHz) and each satellite has 89 small Ka band spot coverage. In addition, Ka-Band traffic collection centers can be established at different points with 6 directable coverage areas of each satellite. GlobalXpress provides 50Mbps download and 5 Mbps upload speeds through 60 cm antennas. Global Xpress provides high speed data communication to air and sea vehicles. Inmarsat Satellite system is used for access between ships and land; 1 terminal will be required for ship and land unit. It is advantageous that this terminal is preferably an Inmarsat-F77 type terminal with high speed data communication capability. Inmarsat negotiations are chargeable and if continuous data will be received from the ship, it is useful to withdraw it with certain periods and to receive it in packages. If the satellite system is preferred, it will be technically possible to use LRIT (Long Range Idintification Tracking) system. Since the LRIT System, also known as the long-distance AIS System, is a system that is also accepted by IMO and its standards are predetermined, it is useful to focus on this. Since the LRIT system is also mandatory, especially in Long Distance vessels, it will be easy to disseminate it and improve its standards. The LRIT system is currently operated via Inmarsat satellites. It is also possible to use HF (Terrestrial Distance) systems in communication between ship / land. In the HF system, the communication will be established since the signal will work on the basis of reflection from ionosphere at long distance; It has to be free. The frequency bands to be used due to the up / down movement of the ionosphere during the day will also vary according to the distance and The communication environment shall be open to interference. For this reason, it is inevitable to encounter interruptions and interruptions from time to time in the communication between ship / land through HF Systems. As a result of these evaluations, it is possible to say that the LRIT devices which are required to be kept in accordance with the legislation on ships with large tonnage and long distance and working on Inmarsat satellites are one of the most suitable systems for this communication. In this regard, in a working group to be established under the coordination of IMO (International Maritime Organization), modifications to the technical standards of LRIT should be made for this purpose.

3. MARINE POLLUTION MONITORING WITH HIGH TECHNOLOGY

The world oceans and sea ares are great parts of the world. Nearly %70 of the water all over the world, like human body. New ships and technologies could help matime transportation and global trade working flow. Also it has many negativities like pollution. Pollution could easily effects basicly for habitats and seacreatures and coastal areas for all humankind. recent developments in software and computation power have led to the increased use of data captured by remote sensing systems. Computer systems can now store and analyze large datasets. Therefore, marine protection agencies and government can utilize the full potential of remote sensing data in geographic information systems (GIS) and decision support systems (DSS) to manage marine resources and pollution. Collaboration between the research community and government is of utmost importance for using the full potential of this data in marine pollution management. Different applications of remote sensing such as detection of floating marine plastic litter and the use of active remote sensing for detecting algal blooms are still in the research. With the advancement of remote sensing sensors, sophisticated methods will be developed in the future for monitoring marine pollution.[7]

4. CONCLUSIONS

Ship Management It is inevitable that 4.0 will develop rapidly in the near future. Considering the technological developments in recent years, no problem is seen in this regard. Especially in recent years, the great opportunities provided in ship systems, data transfer and communication systems, autonomous ships and their monitoring from long distances will easily allow intervening when necessary. In the meantime, the rapid spread of communication between machines, the Internet of Things, developments in sensor technology Ship Management End. 4.0 provides very serious opportunities.

REFERENCES

[1]. Bilisim Teknolojilerinde Egilim – Dr.Tayfun ACARER, 2017
[2]. www.7deniz.net. , Prof. Dr. Soner Esmer, Bildiri, 2017
[3]. i-Marine Deniz Teknolojileri ve Arastirmalari A.S, 2014
[4]. M. Wegmuller, J. P. von der Weid, P. Oberson, and N. Gisin, “High resolution fiber distributed measurements with coherent OFDR,” in *Proc. ECOC’00*, 2000, paper 11.3.4, p. 109.
[5]. R. E. Sorace, V. S. Reinhardt, and S. A. Vaughn, “High-speed digital-to-RF converter,” U.S. Patent 5 668 842, Sep. 16, 1997.
[6]. (2007) The IEEE website. [Online]. Available: http://www.ieee.org/
[7]. Detection and Monitoring of Marine Pollution Using Remote Sensing Technologies, Sidrah Hafeez, Man Sing Wong, Sawaid Abbas, Coco Y. T. Kwok, Janet Nichol, Kwon Ho Lee, Danling Tang and Lilian Pun,2018

ICOEST SARAJEVO
5TH INTERNATIONAL CONFERENCE ON ENVIRONMENTAL SCIENCE AND TECHNOLOGY
October 09-13 2019

The Effects of Marine Sciences on Maritime Transportation and Marine Environment at Turkish Straits

***Hasan Bora Usluer*[1]**

Abstract

The Turkey is a great bridge and correct example of the connecting the Asian and Europe continents. From the history, this sea area has importance of strategical and commercial at maritime trade. The area name is the Turkish Straits Sea Area which is consist of Istanbul Strait (Bosphorus), Canakkale Strait (Dardanelle) and also The Marmara Sea. The Istanbul and Canakkale straits are connecting the Black Sea with the Aegean Sea through by the Marmara Sea. With geographic position, The Turkish Straits has great importance not only strategic but also geopolitics. Recently increasing of energy transportation, The Turkish Straits has become importance and risky waterway at the world maritime transportation. The Turkish Strait Sea Area also Straits have been governed by the Montreux convention, since the 1936. Beside all legalty,The Turkish Republic Maritime Authorities have important responsibilities like on local maritime traffic, innocent passage, safety navigation and marine environmetal management during the maritime transportation. Marine Sciences responsible of the measures all details of marine and environment sciences. Deeply survey of these are could have chance both to making environmental planning for decreasing marine pollution and protect all the straits shoreline by the national and international regulations and making another planning about maritime safety trough the Turkish Straits. This working, try to explain the marine effects and their surveys importance for maritime transportation and environmental management, planning at the Turkish Straits selected area.

Keywords: Turkish Straits, Environment, Pollution, Coastal

1. IMPORTANT INTRODUCTIONS ABOUT TURKISH STRAIT SEA AREA

The Turkish Straits are great important example of the natural seaways all over the world. These all are natural structure and became great valley from water dynamic motions which goes through from Black sea to the Marmara Sea. The sea area is consisting of Istanbul Strait (Bosphorus), Canakkale Strait (Dardanelle) and also the Marmara Sea. Bosphorus and Dardanelles names were came from old times. The Turkey is in a good position which has the gate that connected the asian and europe continental. The Straits of Istanbul and Strait of Canakkale are connecting the Black Sea with the Aegean Sea through by Sea of Marmara and also the area has a really importance from the history because of the geopolitics, strategic and geographic situations. All part of the sovereign sea territory of Turkey and subject to the regime of internal waters. [1] These importances, especially strategic one is that the only water route between the Mediterranean Sea and the Black Sea, so the Turkish Strait sea area has been the site of significant settlement area and also city of Istanbul for a long time in the past. All part of the sovereign sea territory of Turkey and subject to the regime of internal waters. The Turkish Straits have been governed by the Montreux convention, since the 1936. Turkey, due to its treaty obligations under the Montreux Convention, first gave annual reports to the League of Nations Secretary-General and, since 1945, has given these to the United Nations Secretary-General. These reports, which also go to the High Contracting Parties, are entitled,'Rapport Annuel sur le Mouvement des Navires a Travers les Detroits Turcs' (Annual Report Concerning the Movement of Ships through the Turkish Straits). Another important point in favor of using the expression the 'Turkish Straits' comes from a UN document. This is the 'Third United Nations Conference on the Standardization of Geographical Names', held at Athens, in 1977, and attended by 152 participants representing 59 countries, with observers from 11 non-governmental and international scientific organizations. The basic aim of the Conference was to use national names to standardize

[1] *Corresponding author: Galatasaray University, Asst.Prof.Dr., The Director of Maritime Vocational School, Cıragan Cad.,No.36, 34349, Ortakoy-Besiktas/Istanbul, Turkey. hbusluer@gsu.edu.tr*

the names of geographical locations. The Conference resolutions empower Turkey in the use of the name 'Turkish Straits'.[2,3] This document's title is evidence of the international credence of the expression 'Turkish Straits'. [2,4] From past to recent years this gate is the most important trade way of the world cause of the oil and oil products. Throughout the history, this situation due to the geographical location, has lead to conflicts between Turkey and the countries both coasting and not coasting the Black Sea in terms of political, economic and strategic interests. Straits separating Turkey's land into two as Asian side and European side resulted in the facts that Turkey's territorial integrity and independence are directly related to the legal regime which the straits are subject to. [2,5] In Montreux Conference, representative of Romania, Nicolae Titulescu's expression "Straits are the hearts of Turkey, but also lungs of Romania" affirms the importance of the Straits. [2,6] The Turkish Straits sea area has very special ecological conditions in terms of marine environment which includes atmospheric and oceanographic conditions, plant and animal diversity and also terrestrial environment. Besides strategic, economic and geologic situations, this area also has roles as biological corridor and biological barrier between the Mediterranean Sea and the Black Sea and form an acclimatization zone for migrating species. Due to being the only maritime access for the neighboring Black Sea states and the Central Asian Turki Republics, the Istanbul Strait has been exposed to dense marine traffic for centuries and substantial increase has occurred in size and tonnage of the ships passing through the Strait with hazardous cargo varieties and amounts they carry. Increase in the number of vessels that navigates on the Strait and being on the transportation way of hazardous and dangerous materials pose serious environmental and safety hazards for the Istanbul Strait, Marmara Sea and the surrounding residential areas. Geographic and oceanographic features of the Istanbul Strait makes the navigation on the Strait rather difficult and consequently the Strait has faced many casualties that caused severe environmental problems due to thousands tons of oil spill occurring in recent decades. [2,7]

Figure 8.The Turkish Strait Sea Area overview.

2. THE GENERAL CHARACTERISTICS OF THE TURKISH STRAITS

The Istanbul Strait is important narrow waterway of the world.It is also linking Black Sea with the Agean Sea by The Marmara Sea and also separates European and Asian continentals. Istanbul Strait is one of the most important routes of oil transportation, as it connects the Black Sea and the Mediterranean. Also it has most busy and dangerous maritime traffic line like the Malaka Strait. It has really different and special geographic, hydrographic,oceoangraphic and meteorologic conditions. It is not only important narrowest straits of the world but also has sharp turns more than 10 times. 17 Nm length of the Istanbul Strait's european coastline is nearly 55 km, anatolian coastline is 35 km. Istanbul Strait sea bottom topography reveals many banks, holes, shallows and also sinks. [1,2]

The Strait of Canakkale is the other component from Turkish Strait Sea area.It is also about 37 nautical miles long and is generally straightforward than Istanbul, with the exception of two significant turns, near the City of Canakkale, where the Strait reaches its narrowest width about 1,300 metres according to Turkish Surveys. Navigation is less dangerous than in the Strait of Istanbul, although strong currents numerous eddies and counter currents are experienced throughout the strait. A limited number of passenger and car ferries run daily between Canakkale on the Asian side and Eceabat and Kilitbahir on the European side than Istanbul also.

3rd component of the Turkish Strait Sea Area is The Marmara Sea, joins the Istanbul Strait to the Canakkale Strait and sea area distance is about 110 miles. It approaches to the two straits tend to be more congested than the open sea approaches. The approach to Canakkale Strait has limited anchorage space, and that space is close

to the traffic lanes. The Marmara Sea is an intracontinental basin 275 km long and 80 km wide formed as a result of pull-apart tectonics along the North Anatolia Fault.[8]

3. MARINE SCINECES GENERAL

The Marine Science details are very important and have very valuable datas. And not only internationally importance about the sea and environmental research of the world but also maritime transportation. Hydrography, oceanography, meteorology, climatology, marine geology and geophysics etc. are sub-divisions of Marine Sciences. All sub-divisions are working for; measure and describe bodies of sea and try to giving meaningful datas for mariners and also some of marine science disciplines should be known for all mariners and also environmental specialist. All these sub-divisions measures gains are as following, depth of sea, seabed profile, current, velocity, salinity, ecosystem, environment dynamics, pollutions etc. Hydrography is the science that measures and describes the physical features of bodies of sea and the land areas adjacent to those bodies of sea. In according to International Hydrographic Organization-IHO definition, **Hydrography** is the branch of applied sciences which deals with the measurement and description of the physical features of oceans, seas, coastal areas, lakes and rivers, as well as with the prediction of their change over time, for the primary purpose of safety of navigation and in support of all other marine activities, including economic development, security and defense, scientific research, and environmental protection. [9,10] Oceanography **is** scientific discipline and it concerned with all aspects of the world's oceans and seas, including their physical and chemical properties. Also their origin and geologic framework, and the life forms that inhabit the marine environment. Oceanography covers a wide range of topics, including marine life and ecosystems, ocean circulation, plate tectonics and the geology of the sea floor, and the chemical and physical properties of the ocean. Just as there are many specialties within the medical field, there are many disciplines within oceanography. [9,10] Meteorology, the study of the earth's atmosphere, is a component of Earth system science. The temperature, wind, and precipitation that we observe and experience impact, and are impacted on by, various scales. Weather, which is at one end of the meteorological spectrum, generally refers to short-term fluctuations which includes less than a couple of weeks, while the climate is characterized by longer time scales from months to years. On short time scales - convection, like cloud cover, humidity, soil moisture, can all impact a forecast while climate is impacted by solar variations, volcanic eruptions, and changes in the sea circulation. [9]

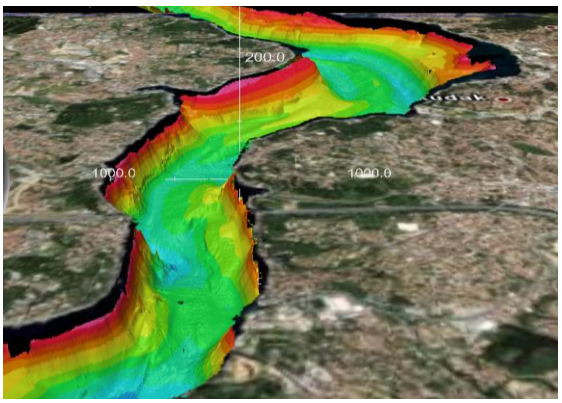

Figure 9.Surveyed part of the Istanbul Strait

4. CURRENT EFFECTS ON THE TURKISH STRAIT WATER DYNAMICS

With this study, the example area had been selected from the Istanbul Strait which published Phd.Thesis H.B.USLUER at 2016. From the all oldest and newest surveys came from one of the Turkish official institution. They shows that, there are different surface and subsurface currents. And also they have been observed at different depths in the Turkish Straits. The office, Turkish Navy-Office of Navigation, Hydrography and Oceanography and which is stands for ONHO that one of the main responsible for marine researches by the Turkish law, had surveyed and researched both at Turkish territorial water and at Turkish Straits Sea Area. All Researches conducted between 2005 and 2007, and also it was showed into an Oceanographic Atlas Book published 2009. This Atlas Book has been examined in different seasons and depths and it shows the different effects of currents at different depths. In the Turkish Straits Sea Area history, many hazardous collusions had been occurred at the Istanbul Strait due to many reasons. Important one of them is currents regime also. Currents

regime can also effect to ship movement and its pollutions during the navigation on the straits. Study trying to find an answers of ,''Can we predict currents before navigation at the Turkish Straits Sea Area? And How could we predict pollutions at the Turkish Strait?''

5. EXAMPLE AREA INTRODUCTIONS

The researches are consisting of 4 sea example areas. With this study trying to explain first one which area is limited from Bebek to Kandilli. Also area limits are between in 41-04.45N & 29-02.85E ile 41-04.75N & 29-03.35E coordinates. This area was surveyed from winter 2005 to summer 2007. [12] Three different depth areas (water columns) which had been selected from 0-10 meters, 10-20 meters and 20-30 meters, were examined separately from 2005's to 2007's summer season. There was a matrix which was examined, had been customized 11x11. In these area each matrix was applied separately to depths of 0-10 meters, depths of 10-20 meters and depths of 20-30 meters. Showed that, study results can predict nearly form %5 to % 10 precision values. In this study, trying to working with prediction analytics from data mining. It was also emphasized that the data which surveyed, have been repeated 3 times in the same season. So it is taking into consideration the availability of more used and reliable results and the acquisition of archival features. [13]

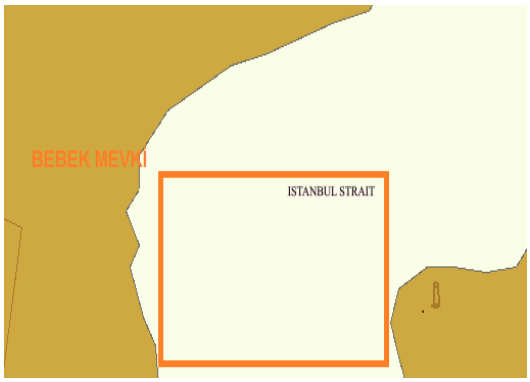

Figure 10.Selected Area scheme from ECDIS Display

6. METHODS

Regression analysis is one of the most popular used statistical techniques. Especially the Least Squares Method (LSM) has been generally adopted because of tradition and ease of computation. In data analysis and trend modelling applications the least squares (LS) estimator is widely used and LS regression is, in most cases, the method of choice. However, the crucial fact that the LSestimator is very sensitive to outlying observations may lead to unreliable results in the regression estimates and, hence, to a misleading interpretation of the data. All datas have been worked with linear regression from regression analysis and Leaast square fits. All surveyed datas are obtained from several experiments. Datas also contain significant amount of random noise caused by measurement errors from the survey circumstances which includes marine science.

6.1. Using Datas in the study

In this study, there are some datas which includes Latitude, Longitude, currents direction and currents values (from the tables of 1,2 and 3) used in MATLAB. Least square and their regression analysis are generally using independent two variable datas. In this study, current and direction are two independent variable datas indeed. some statistical techniques have been developed that are not so easily affected by outliers. These are the robust methods, the results of which remain trustworthy even if a certain amount of data is outlier. One of them is the least median.[14,15] squares method which is using in statistical analysis.

$f(x) = a + bx$ is the main formula for the study, to data is also known as linear regression. In this case the function to be minimized is;

$$S(a, b) = \sum_{i=0}^{n} [y_i - f(x_i)]^2 = \sum_{i=0}^{n} [y_i - a - bx_i]^2. \quad (1)$$

6.2. Study Scenarios

Istanbul Strait's currents directions and speeds values are very different each season. I this study; all example scenarios have been applied about forecasting and the shapes have been determined. And also in the study, flow efficiency vectors appropriate to the ship and water withdrawals were determined taking into account the individual flows for the present region. The study includes different situations. There are two main different moving about ships, first is from Blacksea to Marmara Sea direction. Second one is from Marmara Sea to Blacksea direction.

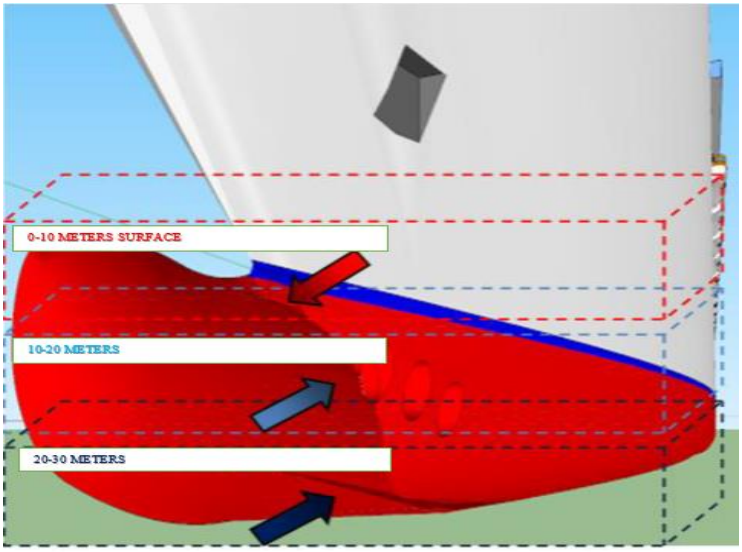

Figure 11.Isanbul Stait Currents Regime

According to the scenario;

1.The Ship is 100 length which has a 7 meters draft and 7 Knots speed,
2. The Ship is 100 length which has a 12 meters draft and 7 Knots speed,
3. The Ship is 100 length which has a 21 meters draft and 7 Knots speed, in the selected area.

This ship is moving from the Blacksea to the Marmara Sea, at a speed of 7 knots at a starting date of 195.35 ° starting from 41.0564N & 29.0466E was considered for a ship moving from the Marmara Sea to the Blacksea at a speed of 7 knots on the 15.05 ° route. [15]

6.3. Scenario Results

Each Scenario's Results and graphics are bellows. Graphics made also from MATLAB programme. All parameters and circumtances were examined separately each depth level and currents status. And it shows that, the effects of the water which includes current direction and speed, high importance factors on the ship movement while navigating on the Turkish Straits. [15]

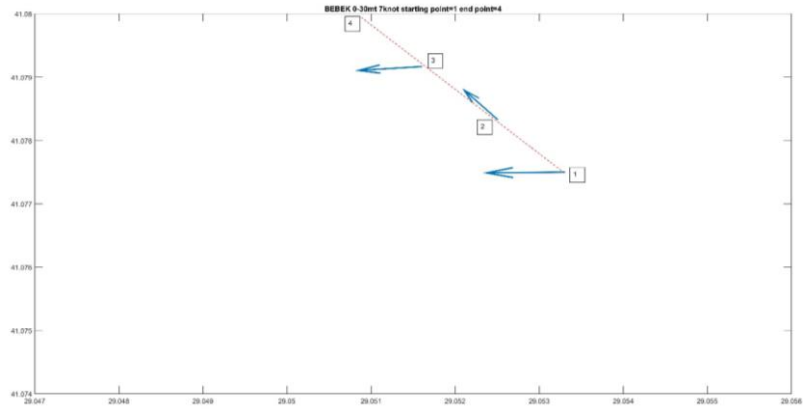

Figure 12.Ship movement from Blacksea to Marmara Sea with currents effects on 0-30 mt.

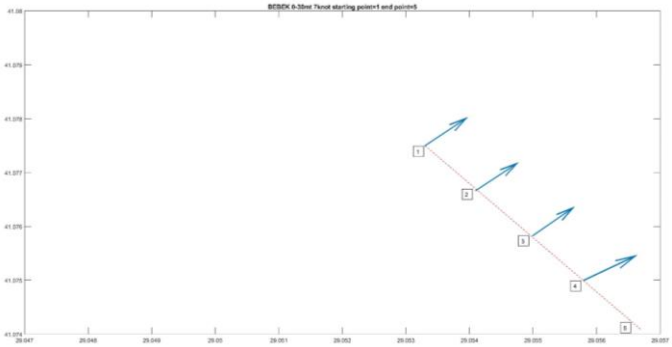

Figure 13.Ship movement from Marmara Sea to Blacksea with currents effects on 0-30 mt.

6.4. How can making schema about Istanbul Strait?

According to the official archive, there were 17 passed through the Istanbul Strait per day at 1936. At the end of 2018, ministry database statics said that this value is 43999 ship were passed. It is showing that nearly 117 ships pass the strait per day and this value 7 times more that 1936. As well known, since 1936, passage through the Turkish Straits has been governed by the Montreux Convention and regarding between Australia, Bulgaria, France, Germany, Greece, Japan, Romania, the dissolved Union of Soviet Socialist Republics, Turkey, the United Kingdom and Yugoslavia, which regulates the legal status of the Canakkale Strait, the Marmara Sea and the Istanbul Strait, was executed on 20.07.1936 and came into force on 9.11.1936. Due to convention all the Merchant ships with any nations can use with thema of innocents passage. Innocent meas very general like, from marine pollution to follow the traffic regulations. As mentioned before, Turkish Straits are also great way for energy transportation between Blacksea to Mediterranean Sea. Both Blacksea and Marmara Sea are close statue. And Balast water or any bilge and chemical waste can negative effect to all components like marine biology and coastal environment. In this study, currents schemas were completed. And it shows that different water column goes different directions and speeds. Attention to not only currents direction but also ships directions and ships drafts and suggest that Turkish Strait could be checked with different water column or level.

7. CONCLUSIONS

The Turkish Straits are in great position and connecting the Black Sea to the Mediterranean Sea by Turkish Strait Sea area which includes Istanbul Strait, Canakkale Strait and Marmara Sea. The Turkish Straits which have an important position in the geographical structure of the natural obstacles to safe navigation and structure is filled with many parameters due to factors because of its strategic importance and geographical political, economic, military, including many areas. The all relevant parameters of obstacles to safe navigation and result a negative effect on environmental management undoubtedly the effect of marine Sciences and marine mapping products is very important. The Benefits of marine science to mariners and environment management, have

enormous impact in ensuring the safety of all marine habitat. Due to the energy source research especially in the Caspian Sea and the Mediterranean Sea, therefore the importance of the use of the Turkish Straits waterways have increased. And this area's currents effects should be examined seasonal and different column values. With this light of the aforementioned remarks that, no doubt that the Turkey has great importance about national and international maritime transportation especially energy transportation. All Straits components should be measured by Marine Science. All measured datas by Marine science and environmental science are using the formation of hydrography, oceanography, cartography and meteorology, such as more emphasis to the data that are important to the safety of navigation and support to environment management further mapping and marine show needs to be taken. And all this experience and useful datas can use for, detection for marine pollutions, Search and Rescue and also environmental control.

ACKNOWLEDGMENT

This studies datas have just used from Phd.Thesis of Dr.USLUER and this paper supported by T.R.Galatasaray University, Scientific Research Programme, under grant project number of 17.600.001.

REFERENCES

[1]. H.,B.,Usluer, G.B.Alkan,''Importance Of The Current Effects On Maritime Transportation And Making Schema About Environmental Planning At The Turkish Straits''3rd Icoest 2017,Budabest-Hungary,2017
[2]. H.,B.,Usluer, G.B.Alkan,''Importance of the Marine Science and Charting about Environmental Planning, Management and Policies at the Turkish Straits''1st.ICOEST 2015
[3]. (1979) Third United Nations Conference on the Standardisation of Geographical Names
[4]. (2001) The Journal of International Affairs. Available http://sam.gov.tr/wp-content/uploads/2012/02/YukselInan.pdf
[5]. (2011) Political,Economic and Strategic and Dimension of the Turkish-Soviet Straits Question Emerged after World War II. International Journal of Business and Social Science,Vol.2,No.15,173-174
[6]. (1948) Bilsel, C. Turk Bogazlari, Istanbul
[7]. (2008) Birpinar,M.E.,Talu,G.F.,Gonencgil,B.,Environmental effects of maritime traffic on the Istanbul Strait
[8]. (2008). McHugh, Gurung, Giosan, Ryan, Mart, Sancar, Burckle, Cagatay The last reconnection of the Marmara Sea (Turkey) to the World Ocean:A paleoceanographic and paleoclimatic.
[9]. (2015) http://dergipark.ulakbim.gov.tr/ejsdr/article/view/5000156097
[10]. (2019) The NOAA website. Available http://oceanservice.noaa.gov/facts/oceanographer.html
[11]. (2015) The Website. Available http://coe.fit.edu/dmes/env_resource.php
[12]. (2015) The Website. Available http://www.csb.gov.tr
[13]. (2016) USLUER,H.B.,PhD.Thesis''INVESTIGATION ABOUT BENEFITS OF EFFECTIVE USING VESSEL TRAFFIC SYSTEM-VTS AT THE TURKISH STRAITS''pg.58-83,2016
[14]. (2008) Regresyon Analizinde Kullanilan en kucuk kareler ve en kucuk medyan kareler yontemlerinin karsilastirilmasi, SDU,Fen Dergisi, Alma G.Ozlem, Vupa Ozgul
[15]. (2016) USLUER,H.B.,PhD.Thesis''INVESTIGATION ABOUT BENEFITS OF EFFECTIVE USING VESSEL TRAFFIC SYSTEM-VTS AT THE TURKISH STRAITS''pg.58-83,2016

BIOGRAPHY

Assist.Prof.Dr. Hasan Bora USLUER is the Director of the Maritime Vocational School of T.R.Galatasaray University. He was served more than 14 years as a cartographer, a hydrographer and an oceanographer at Turkish Navy, Office of Navigation, Hydrography and Oceanography. He graduated from Kocaeli University Deck Science 2001, Army Mapping School Command 2002, Italy International Maritime Academy Electronic Chart Production 2004, Anadolu University, Public Administration 2004, Msc Istanbul University Maritime Politics 2011, International Hydrographic Organization, IHO ICA Applied Hydrography B Category Programme, PhD Istanbul University Maritime Transportation and Management Enginnering 2016.

ICOEST SARAJEVO
5TH INTERNATIONAL CONFERENCE ON ENVIRONMENTAL SCIENCE AND TECHNOLOGY
October 09-13 2019

Determination of cancer risk for maximum PM_{10} values in Izmir vicinity

Aysegul Pala[1], Gunes Kursun[2]

Abstract

The effect of environmental carcinogens on human health is a challenging issue in present type. Environmental carcinogens from various production and consumption activities affect living life on earth. The World Health Organization (WHO) and the International Agency for Research on Cancer (IARC) stated that outdoor air pollution increases the risk of developing lung and bladder cancer. Therefore, air pollution was included in the list of cancer-causing factors. In addition, Particulate Matter (PM), which is one of the parameters that constitute air pollution, has been declared as carcinogenic. In this study, three air quality stations belong to Izmir Metropolitan Municipality were examined from 01.12.2017 to 28.02.2018 including winter months, maximum hourly PM_{10} values in daily data obtained from the vicinity of Izmir was collected. Normal distribution, Log-Normal distribution and Gumbel distribution were applied to observed data to estimate the best fit distribution. By using the Monte Carlo Simulation, randomly generated PM_{10} data were used to calculate carcinogenic risk. As a result of this study, the maximum risk was determined around the vicinity of Izmir in Buca, Karsiyaka and Alsancak.

Keywords: Cancer, Air Quality, Monte Carlo Simulation, Particulate Matter, Risk Analysis, Izmir

1. INTRODUCTION

Air pollution is identified by the World Health Organization (WHO) as responsible for several million deaths per year [1]. Particulate Matter (PM), which is one of the parameters of air pollution, has been declared as a carcinogenic agent. Environmental carcinogens is the statement described by the World Health Organization (WHO) and the International Agency for Research on Cancer (IARC) on 17 October 2013. High exposure to particulate matter (PM) is known to cause several diseases [2].

Studies showed that because of the ambient air pollution, there is a risk of autism of children, depression of elderly people and anxiety of pregnant women [3-4].

Particulate matter with a diameter of 10μ or less, known as PM_{10}. These particulate matters can be produced by natural phenomena such as forest, dust storms and grassland fires. The significant contribution to PM_{10} in a cities release from human activities such as the burning of fossil fuels in vehicles, in airplanes, in power plants and in other industrial processes [5].

The sources of PM comes from both stationary and mobile and also from reactions of primary and secondary pollutants of air by photochemical reactions [6].

2. MATERIALS AND METHODS

The data was provided from three different air quality stations in Izmir (Buca, Karsiyaka, Alsancak) during the period from 01.12.2017 to 28.02.2018 winter months. Maximum hourly PM_{10} values in daily data were collected from the website of the government [7]. Normal, Log-Normal and Gumbel distrubitions were used to find the best fit data with observed PM_{10} values in comparison with determination coefficients (R^2). Monte Carlo simulation used to generate data from given distribution which fitted data includes best. In order to calculate cancer risk exposure by inhalation way Equation 1 and Equation 2 were used.

[1] *Corresponding author: Dokuz Eylul University, Department of Environmental Engineering, 35160, Buca/Izmir, Turkey.* aysegul.pala@deu.edu.tr

[2] *Dokuz Eylul University, Natural and Applied Sciences, 35160, Buca/Izmir, Turkey.,* gunes.kursun1@gmail.com

$$R = \text{ADI} * \text{SF} \quad (1)$$

$$ADI = \frac{C_0 * IR_a * EF * ED}{BW * AT * 365(\frac{day}{year})} \quad (2)$$

Where ADI = Acceptable Daily Intake, R= Cancer Risk, IR_A=Inhalation Rate (m^3/min.), EF=Exposure Frequency (min./years), ED=Exposure Duration (years), BW=Body Weight (kg), AT =Average Time(years), SF= Slope Factor(mg $kg^{-1}day^{1})^{-1}$.

3. RESULTS AND DISCUSSION

According to PM_{10} data collected from Buca Station, the best-fit distribution was Log-Normal Distribution (R^2= 0.8591 while Normal R^2= 0,5562 and Gumbel R^2= 0,7208). The best fit distribution was shown in Figure 1. Then a total of 1000 PM_{10} values were generated by Monte Carlo Simulation based on Log-Normal distribution.

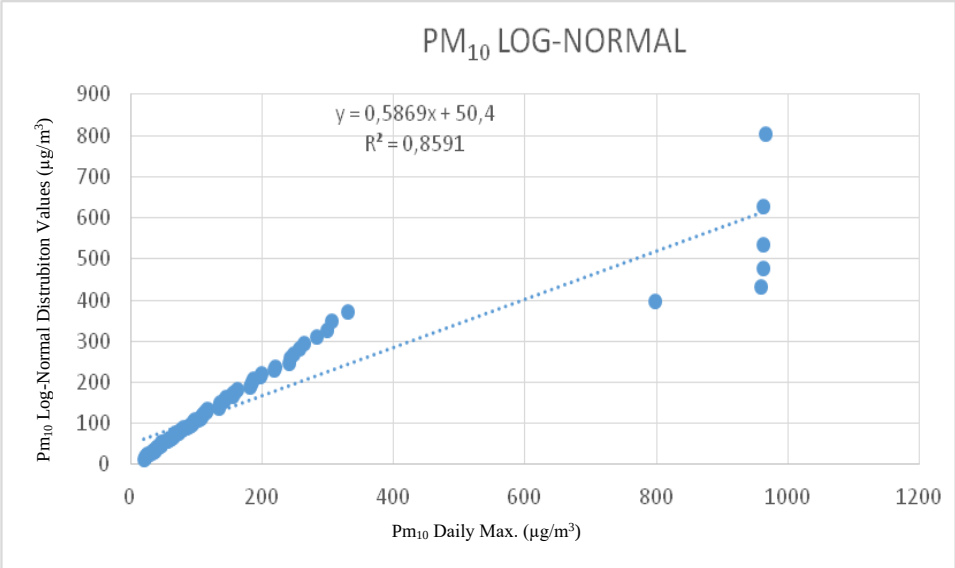

Figure 1. PM_{10} daily max. values vs. PM_{10} log-normal values

According to PM_{10} data collected from Karsiyaka Station, the best-fit distribution was Log-Normal (R^2 = 0.9946 while Normal R^2= 0,9069 and Gumbel R^2= 0,9762). The best fit distribution was shown in Figure 2. Then a total of 1000 PM_{10} values were generated by Monte Carlo Simulation based on Log-Normal distribution.

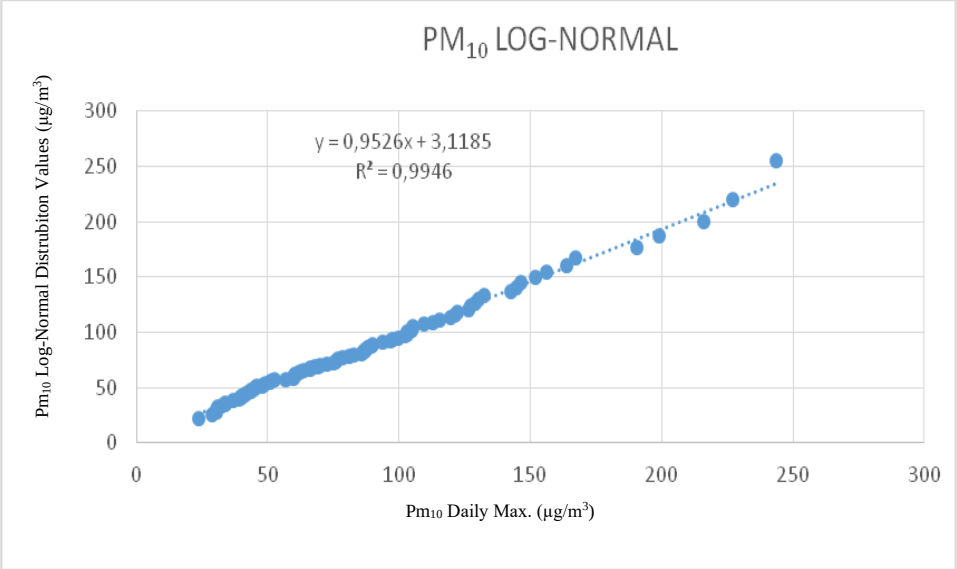

Figure 2. PM_{10} max. values vs. PM_{10} log-normal values

According to PM_{10} data collected from Alsancak Station, the best fit distribution was Log-Normal (R^2 = 0.9835 while Normal R^2= 0,7873 and Gumbel R^2= 0,9274). The best fit distribution was shown in Figure 3. A total of 1000 PM_{10} values were generated by Monte Carlo Simulation based on Log-Normal distribution.

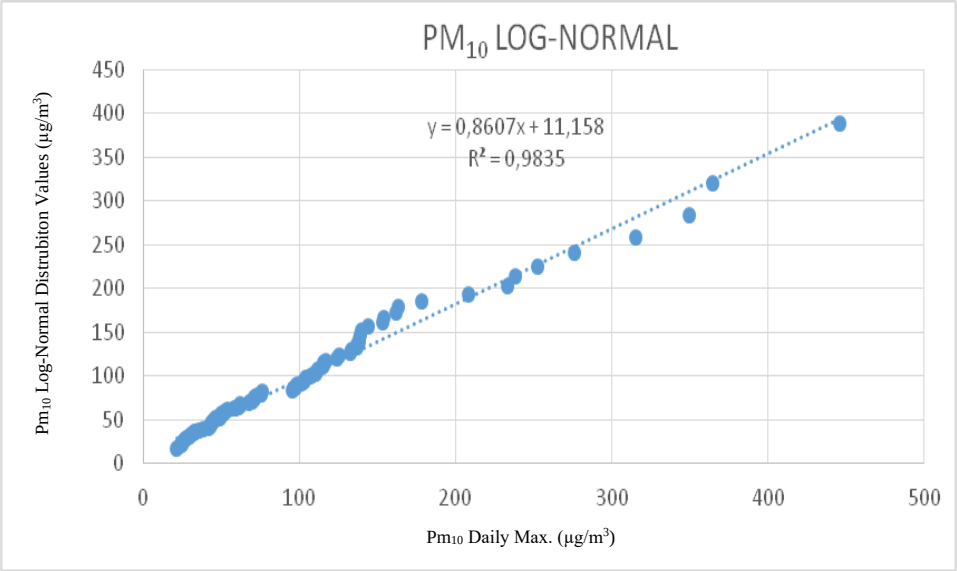

Figure 3. PM_{10} max. values vs. PM_{10} log-normal values

There has been an increase in environmental awareness in wastewater treatment sector. It has been necessary to include tools for evaluating of the processes.

The stations and all districts of Izmir City were shown in Figure 4. The highest cancer risk was found in Buca Station with a percentage of % 0,35 ($3,52*10^{-3}$) and also the lowest cancer risk was found in Karsiyaka Station with a percentage of %0,2 ($2,04*10^{-3}$) as it is shown in Table 1.

Figure 4. The location and districts of Izmir city in Turkey [8].

Table 1. Cancer Risk Exposure of Buca, Karsiyaka and Alsancak regions

Stations	Buca	Karsiyaka	Alsancak
Cancer Risk	$3,52*10^{-3}$	$2,04*10^{-3}$	$2,23*10^{-3}$
	% 0.35	% 0.20	% 0.22

4. CONCLUSIONS

In this study, maximum hourly PM_{10} values in daily data taken from three different air quality stations in Izmir during the period from 01.12.2017 to 28.02.2018 in winter months were examined by statistical methods. Findings are summarized as below.

- The best-fit distribution was Log-Normal for all three air quality stations (Buca, Alsancak, Karsiyaka Stations).
- A total of 1000 PM_{10} values were generated by Monte Carlo Simulation based on Log-Normal distribution. By using these generated data cancer risk was calculated for each three stations.
- The highest cancer risk was found in Buca Station with a percentage of % 0,35 ($3,52*10^{-3}$) and also the lowest cancer risk was found in Karsiyaka Station with a percentage of %0,2 ($2,04*10^{-3}$) as it is shown in Table 1.

REFERENCES

[1]. (2019) The WHO website. [Online]. Available: http://www.who.int
[2]. B. Yang, Z. Qian, S.W. Howard, M.G. Vaughn, S. Fan, K. Liu, et al. "Global association between ambient air pollution and blood pressure: a systematic review and meta-analysis," *Environ. Pollut.*, 235, pp. 576-588, April 2018.
[3]. M.C. Power, M.-A. Kioumourtzoglou, J.E. Hart, O.I. Okereke, F. Laden, M.G. Weisskopf "The relation between past exposure to fine particulate air pollution and prevalent anxiety: observational cohort study" *BMJ*, 350, pp. 1111., March 2015.
[4]. C. Freire, R. Ramos, R. Puertas, M.-J. Lopez-Espinosa, J. Julvez, I. Aguilera, et al., "Association of traffic-related air pollution with cognitive development in children" *J. Epidemiol. Community Health*, 64, pp. 223-228, March 2010.
[5]. Alberto Fortelli, Nicola Scafetta, Adriano Mazzarella, Influence of synoptic and local atmospheric patterns on PM10 air pollution levels: a model application to Naples (Italy), Atmospheric Environment,Volume 143, Pages 218-228, October 2016
[6]. S. Moltchanov, I. Levy, Y. Etzion, U. Lerner, D.M. Broday, B. Fishbain "On the feasibility of measuring urban air pollution bywireless distributed sensor networks" *Sci. Total Environ.*, 502, pp. 537-547, January 2015.
[7]. (2019) The HI website. [Online]. Available: http://www.havaizleme.gov.tr
[8]. (2019) Wikiwand website. [Online]. Available: http://www.wikiwand.com

ICOEST SARAJEVO
5TH INTERNATIONAL CONFERENCE ON ENVIRONMENTAL SCIENCE AND TECHNOLOGY
October 09-13 2019

Examination of Diesel Engine Particle Emissions and Filters

Seref Soylu[1], Nurcan Calis Acikbas[2]

Abstract

Diesel engines have been preferred power sources for a wide range of motor vehicles due to their superior performances and thermal efficiencies. However, their nanometer level particle emissions, which are extremely hazardous for health and environment, are becoming a growing concern. The particle emissions are especially high during rapid engine loadings. During such a period, particle emissions rise up typically to the level of 10^{13} #/cm^3 with a size range approximately from 10 to 200 nm. The typical size distribution has a bell-shaped curve with 45 nm of mode.

Diesel particle filter is the only reliable technology of today to control these nanometer level emissions. A typical diesel particle filter with a porosity content of ~%50 and porosity size of 10-12 micron can easily minimize the particle emission over 90%. On the other hand, exhaust back pressure that increases with filter loading may have a significant adverse impact on engine performance, unless remedied. The alternative filter technologies and microstructures of particle filters were examined to be remedy for the exhaust back pressure. Besides, with the development of needle-like crystals DPF substrate increases the surface area and, hence, increases the filtration efficiency while minimizing the backpressure. Moreover, this kind of microstructure may minimizes the thermal stresses and increases the life time of DPF.

Keywords: Diesel Engines, Particle Matter, DPF, Microstructure, Porosity

1. INTRODUCTION

Although the developments in fuel and combustion technologies significantly minimize particle matter (PM) emissions, diesel engines still generate PM emissions which are known to be one of the most harmful air pollutants for environment and human health (HEI, 2010; Stanek et al., 2011; Briggs et al., 2007; Hess et al., 2010). Diesel engines are power source for many vehicle classes including passenger cars, light and heavy duty vehicles that commonly operate in urban areas where population density is very high. Therefore, diesel engine sourced particle emissions can especially be hazardous for citizens (Hess et al., 2010; Adar et al., 2008). The quantity and chemical composition of the particle emissions released from a diesel engine are strongly dependent on engine combustion technology, exhaust after-treatment systems, fuel quality, and operating conditions (Guan et al., 2015; Erlandsson et al., 2008; Cocker et al., 2004; Haibo et al., 2008; EC Regulation, 2009; Johnson et al., 2009; Durbin et al., 2007; Zhihua et al., 2011; Semercioglu et al.,2010; Andersson et al., 2010; Kittelson et al., 2006). Currently, the legislations bring stringent limits on PM emissions and to meet these limits DPFs become almost necessary for diesel engines. DPF is a device to trap the solid PMs and release the rest of exhaust gas. It is well known from literature that typical wall-flow type DPFs can easily trap well over 90 percent of the PMs (Johnson, 2010; Chandler, 2006; MECA, 2007). As the PMs are accumulated in the DPF, permeability of the filter walls is reduced and exhaust gas back pressure rises up which should not exceed a certain limit. Once the back pressure limit is reached, the accumulated PMs must be burned in order to lower the backpressure. The accumulated PMs, which are mainly soot, starts to burn at a temperature around 600 ^{0}C with oxygen, but the temperature can be reduced in a catalyzed DPF and also with NO_2 oxidation (Guan et al., 2015). Ceramic is the most commonly used DPF materials due to its resistance to high temperatures (Acikbas, 2018). The other important characteristics for a DPF are pore size and filter thickness which are responsible for filtering efficiency and material strength. A typical DPF generally has a pore size of 10 - 30 μm, pore volume 50%, thickness of 400 μm which guarantee 90% of filtering efficiency (Adler, 2005). DPF

[1] *Corresponding author: Bilecik S. Edebali University, Department of Mechanical Engineering, 11230, Gulumbe / Bilecik, Turkey. serefsoylu@gmail.com*

[2] *Bilecik S. Edebali University, Department of Metallurgical and Materials Engineering, 11230, Gulumbe / Bilecik, Turkey. ncalis@gmail.com*

material must be able stand to high temperature of the regeneration process, which can be as high as 1200℃. Temperature rise during regeneration leads to thermo-mechanical stresses in the DPF. (Benaqqa et al. 2014). The filter material must be able to withstand such stresses that may occur. This kind of stresses can be controlled by microstructural design. In the previous studies, it was stated that by increasing the needle mullite crystals on DPF cell walls, the surface area was increased and filtration efficiency was increased and the back pressure remained at optimum level. At the same time, the fibrous structure increases porosity and permeability and provides better mechanical strength with the open pore network structure formed between intertwined ceramic fibers. (Gallant et al. 2016). Three basic mechanism of the filtration process are "sieve", "deep-bed" and "cake filtrations". DPFs are able to reduce not only the course particles (1-10 μm), but also the nuclei mode particles in nanometer range (<50 nm) (Guan, 2015).

2. METHODOLOGY

In this work test engine to complete PM number and size measurements were 6.7 liter Cummins diesel engine (ISB6.7) which is certified to EURO 5. It delivers 186 kW at 2500 rpm. The testing was completed in the project entitled "Measurement and Modeling of Real World Emissions of a Hybrid City Bus". This project was coordinated by Sakarya University and supported by the Turkish Ministry of Science, Industry and Technology and TEMSA R&D. Figure 1 shows a schematic of emissions measurement system. Engine operating parameters, ambient conditions, vehicle location and tailpipe gaseous emissions measurements were made by using a SEMTECH DS from SENSORS Inc. The exhaust mass flow-rate was measured using a SEMTECH EFM which operates based on Pitot Tube technology. Because of better sensitivity, solid particle number (PN) emissions and their size were measured instead of particle mass emissions (Giechaskiel, 2012). PN and size measurement systems involve a rotating disc thermo-dilution system from Matter Engineering, a condensation particle counter (CPC 3097) and a particle sizer (EEPS 3090) both from TSI.

The performance of DPFs is controlled by microstructure. Especially the por structure is the most effective parameter. It is expected that the problem of both high filtration ability and back pressure increase will be minimized by the development of needle-like Si3N4/SiAlON crystals in the por walls. This can be provided by judicious selection of sintering aids to form needle-like crystals on the DPF wall. In addition, thermo-mechanical properties are expected to improve.

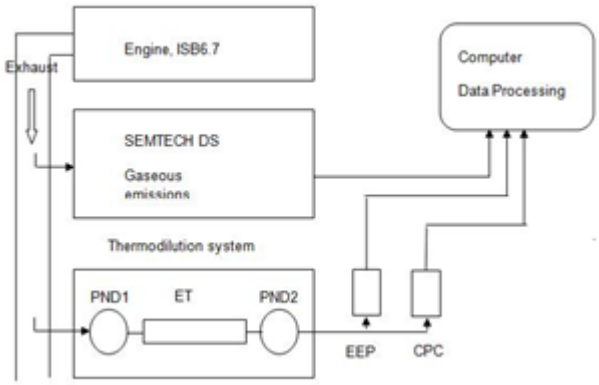

Figure 1. *Schematic of emissions measurement system.*

3. RESULTS AND DISCUSSION

In this section characteristics of diesel engine PMs and DPF technologies including substrate materials will be examined in detail.

a. Particle Emissions of the Diesel Engine

Particle emissions and basic engine operating parameters in a synchronized manner were examined under rapid engine loading condition, which is a common operating condition for a typical diesel engine. Figure 2 indicates

basic engine operating parameters and corresponding Particle Number (PN) emissions. This is very useful figure to understand the effects of the engine operating parameters on the PN emissions. At this engine loading, while the engine speed and power start to rise up, the excess air ratio (lambda) decreases immediately from approximately 5.0 to 1.7. Turbocharger lag may also have some contribution for such sharp decrease in lambda. During this period, turbulent engine combustion is probably highly instable and PN emissions rise up immediately to the maximum. Once engine speed and power become stable at their maximum, PN emissions decrease sharply. As the turbocharger operation is stabilized, the lambda rises up to 2.0 at this condition. Diesel engines are very efficient power source to deliver high power demands of heavy duty vehicles, but as can be seen from Figure 2, during the acceleration period, there is almost a linear relationship between engine power and PN emissions. During this period while the engine is accelerating for maximum power, PN emissions rise up to approximately 7.50E+6 #/cm3 of exhaust gas. It is actually very important to note that while the engine is accelerating from idle to higher powers, the PN emissions immediately increase up to the maximum. Then, once the engine power becomes stable at the maximum, as shown in Figure 2, the PN emissions sharply decrease to about 30% of the maximum. There is almost a direct relation between sudden increase of engine power and PN emissions. It is probably true that during such a full load acceleration of the engine, insufficient turbulent mixing of the locally rich fuel-air mixture in the cylinder is the main reason for very high number of the particle emissions.

In order to get statistically significant PN emission results, the engine loadings and measurements were repeated several times. During these tests, PN emissions sharply increased from about $1.0*10^6$ to the maximum values, which were in a range from $6.5*10^6$ to $7.9*10^6$ #/cm^3 for 10 consecutive tests. Once the engine power became stable at the maximum, PN emissions are reduced to about 30% of the maximums and then during deceleration period the PN emissions reduced to as low as $1.0*10^6$ #/cm^3. Table 1 indicates some of the PN test results. As can be seen from the table PN per kW-h of engine energy (PNEE) is as high as $1.30*10^{13}$. Figure 3 indicates total PN emissions and engine power. Total PN is the summation of all particles without a size limitation in the measureable range of the EEPS. As can be seen from the figure, the peaks of PN emissions and the peaks of engine power overlap.

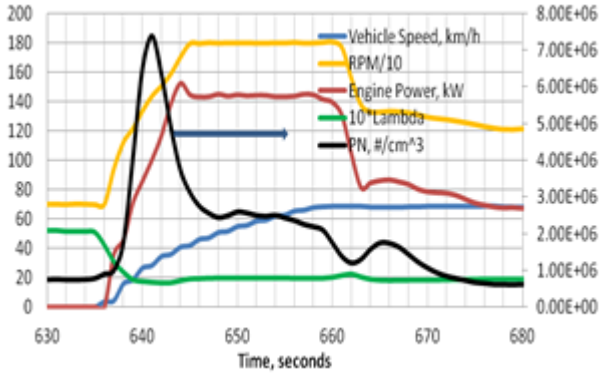

Figure 2. *Effects of city bus acceleration on the engine parameters and PN emissions.*

Figures 4a and 4b show the particle size distributions at 1460th and 1320th seconds for better comparison of the size distributions for acceleration and cruising conditions of the bus. As can be seen from the figures, the acceleration condition size distributions have a bell shaped curve with 45 nm of mode and a size range approximately from 10 to 200 nm. At this condition, the engine is accelerating to reach its maximum power and total PN emissions are at the maximum. This means that PN emissions from 20 to 200 nm are very sensitive to change in engine power. During the cruising, creeping and idling conditions, as shown in Figure 4b, PNs sized less than 20 nm are slightly dominant. It is worth mentioning again that a DPF can reduce the PN emissions much more efficiently but these reductions come with additional costs. Therefore, it is better to minimize the PN emissions at its source as much as possible.

Table 1. PN emissions of the engine over the test

Parameters	Text
Averaged Peak PN, #/cm^3	6.88*10^6
Total PN, #/test	7.74*10^{13}
PNEE, #/kW-h	1.30*10^{13}

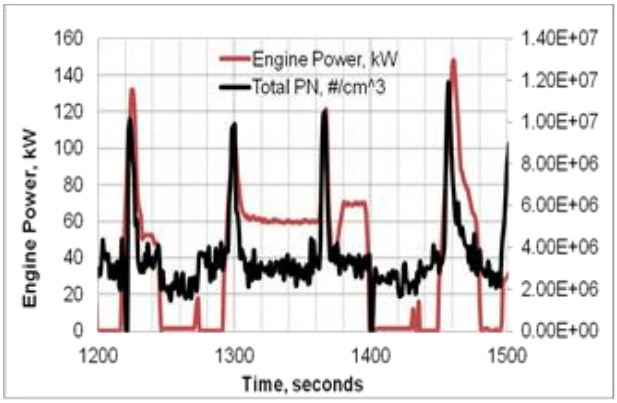

Figure 3. *The effects of the engine power on total PN from 1200 to 1500 seconds of sampling period.*

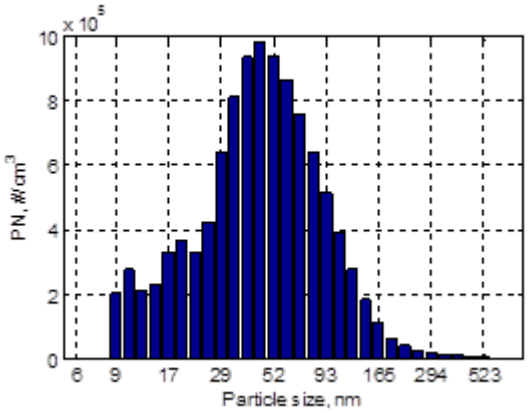

Figure 4a. *Effects of engine power on particle size distribution - acceleration condition size distribution (Time= 1460th second).*

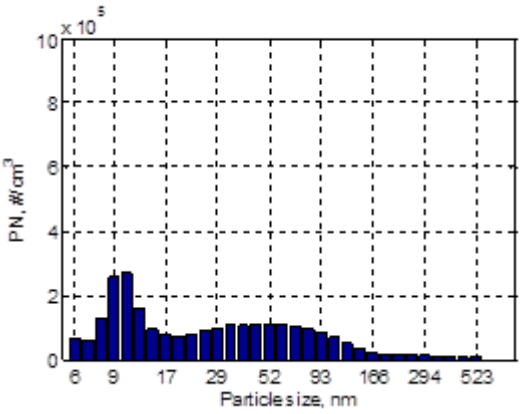

Figure 4b. *Effects of engine power on particle size distribution - cruising condition size distribution (Time=1320th second).*

b. Control strategies for particle emissions

The most common methodology to control PM emissions is to simply trap PMs in a ceramic wall-flow type porous filter. Ceramic is especially preferred material for a DPF due to its resistance to high temperature to withstand the temperature of exhaust gas. As can be seen from Figure 5, alternatively plugging the channels of a ceramic filter at the beginning and end, forces the PM loaded exhaust gases to pass through porous wall and hence trap the solid PMs in the channels. The porous filter generally have 200 to 300 channels per square inch (cpsi) of the substrate and the channel walls generally have pore diameters from 10 to 30 micro-meter and wall thickness from 300 to 500 micro-meter (Adler, 2005; Guan, 2015). However, the trapped PMs accumulated in the channels rises up the exhaust back pressure, which has an adverse effect on engine performance. Therefore, the accumulated PMs have to be removed as it is necessary in a reliable technique to reduce the backpressure. The removing process of the accumulated PMs by burning them up is called regeneration. In order to regenerate the trapped PM, either the exhaust gas must be at a certain temperature, which is around 600 ^{0}C, or the ignition temperature of the PMs must be lowered by a different oxidizer, which is NO2, or a catalyst (Kostoglou, 2000). Exhaust gas temperatures of diesel engines rarely exceeds 300 ^{0}C under real world operating conditions, and therefore, it is not guarantee that the trapped PMs regenerate themselves in a reliable way. For this reason, either the exhaust gas temperature or the filter temperature has to be increased to a reliable level by an external means which is called "active regeneration". The other technique to regenerate the trapped PMs is to reduce ignition temperature of the PMs to lower levels and continuously regenerate the trapped PMs under real world operating conditions of the engine. This technique is called "passive regeneration".

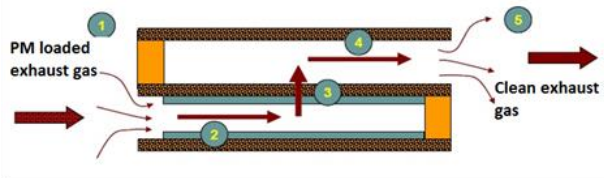

Figure 5. Wall-flow type particle filter.

2.2.1 Active regeneration DPF

Since diesel combustion is a globally lean combustion, the exhaust gas involves plenty of O2 to oxidize the accumulated PMs in the filter. However, ignition temperature of the PMs is as high as 600 ^{0}C if the oxidizing agent is O2, and exhaust gas temperature of a diesel engine cannot reach to such high level of temperature under normal operating conditions. Therefore, in active regeneration technique, as seen in Figure 8, the exhaust

temperature is raised externally by any of the following techniques; in-cylinder post injection, in exhaust fuel injection, flame burner or electrical heating of the filter. The main advantage of the active regeneration is independence of it from engine operating conditions. Active regeneration is initiated by the electronic control module as PM loading of the filter reaches a certain level which has direct impact on the exhaust back pressure.

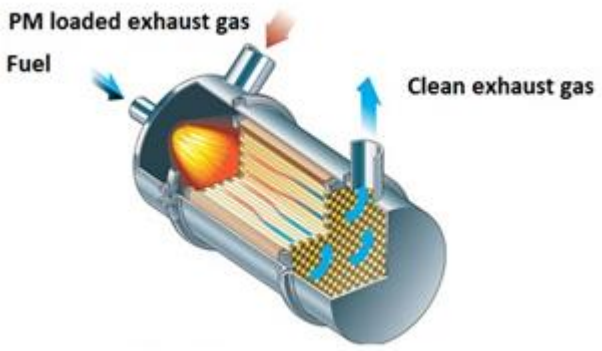

Figure 8. Active regeneration with a flame burner.

2.2.2 Passive regeneration DPF

Passive regeneration does not require an external heat source to ignite the trapped PMs instead PM ignition temperature is lowered either by using a catalyst or a more reactive oxidant such as NO2. There are three mechanisms of the passive regeneration, which are catalyzed DPF, continuously regenerating trap (CRT) and fuel born catalyst (FBC). In catalyzed DPF, catalyst materials, which is generally platinum group materials, are coated to inlet channels of the substrate so that ignition temperature of the trapped PMs is reduced sufficiently (~300 ^{0}C) that allows self-regeneration of the PMs under high load operations of the engine. A catalyzed DPF can easily reduce PM emissions with an efficiency over 90% (Southward, 2010). In a CRT, as seen in Figure 9, regeneration is realized in two steps. First, exhaust gas enters to an oxidation catalyst to generate the reactant agent NO2, which is much more reactive than O2. Then the exhaust gas with enriched NO2 enters the DPF to react with the trapped PMs. The reaction takes place at substantially lower temperature (~250 ^{0}C) so that the self-regeneration of the PMs is realized in a wide range of diesel engine operation (Ootake, 2007;). Catalyzed type CRT applications can further reduce the regeneration temperatures.

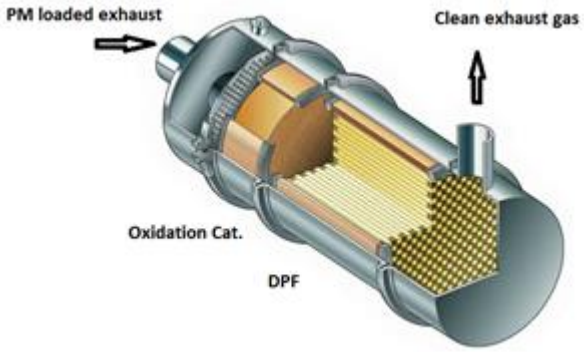

Figure 9. CRT for passive regeneration of the PM.

In FBC, a metallic fuel additive which are generally compounds of iron, cerium, or platinum, is used to lower ignition temperature of the PMs (Harle, 2008). The metallic components of the additive leaves the combustion chamber as metal oxides which act as a catalyst to lower the ignition temperature of the trapped PMs. Therefore, the regeneration is realized in a wider range of engine operation.

2.2.3 Microstructure for minimizing the backpressure

The microstructure design is given schematically in Figure 10. With the proposed microstructure design, it is expected that the release of nanoparticles into the environment during the initial phase will be prevented. A high surface area is required to effectively collect PM. The surface area will increase with needle-like crystals, the filtration efficiency will be increased by capturing the nanoparticles more effectively and the release of the nanoparticles to the environment will be prevented. The objective is to determine the optimum pore size and structure containing needle-like crystals for effective filtration. Therefore the aim of the study is to develop Si3N4 / SiAlON needle crystals which are homogeneously distributed on the porous walls in order to increase filtration efficiency, prevent the release of the initial nanoparticles to the environment and to ensure optimum back pressure.

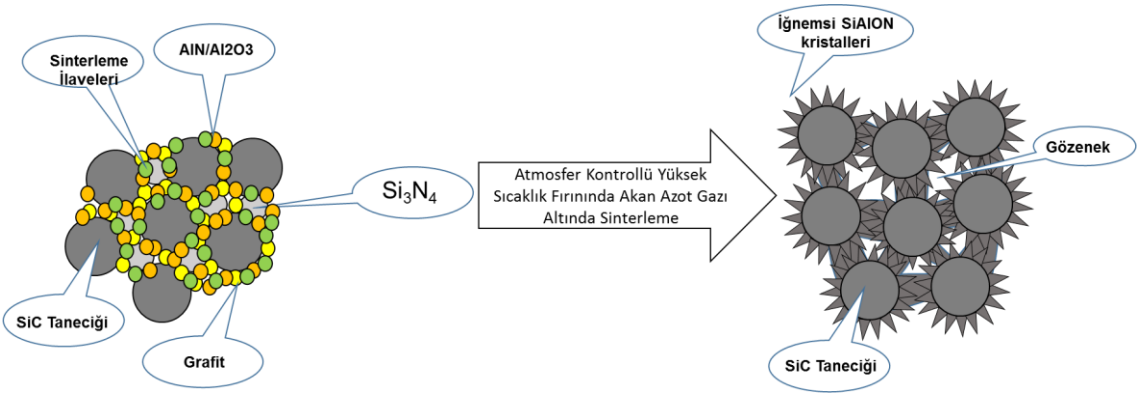

Figure 10. Modeling the development of needle-like Si3N4 / SiAlON grains on SiC grains

4. CONCLUSIONS

Rapid loading of the diesel engine from idle to full power strongly influence the particle formation and increase them to their maximum. Once the engine power becomes stable at the maximum, particle emissions decrease sharply to about 30% of the maximum.

During rapid loading of the engine, particle size distributions have a bell shaped curve with 45 nm of mode and a size range approximately from 10 to 200 nm. This means that PN emissions from 20 to 200 nm are very sensitive to change in engine power. During the cruising, creeping and idling conditions, PNs sized less than 20 nm are slightly dominant.

Active and Passive regeneration DPFs are currently the only reliable technologies to meet requirements of stringent particle emissions standards

DPF substrate with the development of needle-like crystals may increase the surface area and, hence, increases the filtration efficiency while minimizing the backpressure.

ACKNOWLEDGMENT

Turkish ministry of science and technology is acknowledged for their financial support

REFERENCES

[1]. Acikbas, NC., Ture, Y., Gurlek, E., Ozcan, S., Soylu, S., Acikbas G. and Gudu, T., 2018, Microstructural Characterization, Mechanical, Physical and Thermal Properties of a Diesel Particulate Filter, *The Arabian Journal for Science and Engineering*, DOI: 10.1007/s13369-017-2872-9

[2]. Adar., S. D., Davey, M., Sullivan, J. R., Compher, M., Szpiro, A. and Liu, L., 2008, Predicting airborne particle levels aboard Washington State school buses. *Atmospheric Environment*, 42, 7590−7599.

[3]. Adler, J., 2005, Ceramic Diesel Particulate Filters, Int. J. Appl. Ceram. Technol., 2 [6] 429–439.
[4]. Andersson, J., Mamakos, A., Giechaskiel, B., Carriero, M. and Martini, G., 2010, Particle Measurement Programme (PMP) Heavy-duty Inter-laboratory Correlation Exercise (ILCE_HD) *Final Report.* EC-JRC Scientific and Technical Reports.
[5]. Benaqqa, C., et al., Morphology, physical, thermal and mechanical properties of the constitutive materials of diesel particulate filters, Applied Thermal Engineering 62 (2014) 599 – 606.
[6]. Briggs, D. J., de Hoogh, K., Morris, C. and Gulliver, J., 2007, Effects of travel mode on exposure to particulate pollution. *Environment Int*., 34, 12−22.
[7]. Cocker, D. R., Shah, S. D., Johnson, K., Miller, J. W. And Norbeck, J. M. (2004). Development and application of a mobile laboratory for measuring emissions from diesel engines. 1. Regulated gaseous emissions. *Environmental Science & Technology*, 38, 2182−2189.
[8]. Chandler, K. and Walkowicz, K. (2006). King County Metro Transit Hybrid Articulated Buses: Final Evaluation Results. *Technical Report NREL/TP*-540-40585, USA.
[9]. Durbin, T. D., Johnson, K., Cocker, D. R. and Miller, J. W. (2007). Evaluation and comparison of portable emissions measurement systems and federal reference methods for emissions from a back-up generator and a diesel truck operated on a chassis dynamometer. *Environmental Science & Technology*, 41, 6199−6204.
[10]. EC Regulation (2009). No 595/2009 of the European Parliament and of the Council. *Official J. European Union.*
[11]. Erlandsson, L., Almen, J. and Johansson, H. (2008). Measurement of emissions from heavy duty vehicles meeting Euro IV/V emission levels by using on-board measurement in real life operation. 16th *Int. Symp. "Transport and Air Pollution",* Graz.
[12]. EPA Regulation (2008). In-Use Testing for Heavy-Duty Diesel Engines and Vehicles; Emission Measurement Accuracy Margins for Portable Emission Measurement Systems and Program Revisions. EPA, 40 CFR Part 86, *Federal Register* 73, 50 / Rules and Regulations.
[13]. Giechaskiel, B., Mamakos, A., Andersson, J., Dilara, P., Martini, G., Schindler, W. and Bergmann, A. (2012). Measurement of automotive nonvolatile particle number emissions within the European legislative framework: A review. *Aerosol Science and Technology* 46, 7, 719−749.
[14]. Guan, B., Zhan, R., Lin, H., Huang, Z., (2015). Review of the state-of-the-art of exhaust particulate filter technology in internal combustion engines. *Journal of Environmental Management* 154 (2015) 225 - 258.
[15]. Haibo, Z., Frey, H. C. and Rouphail, N. M. (2008). A vehicle-specific power approach to speed- and facilityspecific emissions estimates for diesel transit buses. *Environmental Science & Technology*, 42, 7985−7991.
[16]. Harle, V., Pitois, C., Rocher, L. and Garcia, F. (2008). Latest Development and Registration of Fuel Borne Catalyst for DPF Regeneration. *SAE Technical Paper* 2008-01-0331.
[17]. Hess, D. B., Ray, P. D., Stinson, A. E. and Park, J. (2010). Determinants of exposure to fine particulate matter (PM2.5) for waiting passengers at bus stops. *Atmospheric Environment*, 44, 5174−5182.
[18]. HEI (2010). Traffic Related Air Pollution: A Critical Review of the Literature on Emissions, Exposure, and Health Effects. *Health Effects Institute*, Boston, MA. Special Report 17.
[19]. Johnson, K. C., Durbin, T. D., Cocker, D. R., Miller, W. J., Bishnu, J. K., Maldonado, H., Moynahan, N., Ensfield, C. and Laroo, C. A. (2009). On-road comparison of a portable emission measurement system with a mobile reference laboratory for a heavy-duty diesel vehicle. *Atmospheric Environment*, 43, 2877−2883.
[20]. Johnson, T.V., 2010. Review of Diesel Emissions and Control. *SAE Technical Paper* 2010-01-0301. http://dx.doi.org/10.4271/2010-01-0301.
[21]. Kittelson, D. B.,Watts, W. F., Johnson, J. P., Rowntree, C., Payne, M., Goodier, S.,Warrens, C., Preston, H., Zink, U., Ortiz, M., Goersmann, C., Twigg, M. V., Walker, A. P. and Caldow, R. (2006). On-road evaluation of two diesel exhaust aftertreatment devices. *J. Aerosol Science*, 37, 1140−1151.
[22]. Kostoglou, E.S.M., Papaioannou, E., Zarvalis, D. and Kladopoulou, E. (2000) "Fundamental Studies of Diesel Particulate Filters: Transient Loading, Regeneration and Aging," *Society of Automotive Engineers, Inc.*, vol. 2000-01-1016.
[23]. MECA white paper, Emission control technologies for diesel-powered vehicles, December 2007, Available at: http://www.meca.org/.
[24]. Ootake, M., Kondou, T., Ikeda, M., Daigo, M., Nakano, M., Yokoyama, J. And Miura, M. (2007). Development of Diesel Engine System with DPF for the European Market. *SAE Technical Paper* 2007-01-1061
[25]. Semercioglu, H., Bal, A. and Soylu, S. (2010). Examination of real world operating conditions and emissions of a hybrid city bus. ICAT 2010, *5th Int. Conf. Energy and Automotive Technologies*, Istanbul.
[26]. Southward, B.W.L., Basso, S. and Pfeifer, M. (2010). On the Development of Low PGM Content Direct Soot Combustion Catalysts for Diesel Particulate Filters. *SAE Technical Paper* 2010-01-0558.
[27]. Stanek, L. W., Sacks, J. D., Dutton, S. J. and Dubois, J. Croatia, B. (2011). Attributing health effects to apportioned components and sources of particulate matter: An evaluation of collective results. *Atmospheric Environment*, 45, 5655−5663.
[28]. Zheng, Z., Johnson, K. C., Liua, Z., Durbin, T. D., Hub, S., Huai, T., Kittelson, D. B. and Jung, H. S. (2011). Investigation of solid particle number measurement: Existence and nature of sub-23 nm particles under PMP methodology. *J. Aerosol Science*, 42, 883−897.
[29]. Zhihua, L., Ge, Y., Johnson, K. C., Shah, A. N., Tan, J.,Wang, C. and Yu, L. (2011). Real-world operation conditions and on-road emissions of Beijing diesel buses measured by using portable emission measurement system and electric low-pressure impactor. *Science of the Total Environment*, 409, 1476−1480.

ICOEST SARAJEVO
5TH INTERNATIONAL CONFERENCE ON ENVIRONMENTAL SCIENCE AND TECHNOLOGY
October 09-13 2019

Preparation and Characteristics of Activated Carbon Supported Fe-Based Catalyst from Biomass Mixture

Hatice Erdem[1], Mehmet Erdem[2]

Abstract

Activated carbons (ACs) are the most widely used as supporting material for commercially available precious metal catalysts due to controllability of their surface properties, resistance to acidic and basic media, and ease of regeneration. ACs are relatively expensive due to high cost of precursors and production methods. Recently, intensive researches have been carried out on the synthesis of AC from biomasses by physical and chemical activation methods in order to produce cheaper ACs. In these studies, it has been shown that high quality ACs can be obtained from biomasses. In their use as catalyst support, the AC surfaces are coated by chemical precipitation or impregnation of the catalyst material. However, it is possible to prepare by impregnation of biomass with direct catalyst material and then pyrolysis. This method will not only reduce production costs, but will also provide catalysts with desired properties. In this study, AC supported Fe-based catalysts were prepared by impregnation method from the waste biomasses mixture by $FeSO_4$ activation and then pyrolysis. Desired catalyst was synthesized by pyrolysis of the chemically activated biomass at impregnation ratio of 20:40 at 700°C for 60 minutes in CO_2 atmosphere. The surface area, total pore volume and pore diameter were found to be 375.28 m^2/g, 0.2391 cm^3/g and 2.5486 nm, respectively. It has been found that iron having catalytic effect is transformed into magnetite crystal structure having chemical formula of $Fe_{2.9}O_4$. The results showed that cheaper catalysts with desired surface properties can be obtained by the proposed method.

Keywords: *Activated carbon, biomass, catalyst, ferrous, support material*

1. INTRODUCTION

Activated carbon (AC) also called activated charcoal, activated coal or carbo activatus is the most well-known form of carbon as catalyst or catalyst supports. AC is a type of amorphous carbon that has been processed to make it extremely porous and thus to have a very large surface area available for adsorption or chemical reactions [1,2]. Nowadays AC is mainly employed in filtering air and gases, wastewater treatment, removal of liquid-phase contaminants, including organic pollutants, heavy metal ions, organic dyes and as catalyst support [1]. ACs can be prepared from any carbon-containing raw material, including bituminous coal and lignite, from which a large part of the ACs on the market is produced [3]. The use of waste and inexpensive materials for the synthesis of porous carbons has attracted the considerable attention of researchers towards utilisation of carbon in a variety of processes. The use of biomass wastes for preparing activated porous carbon materials has enhanced considerably in the last years [4,5]. Low-cost, quite abundance, renewability, and high lignocellulosic content of agricultural biomass make them promising precursors for cost-effective activated carbons. Fruit stones are of particular interest for their generation as by-products from food processing industries, in amounts sufficient for obtaining good adsorbing carbons with appreciable hardness and better porous structure [6]. Biomass wastes such as olive stones [7,8], peach stones [9]-[11], apricot stones [12,13], cherry stones [14,15], grape stones [16,17], chestnut shell [18] and date stones [19,20] have been effectively utilized as precursors for production of activated carbons. They are produced from these kind of precursors by physical and/or chemical activation methods. Chemical activation methods are widely used to produce ACs with larger surface area and desired surface properties. In the chemical activation, precursor is impregnated with a convenient chemical activator such as KOH, K_2CO_3, NaOH, Na_2CO_3, $AlCl_3$, $ZnCl_2$, $FeSO_4$, H_3PO_4 and H_2SO_4 and then pyrolized in an inert atmosphere. They are dehydrating agents that influence pyrolytic decomposition and

[1] *Corresponding author: Firat University, Department of Environmental Engineering, 23200, Elazığ, Turkey.* herdem@firat.edu.tr, erdemhatice23@gmail.com

[2] *Firat University, Department of Environmental Engineering, 23200, Elazığ, Turkey.* merdem@firat.edu.tr

inhibit formation of tar. By the catalytic effect of the activators, macromolecules are fragmented, volatile components formed leave the structure and a carbonaceous material containing activator remains [21, 22]. This shows that AC supported catalyst can be prepared by direct chemical activation of the precursor.

In order to improve their catalytic properties and stability, the active metal component of the catalyst is usually dispersed by impregnation or by precipitation-deposition. Impregnation is a simple technique for insertion of metals into the pore network of the carbon support. In most cases, the precursor metal solution is mixed together with the support carbon materials, and is allowed to enrich the surface with metal centres through contact and evaporation. The mixed solution can be subjected to mixing by methods such as sonication or stirring to ensure maximum metal dispersion in the solution. Then, the material is dried and subsequent heat treatment under inert gas is usually performed to further stabilize the metal catalyst. Because of its simplicity and ease of metal loading control, this is a well-established catalyst preparation procedure, which has been widely reported in the literature [23]. In this study, an AC-supported Fe-based catalyst was firstly prepared from almond and apricot and peach stones by $FeSO_4$ activation and then pyrolysis. The effects of $FeSO_4$:biomass mixture ratio on the catalyst properties were investigated. The synthesized catalysts were characterized by surface area, total pore volume, pore diameter, pH_{pzc}, Boehm titration, SEM, EDS, XRD and VSM analysis.

2. MATERIAL AND METHODS

2.1. Materials

In the study; in the production of activated carbon which will be used as catalyst support material, the triple biomass mixture prepared from almond and apricot and peach stones was used as raw material. These products were purchased from agricultural markets. After the products were supplied, they were washed first with tap water and then with demineralized water and dried for three days at 80ºC. The dry samples were milled in a knife grinder and sieved to prepare the -30+50 mesh fraction (0.3-0.5 mm) for use in the experiments. The dry samples classified were homogenized by mixing in 1/1/1 ratios and stored in jars with lids for use [24].

The catalyst was prepared by chemical activation of the related raw material with the salt of the metal to be filled followed by pyrolysis. For this purpose, $FeSO_4.7H_2O$ (Merck, 1.03965) salt was used as chemical activator and pure CO_2 gas was used to form inert environment in pyrolysis experiments. HCl (Merck, 10.0317) ve NaOH (Merck, 10.6462) for adjusting the pH of the solutions; HCl, NaOH, $NaHCO_3$ (Carlo Erba, 478537), Na_2CO_3 (Merck, 10.6392) and phenolphthalein indicator for Boehm titration were used.

2.2. Catalyst Preparation

In the study, the activated carbon supported iron-based catalyst was prepared by chemical activation of the related raw material with the salt of the metal to be filled, followed by pyrolysis. For this purpose; the triple biomass mixture with -30+50 mesh fraction was activated with $FeSO_4$ solution at 25 °C for 24 hours to provide different triple biomass mixture/$FeSO_4$ ratios. At the end of the 24 hour, the mixtures were dried in an oven at 105 °C, the dried samples were filled into a sealed stainless steel reactor as shown in Fig. 1, and the reactor was placed in a muffle furnace. In order to remove the air in the reactor before pyrolysis and thus to form an inert environment to prevent combustion, pure CO_2 was passed through the system for a flow rate of 2.5 L/min. Then, the furnace was operated, the temperature of the furnace was adjusted to operating temperature and the carbonization processes were carried out for 60 min at the same CO_2 flow rate. At the end of this process, the furnace was closed and the reactor was allowed to cool under inert gas flow.

2.3. Catalyst Characterization

Textural properties such as surface area, total pore volume and pore size of the catalysts synthesized were investigated by nitrogen adsorption analysis at 77 K using Micromeritics ASAP 2020 analyzer. The surface area was determined according to BET (Brunauer-Emmett-Teller) method. The total pore volume (V_T) was derived from the amount of N_2 adsorbed at relative pressure (P/P°) of 0.99. The pore size was calculated from the relation $4V_T$/BET-surface area. The morphology and chemical composition of the representative catalyst were investigated by using JEOL-JSM-6510 scanning electron microscopes (SEM) coupled with EDS.

The magnetic property of the sample was measured on a vibrating sample magnetometer at room temperature under a magnetic field ranging from -8000 to 8000 Oe. (VSM; Versalab, Quantum Design Company, USA). The X-ray diffraction (XRD) pattern of the sample was obtained on Rigaku Ultima IV. Diffraction intensities were measured between 3 and 90° 2θ with increments of 0.02° at 1 deg/min scan speed, 40 kV and 30 mA. The main surface functional groups on the catalyst were gravimetrically analyzed with Boehm's titration [25]. The

pH of zero point of charge, pHzpc, of the activated carbon supported Fe-based catalyst was measured by using drift method described by Lopez-Ramon et al. [26].

Figure 1. Reactor and muffle furnace for pyrolysis experiments

3. RESULTS AND DISCUSSION

3.1. Effect of Impregnation Ratio

The cost of catalysts will vary depending on the catalyst used and the preparation techniques. The aim is to prepare an effective catalyst with desired surface area. Therefore, it was tried to determine the conditions in which the largest surface area catalyst was obtained with the lowest amount of activator. Effect of activator dosage on the textural properties of the catalyst was investigated by changing the weight ratio of $FeSO_4$/ biomass mixture in the range of 5/40 – 60/40. By the increasing impregnation ratio from 5/40 to 20/40, specific surface area of the catalyst increased from 273.98 to 375.28 m2/g. The total pore volume increased in the same trend. But, both surface area and total pore volume decreased over the weight ratio of $FeSO_4$/ biomass mixture of 20/40. In the impregnation ratio was greater than 20/40, precursor surfaces coated with a thick activator layer. These layers prevented volatile components from moving away from the mass during pyrolysis and thus surface areas of the catalysts could not expand. Therefore, it can be said that the catalyst obtained at the $FeSO_4$/biomass mixture ratio of 20/40 is the most suitable catalyst.

Table 1. Properties of activated carbon supported Fe-based catalyst

$FeSO_4$/Biomass mixture ratio	**BET-Surface Area, m^2/g**	**Total Pore Volume cm^3/g**	**Pore Diameter, nm**
5/40	273.98	0.1682	2.5765
10/40	294.74	0.1705	2.5265
20/40	375.28	0.2391	2.5486
30/40	269.58	0.1296	2.3862
40/40	251.52	0.1456	2.3159
50/40	262.83	0.1543	2.3117
60/40	251.23	0.1432	2.2804
80/40	216.98	0.1301	2.3981

3.2. Surface Functional Groups of the Catalyst

The types and amounts of surface functional groups in the catalyst were determined by Boehm's titration method. The amounts of carboxylic, lactonic and phenolic groups (acidic surface groups) were determined by neutralizing with $NaHCO_3$, Na_2CO_3 and NaOH solutions. The total basic group content was determined by the titration with HCl solution. Table 2 shows the surface functional groups of the catalyst determined by Boehm titration. When the values in Table 2 are examined, it was seen that acidic functional groups were dominant on

the catalyst surface. In particular, it was determined that the phenolic and lactonic groups were high in quantity and the total acidic functional groups were almost twice the total basic groups in Fe-based catalyst.

Table 2. Boehm results of activated carbon supported Fe-based catalyst

Asidic Groups, mesg/g				Total Basic Groups, mesg/g
Phenolic	**Lactonic**	**Carboxylic**	**Total Acidic**	
0.1944	0.2103	0.0628	0.4675	0.2315

The pH of zero point of charge (pH_{zpc}) corresponds to the pH value at which the net surface charge of the catalyst becomes electrically neutral. The experimental results of pH_{zpc} determination are shown in Fig. 2. At $pH < pH_{zpc}$, the catalyst surface becomes positively charged, while at $pH > pH_{zpc}$, the catalyst surface is negatively charged. The point at which the curve cut off the apse gives the pH_{zpc} of that catalyst. Accordingly, it can be seen that the pH_{zpc} value for the catalyst is 5.4. This result is consistent with the surface functional groups determined by Boehm titration. When the obtained pH_{zpc} value and surface functional groups are compared, it can be said that the dominant of acidic surface functional groups causes the acidic pH_{zpc} value.

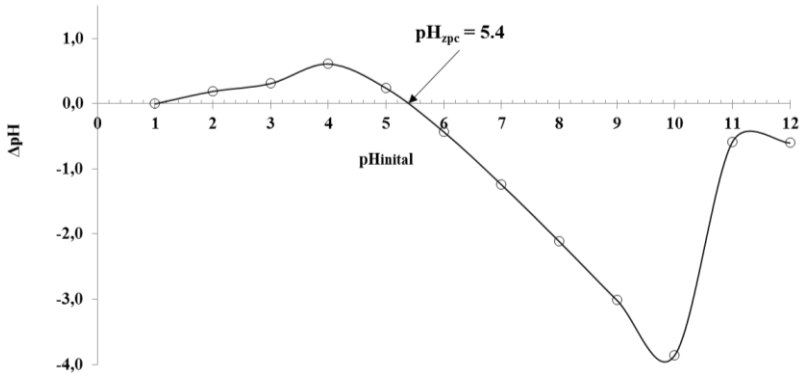

Figure 2. pHzpc value of activated carbon supported Fe-based catalyst

3.3. XRD Analysis of the Catalyst

The catalyst was subjected to XRD analysis to determine the crystalline form of iron in the catalyst, which would exhibit the actual catalytic effect. Fig. 3 shows the XRD pattern of the Fe-based catalyst. $FeSO_4$ salt was used for Fe-based catalyst production in the process of converting lignocellulosic biomass into activated carbon during the activation of the triple biomass mixture and thus dispersing to each point in the structure and synthesizing large surface area catalyst. The XRD result shows that the pyrolysis process carried out under inert carbon dioxide breaks down the structures of this salt and that the Fe-based catalyst transforms the iron to a magnetite crystal structure with only $Fe_{2.9}O_4$ chemical structure. It was also observed that there were no other crystal structures in the catalyst.

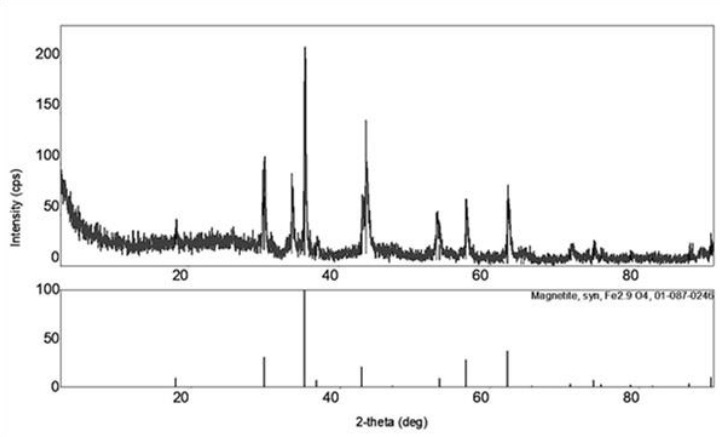

Figure 3. XRD graph of activated carbon supported Fe-based catalyst

3.4. SEM Analysis of the Catalyst

In order to determine the morphological structure of the catalyst, SEM analysis and EDX results of the surface chemical composition and the obtained image is shown in Fig. 4. From the SEM image, it can be seen that the catalyst has a very rough and porous structure. On the other hand, EDX analysis showed that iron and carbon, one of the main components determined by XRD analysis, were found to be 77.57% and 10.02% in the catalyst structure, respectively. Since there is no iron loss in the applied processes, all iron used for activation remains trapped in the active carbon skeleton.

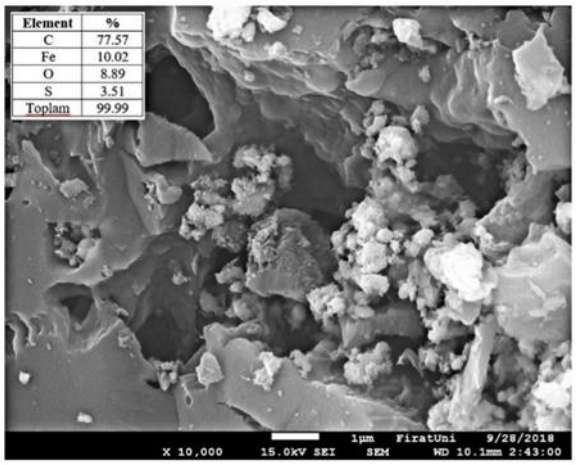

Figure 4. SEM image of activated carbon supported Fe-based catalyst

3.5. Magnetic Characteristic of the Catalyst

The magnetic properties of the catalyst were investigated using VSM analysis at room temperature, on the magnetic field range from -8000 to 8000 Oe. The hysteresis cycle of the catalyst is presented in Fig. 5. In the VSM analysis of the synthesized catalyst, it was determined that the iron having the catalytic effect and magnetic properties gained magnetic properties by binding to the structure. Fe-based catalyst has high magnetic saturation values. The fact that an external magnet applied to the aqueous mixtures containing the catalysts also collects almost all solid particles indicates that the catalysts can be easily separated from the mixture by magnetic separation

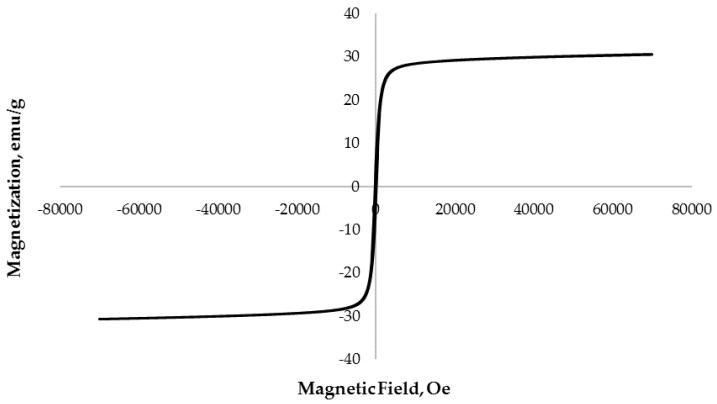

Figure 5. VSM graph of the activated carbon supported Fe-based catalyst

4. CONCLUSIONS

The results showed that the carbonization temperature and impregnation ratio have significant effect on the surface area and pore structure of the catalyst. The optimum conditions for preparing the catalyst having the highest surface area were found to be a carbonization temperature of 700°C, time of 60 min and $FeSO_4$/biomass ratio of 20/40. The surface area, total pore volume and pore diameter were found to be 375.28 m^2/g, 0.2391 cm^3/g and 2.5486 nm, respectively. It was found that the triple biomass mixture from almond and apricot and peach stones was effective precursors for the activated carbon supported Fe-based catalyst production. The catalyst obtained is very promising because it is cost-effective and has a large surface area.

ACKNOWLEDGMENT

This study was financially supported by The Scientific and Technological Research Council of Turkey (TUBITAK) [Project number: 117Y300].

REFERENCES

[1]. L.J. Konwar, J. Boro, D. Deka, "Review on latest developments in biodiesel production using carbon-based catalysts", Renewable and Sustainable Energy Reviews, 29, 546-564, 2014.
[2]. R.V. Quah, Y.H. Tan, N.M. Mubarak, M Khalid, E.C. Abdullah, C. Nolasco-Hipolitod, "An overview of biodiesel production using recyclable biomass and nonbiomass derived magnetic catalysts", Journal of Environmental Chemical Engineering, 7, 103219, 2019.
[3]. A. Rusanen, R. Lahti, K. Lappalainen, J. Kärkkäinen, T. Hu, H. Romar, U. Lassi, "Catalytic conversion of glucose to 5-hydroxymethylfurfural over biomass-based activated carbon catalyst", Catalysis Today, Available online 18 February 2019
[4]. M. Daoud, O. Benturki, P. Girods, A. Donnot, S. Fontana, "Adsorption ability of activated carbons from Phoenix dactylifera rachis and Ziziphus jujube stones for the removal of commercial dye and the treatment of dyestuff wastewater", Microchemical Journal, 148, 493-502, 2019.
[5]. D. R. Lima, A. Hosseini-Bandegharaei, P.S. Thue, E.C. Lima, Y.R.T. de Albuquerque, G.S. dos Reis, C.S. Umpierres, S.L.P. Dias, H.N. Tran, "Efficient acetaminophen removal from water and hospital effluents treatment by activated carbons derived from Brazil nutshells", Colloids and Surfaces A: Physicochemical and Engineering Aspects, Volume 583, 123966, 20 December 2019.
[6]. M.J. Ahmed, "Preparation of activated carbons from date (*Phoenix dactylifera L.*) palm stones and application for wastewater treatments: Review", Process Safety and Environmental Protection, 102, 168-172, 2016.
[7]. N. Bader, U. Sager, U. Schneiderwind, A. Ouederni, "Foam and granular olive stone-derived activated carbons for NO_2 filtration from indoor air", Journal of Environmental Chemical Engineering, 7, 103005, 2019.
[8]. Z. Rajah, M. Guiza, R.R. Solís, N. Becheikh, F.J. Rivas, A. Ouederni, "Clopyralid degradation using solar-photocatalytic/ozone process with olive stone activated carbon", Journal of Environmental Chemical Engineering, 7, 102900, 2019.
[9]. J.J. Arroyo-Gómez, D. Villarroel-Rocha, K.C. de Freitas-Araújo, C.A. Martínez-Huitle, K. Sapag, "Applicability of activated carbon obtained from peach stone as an electrochemical sensor for detecting caffeine", Journal of Electroanalytical Chemistry, 822, 171-176, 2018.
[10]. F. Khemmari, K. Benrachedi, "Valorization of peach stones to high efficient activated carbon: Synthesis, characterization, and application for Cr (VI) removal from aqueous medium", Energy Sources, Part A: Recovery, Utilization, and Environmental Effects, 1-12, 2019.
[11]. M. Martin-Martinez, S. Álvarez-Torrellas, J. García, A.M.T. Silva, J.L. Faria, H.T. Gomes, "Exploring the activity of chemical-activated carbons synthesized from peach stones as metal-free catalysts for wet peroxide oxidation", Catalysis Today, 313, 20-25, 2018.
[12]. B. Petrova, T. Budinova, B. Tsyntsarski, V. Kochkodan, Z. Shkavro, N. Petrov, "Removal of aromatic hydrocarbons from water by activated carbon from apricot stones" Chemical Engineering Journal, 165, 258-264, 2010.
[13]. A.M. Youssef, N.R.E. Radwan, I. Abdel-Gawad, G.A.A. Singer, "Textural properties of activated carbons from apricot stones" Colloids and Surfaces A: Physicochemical and Engineering Aspects, 252, 143-151, 2005.
[14]. D. Angin, 2014. Production and characterization of activated carbon from sour cherry stones by zinc chloride. Fuel 115, 804-811.
[15]. M. Olivares-Marín, C. Fernández-González, A. Macías-García, V. Gómez-Serrano, "Preparation of activated carbon from cherry stones by physical activation in air. Influence of the chemical carbonisation with H_2SO_4", J. Anal. Appl. Pyrolysis, 94, pp. 131-137, 2012.
[16]. I. Okman, S. Karagoz, T. Tay, M. Erdem, "Activated carbons from grape seeds by chemical activation with potassium carbonate and potassium hydroxide", Appl. Surf. Sci., 293, pp. 138-142, (2014),
[17]. D. Jimenez-Cordero, F. Heras, N. Alonso-Morales, M.A. Gilarranz, J.J. Rodríguez, "Preparation of granular activated carbons from grape seeds by cycles of liquid phase oxidation and thermal desorption", Fuel Processing Technol., 118 (2014), pp. 148-155
[18]. D. Ozcimen and A. Ersoy-Mericboyu, "Removal of copper from aqueous solutions by adsorption onto chestnut shell and grapeseed activated carbons", Journal of Hazardous Materials 168, 1118-1125, 2009.
[19]. B.H. Hameed, J.M. Salman, A.L. Ahmad, "Adsorption isotherm and kinetic modeling of 2,4-D pesticide on activated carbon derived from date stones", Journal of Hazardous Materials, 163, 121-126, 2009.

[20]. G. Yamina, A. Abdeltif, T. Youcef, H.M. Mahfoud, G. Fatiha, B. lotfi "A comparative study of the addition effect of activated carbon obtained from date stones on the biological filtration efficiency using sand dune bed", Energy Procedia, 36 (2013), pp. 1175-1183

[21]. J.M. Dias, M.C.M. Alvim-Ferraz, M.F. Almeida, J. Rivera-Utrilla, M. Sánchez-Polo, "Waste materials for activated carbon preparation and its use in aqueous-phase treatment: a review", Journal of Environmental Management, 85,4, 833-846, 2007.

[22]. M.A.Yahya, Z. Al-Qodah, C.W.Z. Ngah, "Agricultural bio-waste materials as potential sustainable precursors used for activated carbon production: A review", Renewable and Sustainable Energy Reviews, Volume 46, 218-235, 2015.

[23]. Y. Yang, K. Chiang, N. Burke, "Porous carbon-supported catalysts for energy and environmental applications: A short review", Catalysis Today, Volume 178, Issue 1, Pages 197-205,15 December 2011.

[24]. O. Akcakal, M. Sahin and M. Erdem, "Synthesis and characterization of high-quality activated carbons from hard-shelled agricultural wastes mixture by zinc chloride activation", Journal Chemical Engineering Communications, Volume 206, Issue 7, Pages 888-897, 2019.

[25]. H.P. Boehm, (2002). Surface oxides on carbon and their analysis: A critical assessment, Carbon, 40, 145–149.

[26]. M. Lopez-Ramon, F. Stoeckli, C. Moreno-Castilla, and F. Carrasco-Marin, "On the characterization of acidic and basic surface sites on carbons by various techniques", Carbon, 37, 1215–1221, 1999.

ICOEST SARAJEVO
5TH INTERNATIONAL CONFERENCE ON ENVIRONMENTAL SCIENCE AND TECHNOLOGY
October 09-13 2019

Effect of Sunflower Seed Shells Ash on Properties of Self-compacting Concrete

Sandra Juradin[1], Ivanka Netinger Grubeša[2], Nives Ostojić-Škomrlj[3], Ivana Rušinović[4]

Abstract

There are numerous researches in the field of civil engineering that attempt to find a possible application of biomass ash. The purpose of this study is to investigate the possible use of the sunflower seed shells ash as powder material in self-compacting concrete. Four mixtures of self-compacting concrete have been made and tested. In all the mixtures there were equal amounts of cement, the total amount of fines, additives and aggregates. The water to binder ratio is maintained 0.55 for all mixtures. The reference mixture is made with cement, silicate fume and stone powder. In two mixtures, a part of the stone powder was replaced with the sunflower seed shells ash and in the last mixtures, silica fume was replaced with fly ash. Mixtures were tested for air content and workability of the fresh concrete is determined by using V funnel method, slum flow, T 500, L - box, and visual check of stability. The dynamic modulus of elasticity and compressive strength were tested after 7 and 28 days. According to the obtained results, the higher ash content of the sunflower seed shells reduces the mechanical properties of the concrete and in the fresh state affects on the setting time. The workability depends on the ratios and types of powders. Specimens of lime mortar with the addition of sunflower seed shells ash were also made. The obtained results do not indicate that sunflower seed shells ash has pozzolanic activity.

Keywords: sunflower seed shells ash, self-compacted concrete, workability, mechanical properties, pozzolanic activity

1. INTRODUCTION

The wide-ranging research works have been successfully carried out to integrate biomass in concrete or mortar. The origin of biomass can be wood biomass, agricultural biomass and biomass from waste. The use of agricultural biomass in industry produces large quantities of ash as a waste. That is an ecological problem but, on the other hand, that is also cheap and easily accessible material [1] - [3].

According to [4], the wood ash as a replacement part of cement in concrete reduces the workability of concrete. Cuenca et al. [5] used olive residue biomass fly ash as filler in self-compacting concrete. The strengths obtained were the same or even greater than the strength of the control mixture. Sua-iam et al. [6] used the blends of Portland cement with residual rice husk ash and limestone powder to improve the fresh and mechanical properties of self-compacting concrete. Their mixture of SSC resulted in greater mechanical properties than the conventional SCC. Krishnasamy and Palanisamy [7] investigated bagasse ash and rice husk ash as cement replacement in self-compacting concrete. Their results were used as the basis for defining three optimum cement replacement mix proportions, for several structural applications. Frías et al. [8] incorporated 10 and 20 percentages by mass of Bamboo Leaves Ash in concrete and noted a small reduction in compressive strength on the 7th day compared to controlled reference concrete.

[1] *Corresponding author: University of Split, Faculty of Civil Engineering, Architecture and Geodesy, Matice hrvatske 15, 21000 Split, Croatia* sandra.juradin@gradst.hr

[2] *University Josip Juraj Strossmayer of Osijek, Faculty of Civil Engineering, Vladimira Preloga 3, Osijek, Croatia,* nivanka@gfos.hr

[3] *University of Split, Faculty of Civil Engineering, Architecture and Geodesy, Matice hrvatske 15, 21000 Split, Croatia,* nives.ostojic@gradst.hr

[4] *University of Split, Faculty of Civil Engineering, Architecture and Geodesy, Matice hrvatske 15, 21000 Split, Croatia* ivana.rusinovic@gmail.com

Sunflower seed shells are used as fuel in oil factory Čepin in Croatia and per one year about 84 t of ash is generated. The possible use of this ash as a partial replacement for cement in concrete and mortar were investigated in [2], [3], [9] and [10]. The authors in [3] recommended the replacement of up to 5 % of cement mass with sunflower seed shells ash in concrete because a higher ash content decreases the compressive strength of concrete. This study investigate the possibility of applying this ash as a partial replacement for limestone powder in self compacted concrete.

2. EXPERIMENTAL PART

2.1. Materials and methods

For the purpose of testing the effect of sunflower seed shells ash on the properties of self-compacting concrete, four mixtures were made. Cement CEM I 42.5 R (3.14 kg/dm^3), crushed limestone aggregate (2.68 kg/dm^3) and liquid PCE (poly-carboxylic-ether) superplasticizer (1.05 kg/dm^3) were used for all mixtures and in equal quantities. The fractions of the aggregate were 0-4, 4-8 and 8-16 mm, with grain-size distribution curves are shown in Figure 1. Admixtures for concrete were fly ash (2.25 kg/dm^3), silica fume (2.2 kg/dm^3), limestone powder (2.7 kg/dm^3) and sunflower seed shells ash (2.4 kg/dm^3). The total sum of admixtures for all mixtures was the same. Water-binder ratio was 0.55. The reference mixture (E) was made with cement, silicate fume (10% of the cement mass) and limestone powder. Two concrete mixtures (S5 and S10) with different shares of limestone powder replacement by sunflower seed shells ash (SSSA) were prepared. Replacement was 19.5 and 39% in value from the mass of limestone powder, corresponding to 5 and 10% by weight of cement, respectively. The mixture FA was made like S10, with the difference that silica fume has been replaced with fly ash. The composition of the mixtures is given in Table 1.

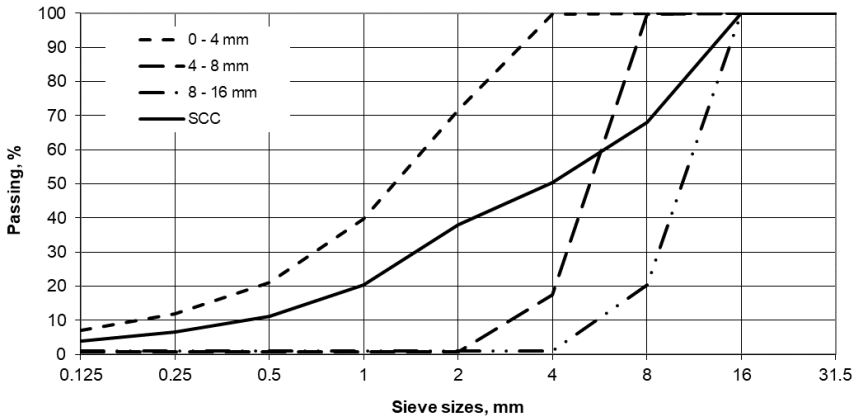

Figure 2. Grain-size distribution curves of aggregate fractions and concrete

Table 2. Mixture compositions

Mixture	Cement (kg)	w/b	Silica fume (kg)	Limestone powder (kg)	Fly Ash (kg)	Sunflower seed shells ash (kg)	Admixture (kg)	Aggregate (kg)		
								0-4 mm	4-8 mm	8-16 mm
E	363	0.55	36.3	93.5	-	-	5.9	768.30	153.66	614.64
S5	363	0.55	36.3	75.35	-	18.15	5.9	767.20	153.44	613.76
S10	363	0.55	36.3	57.2	-	36.3	5.9	766.05	153.21	612.84
FA	363	0.55	-	57.2	36.3	36.3	5.9	766.55	153.31	613.24

The solids components of mixtures were dry mixed in the laboratory pan mixer for about 1 min. After that, the mixture of water and superplasticizer were added and the wet mixing was done for 5 min.

2.2. Test results of fresh concrete

The mixtures were tested for workability in fresh state. The workability of mixtures was examined on specimens using the slump-flow method, visual check of stability, T500 time and with V-funnel. The passing ability of

concretes was determined using the L - box test. Results were selected according to the specifications that meet the requirements of EFNARC guidelines [11].

Table 2. V-funnel, T500 and slump-flow results, passing ability and classification according to EFNARC[11]

Mixture	V-funnel (s)		T500 (s)		Slump-flow (mm)		L-box (PL)	
	measured	Class	measured	class	measured	class	measured	class
E	7.35	VF1	1.33	VS1	655	SF2	0.8	PL2
S5	20.34	VF2	2.48	VS2	670	SF2	0.7	-
S10	5.75	VF1	2.04	VS2	580	SF1	0.5	-
FA	23.26	VF2	2.95	VS2	697.5	SF2	0.8	PL2
EFNARC min	6		2		650		0.8	
EFNARC max	12		5		800		1	

Figure 2. (a) Mixture S10 – slump-flow

(b) Mixture FA – slump-flow

Figure 3. (a) Mixture S5 – slump-flow

(b) Mixture E – L-box

The three mixtures (E, S5 and FA) achieved slump flow values around 675 ± 20 mm and S10 achieved the lowest slump flow value, Figure 2(a). Acceptable range for SCC is from 650 to 800 mm according to EFNARC and the mixtures E, S5 and FA achieved that requirement, table 2, Figure 2(b) and Figure 3(a). The mixtures with the highest SSSA content (S10 and FA) achieved the lowest and the highest slump flow values. During the slump flow test, the time required to reach the 500mm diameter was also measured and recorded as T500 where a lower flow time indicates greater flow ability. Only the control mixture had T500 time under the EFNARC requirement, while S5, S10 and FA had properly time. The V-funnel flow time for S10 mixtures was less that time for the control mixture E while the values for S5 and FA exceeded time of 20 seconds. Again, the mixtures with the highest SSSA content (FA and S10) achieved the lowest and the highest flow time values. L-box test is used to measure the filling and passing ability of SCC. A blocking ratio between 0.8 and 1.0 is considered appropriate according to EFNARC because there is a risk of blocking when the L-box ratio is below 0.8. Only mixtures E and FA achieved that requirement, Figure 3(b).

The density of SCC was tested based on EN 12350-6, air content was tested based on EN 12350-7, and temperature was tested with digital thermometer after workability testing, Figure 4. The fresh SCC properties are listed in Table 3. Stone powder replacement with SSSA did not significantly influence the density of concrete but mixture with 10 % of SSSA had evidently increased air content in mixture S10 and decreased in FA.

Figure 4. Mixture FA – air content

Table 3. Properties of fresh concrete

Mixture	Temperature, °C	Air content, %	Density, kg/m^3
E	22.2	1.2	2.360
S5	22.8	1.4	2.365
S10	22	4.2	2.325
FA	22.5	0.8	2.379

All specimens were cast in cubes of 15 cm. The specimens of mixture E were extracted from the molds 24 hours after the casting and the specimens of other three mixtures were extracted from the molds about 4 days after casting. The specimens containing the sunflower seed shells ash were later removed from the mold because the cement had not finished setting time in the first 24 hours. According to research in [3] the content of MgO in SSSA exceeds the proposed values in CEN EN 450 – 1, Fly ash for concrete (Part 1) and high percentage of MgO retards the initial hydration of cement and increases the setting time of cement [7].The same phenomenon was observed in the paper [10]. After extraction, all specimens were placed in a water tank at a temperature of 20 ± 5 °C until taken out for testing. The dynamic modulus of elasticity and the compressive strength were tested on specimens at ages corresponding to 7 and 28 days. The remaining specimens were dried at room temperature to constant weight and tested for water absorption.

3. RESULTS AND DISCUSSION

3.1. Test results of hardened concrete - Dynamic modulus of elasticity

The dynamic modulus of elasticity was determined according to the expression:

$$E_{din} = \frac{v^2\rho(1+\mu)(1-2\mu)}{1-\mu} \quad (1)$$

where: v is mean ultrasonic wave speed (m/s), ρ is concrete density (kg/m^3) and μ is Poisson coefficient (μ = 0.2).

Figure 5 shows the test results of 7-days and 28-days. Two control mixtures E and FA achieved almost the same values after 7 and 28 days. In the case of 28-days, the mixture S5 reached almost the same value as control mixtures. The mixture with 10 % of SSSA (S10) had the lowest values of dynamic modulus of elasticity for all measuring times.

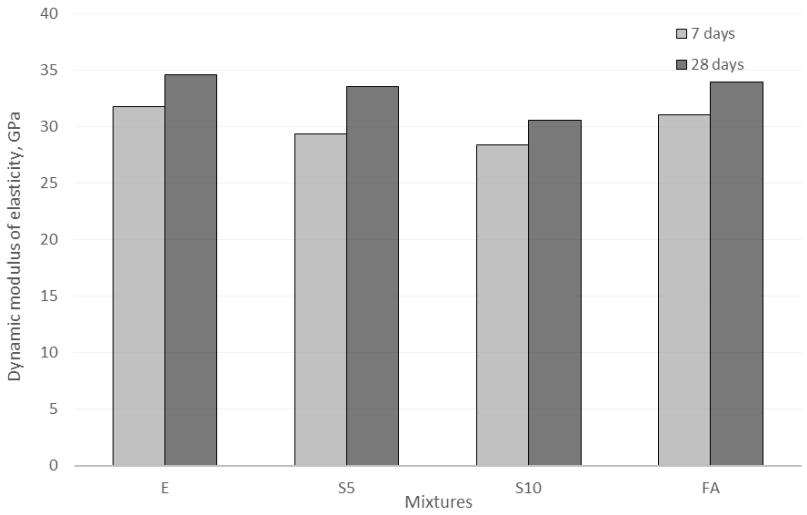

Figure 5. Dynamic modulus of elasticity after 7 and 28 days

3.2. Test results of hardened concrete – Compressive strength

The results of compressive strength based on [12] for 7-days and 28-days are shown in Figure 6.

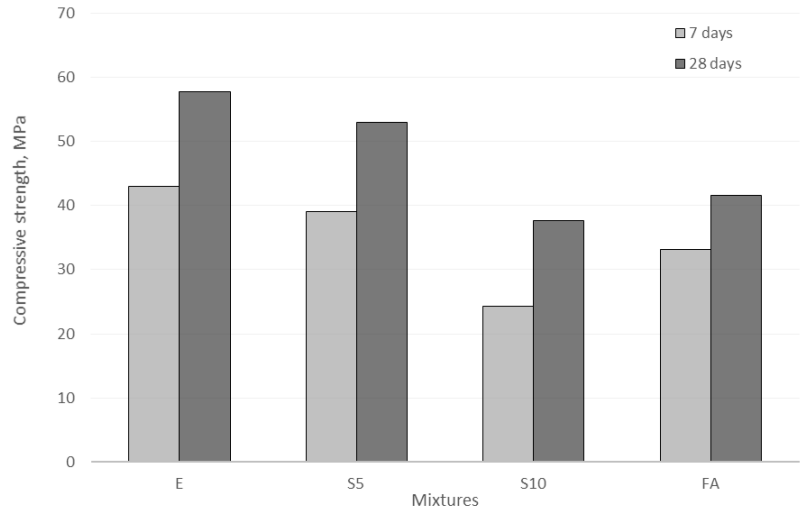

Figure 6. Compressive strength after 7 and 28 days

The maximum compressive strength was (42.98 and 57.67 MPa) obtained for control concrete mixture (E) at 7 and 28 days respectively. Reduction in compressive strength was about 9% (at 7 days) and 8.1% (at 28 days) for concrete mixtures S5. The mixture S10 achieved 24.23 and 37.67 MPa, which represented only 56.4% and 65.3% of control mixture compressive strength. The replacement of silica fume with fly ash (FA) caused a decrease in strength for 23% and 27.9% in regard to control mixture (E) but this mixture achieved 136.6% and 110.4% of compressive strength of mixture S10. Figure 7 shows a cross section of the specimens after testing.

Figure 7. Cross section of the specimens after testing: S5, S10, E and FA

3.3. Absorption

The concrete cube specimens dried to a constant weight at room temperature were exposed to water only on one side and the change in weight was measured after 2, 4, 8, 15, 30, 45, 60 min, and 4 and 24 h. The change in the amount of absorbed water (g) in relation to the initial weight of the sample is plotted with time (min) for measuring period of 24 h in Figure 8(a) and for the first hour in Figure 8(b).

The least water absorption is observed in specimens E while the other samples had an almost identical absorption curve, especially in the first 60 minutes of testing. The mixture S10 exhibited the worst results, considering that the weight increased by only 0.34% in relation to the initial sample weight after 24 h.

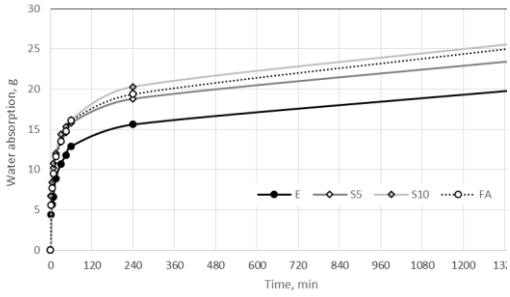

Figure 8. (a) Absorbed water (g) in samples during 24 h - flow

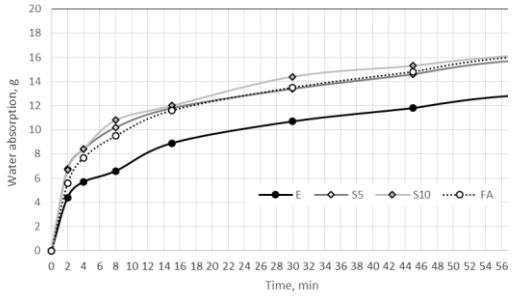

(b) Absorbed water (g) in samples during 1 h

3.4. Lime mortar testing

Some biomass ash have pozzolanic activity so as admixture in concrete can improve property. The pozzolanic activity of material is the ability to react with calcium hydroxide [13]. Three specimens of lime mortar were made for the purpose of determining possible pozzolanic activity of SSSA. Table 4 and Figure 9 list the proportions of all constituents in the mortars. Lime used was CL 80-S. In mixtures SSSAL and SFL 13 % lime was replaced with SSSA and silica fume in regard to the referent lime mortar L. The presented quantities in Table 4 are sufficient for one three gang mold 40x40x160 mm. The mortars were mixed in an automatic mortar mixer with the standard mixing program for cement mortar in accordance with EN 196.

Table 4. Composition of the mortars

Mixture	Lime, g	SSSA, g	Silica fume, g	Water, g	Quartz sand, g
L	460	-	-	350	1380
SSSAL	400	60	-	350	1380
SFL	400	-	60	350	1380

Mortar mixtures were compacted on a vibrating table. The specimens were demolded 96 hours after casting and moved in a storage chamber (20 ± 2 °C and 50 ± 5 % humidity) until testing at the age of 28 days.

The results for relative compressive and flexural strength in the percentage of reference lime mortar strength are shown in Figure 10.

Figure 9. Lime, sunflower seed shells ash and quartz sand

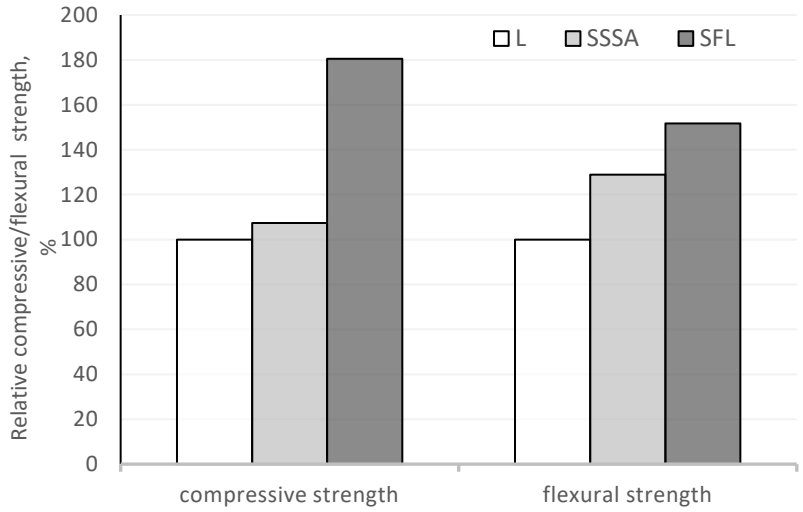

Figure 10. Relative compressive/ flexural/strengths of mortars

The silica fume addition in both cases gave significantly higher strengths than the control mortar mixture, as expected. The mixture with SSSA achieved slightly better results than lime mortar. This result indicate that SSSA does not exhibit pozzolanic activity but it doesn't seem to be completely chemically inert admixture. The same conclusion was reached by Grubeša et al. in [3]

4. CONCLUSION

One disadvantage of self-compacted concrete is its high cost because of high volume of Portland cement and powder materials used to manufacture it. The good way to reduce the cost of SCC is by adding mineral additives such as limestone powder, fly ash or some other similar materials. Limestone powder is obtained by grinding limestone, a material from non-renewable sources. Therefore, the possibility of replacing part of limestone powder with biomass waste such as sunflower seed shells ash was examined in this paper. Based on the test results, it can be concluded:

- The workability of self-compacted concrete depends on the ratios and types of powders.
- Sunflower seed shells ash affects on the setting time of concrete.
- The higher content of the sunflower seed shells ash reduces the mechanical properties of self-compacted concrete. For higher sunflower seed shells ash content, mixture with fly ash has better results than mixture with silica fume.
- The replacement of up to 20% of powder material mass like limestone powder with sunflower seed shells ash is recommended amount.
- Sunflower seed shells ash does not exhibit pozzolanic activity but is not completely chemically inert material.

REFERENCES

[1]. S. Luhar, T.-W. Cheng and I. Luhar, "Incorporation of natural waste from agricultural and aquacultural farming as supplementary materials with green concrete: A review", *Composites Part B* 175 (2019) 107076, Available: https://doi.org/10.1016/j.compositesb.2019.107076

[2]. I. Barišić, I. Netinger Grubeša, T. Dokšanović and B. Marković,, "Feasibility of Agricultural Biomass Fly Ash Usage for Soil Stabilisation of Road Works", *Materials*, 12, 1375, 2019., Available: https://doi.org/10.3390/ma12091375

[3]. I. Netinger Grubeša, M. Radeka, M. Malešev, V. Radonjanin, A. Gojević and R. Siddique "Strength and microstructural analysis of concrete incorporating ash from sunflower seed shells combustion" *Structural Concrete* 20 (1), 396-404, 2019. Available: https://doi.org/10.1002/suco.201800036

[4]. S. Wang, A. Miller, E. Llamazos, F. Fonseca and L. Baxter, "Biomass fly ash in concrete: Mixture proportioning and mechanical properties", *Fuel*, 87, 365–371, 2008

[5]. Cuenca, J., Rodríguez, J., Martín-Morales, M., Sánchez-Roldán, Z., Zamorano, M.: Effects of olive residue biomass fly ash as filler in self-compacting concrete, Construction and Building Materials 40, 702–709, 2013., Available: https://doi.org/10.1016/j.conbuildmat.2012.09.101

[6]. G. Sua-iam, P. Sokrai and N. Makul, "Novel ternary blends of Type 1 Portland cement, residual rice husk ash, and limestone powder to improve the properties of self-compacting concrete", *Construction and Building Materials* 125, 1028–1034, 2016., Available: http://dx.doi.org/10.1016/j.conbuildmat.2016.09.002

[7]. T.R. Krishnasamy and M. Palanisamy, „Bagasse ash and rice husk ash as cement replacement in self-compacting concrete", *GRAĐEVINAR*, 67, 1, 23-31, 2015., Available: https://doi.org/10.14256/JCE.1114.2014

[8]. M. Frías, H. Savastano, E. Villar. MISD Rojas and S. Santos, C"haracterization and properties of blended cement matrices containing activated bamboo leaf wastes" *Cement and Concrete Composites*, 34, 1019–23, 2012., Available: https://doi.org/10.1016/j.cemconcomp.2012.05.005.

[9]. I. Netinger Grubeša, S. Juradin, I. Boko and S. Crnojevac, The effect of ash from sunflower seed husk and Spanish broom on mortar properties// 14th International scientific conference on planning, design, construction and building renewal / Radonjanin, Vlastimir ; Folić, Radomir (ur.). Novi Sad: Departman za građevinarstvo i geodeziju Fakulteta tehničkih nauka, Novi Sad, 2018. str. 144-144

[10]. S Juradin, I. Netinger Grubeša, I. Boko, D. Jozić, D. Dumanić and L. Štraus, The effect of bio-ash from soy, sunflower seed husk and Spanish broom on properties of fresh and hardened mortar, Contemporary Civil Engineering Practice Eco build 2019, Fakultet tehničkih nauka, Departman za građevinarstvo i geodeziju, Novi Sad, 49-56, 2019.

[11]. EFNARC, Specifications and guidelines for self-compacting concrete, in: European Federation of Producers and Applicators of Specialist Products for Structures, 2002,, Available: http://www.efnarc.org/pdf/SandGforSCC.PDF

[12]. EN 196-1:2016 Methods of testing cement. Determination of strength

[13]. M.D.A.Thomas, Supplementary Cementing Materials in Concrete. CRC Press, Boca Raton, FL, 210 pp. 2013.

ICOEST SARAJEVO
5TH INTERNATIONAL CONFERENCE ON ENVIRONMENTAL SCIENCE AND TECHNOLOGY
October 09-13 2019

Biosurfactant Production Using Industrial Wastes from Bacteria which is Natural and Clinical Isolates

Fatih Sezer[1], Fatima Masume Uslu[1], Sadik Dincer[1,2]

Abstract

Many microorganisms synthesize biosurfactants of different structures in different culture environments. Biosurfactants are amphilic compounds capable of reducing surface and internal surface tension between solids, liquids and gases. In this study, production of biosurfactant was be carried out using waste frying oil and corn steep liquor by bacillus sp. isolated from soil, clinical isolates Pseudomonas aeruginosa and Escherichia coli. These bacteria were incubated for 72 hours at 37 °C in the corn steep liquor(CSL) and LB broth containing 5% waste oil. Then, these produced biosurfactants were detected by oil spreading technique. All samples with a zone diameter exceeding 1.5 cm were considered positive. Biosurfactant from bacillus sp. incubated in the oil waste has showed 8.6 cm zone diameter which is even higher than tween 80 used as a control. Surface tension of biosurfactants were determined using pendant drop method. It has been determined that the biosurfactants obtained can reduce the surface tension range %23.6 to %44.8 for vegetable oil waste and range to %3 to 18% for corn steep liquor. As a result, it is shown that industrial wastes are appropriate growth mediums for biosurfactant production from microorganisms.

Keywords: *Bacillus, Biosurfactant. industrial waste, Pseudmonas, Escherichia coli*

1. INTRODUCTION

Biosurfactants are chemicals which have both hydrophilic and hydrophobic groups that are synthesized by microorganisms in the cell membrane and released outside the cell and act on the interfaces. It is used in many industrial fields such as food, cosmetics, pharmaceutical, petroleum industry and environmental technologies due to their properties that increase the solubility and biodegradability of hydrophobic pollutants and emulsion properties [1].

Environment pollution with hydrophobic hydrocarbons is serious problem that requires development of efficient strategies that would lead to bioremediation of contaminated areas. One of the common methods used for enhancement of biodegradation of pollutants is the addition of biosurfactants [2]. Especially when they are released into the environment as extracellular emulsify hydrocarbons and when they are located in the structure of the cell wall facilitate the penetration of hydrocarbons periplasmic surface. For these reasons, the use of biosurfactants comes to the forefront [3].

In this study, production of biosurfactant was be carried out using waste frying oil and corn steep liquor by *Bacillus* sp. isolated from soil, clinical isolates *Pseudomonas aeruginosa* and *Escherichia coli* strains.

2. MATERIALS AND METHODS.

2.1. Microorganisms

Bacillus sp. used in the study was isolated from soil samples were collected from different regions of the Cukurova University campus.

For the isolation of *Bacillus* spp. strains, 5 g from each soil samples were weigthed and homogenized in 10 ml serum physiologic by vortexing then, soil suspension were incubated for 15 min at 85 ° C to eliminate non-

[1] *Cukurova University, Science and Letter Faculty,Biology Department, Balcalı/ADANA, Turkey*

[2] *Corresponding author: sdincer@cu.edu.tr*

spore forming bacteria. At the end of the incubation, 100 µl from each samples were seeded onto nutrient agar plate by spread method and incubated for 24 hours at 37 ° C. Colonies grown on nutrient agar were selected and identified as *Bacillus* sp. by gram stain and biochemical tests.

Pseudomonas aeruginosa and *Escherichia coli* strains used in the study were obtained from the Balcali Hospital of Cukurova University. In the former studies it was determined that the strains have high hemolytic activity.

In order to detect biosurfactant producing *Bacillus* sp., the isolates were planted on blood agar and incubated at 37 ° C for 2-7 days to see if there was hemolytic activity. [4] The strains with hemolysis zone formed around the colonies at the end of incubation were evaluated as biosurfactant positive.

2.2. *Biosurfactant Production*

Biosurfactant production was carried out on rotary shaker incubator at a volume of 150 mL in conical flasks of 250 mL for 72 hours at 37 °C and 150 rpm . The growth medium were, for each bacteria both Corn Steep Liquor (CSL) and LB broth containing 5% waste oil.

2.3. *Biosurfactant Extraction*

Precipitation method with ethyl acetate was used for biosurfactant extraction. In this method, at the end of the incubation period, the cells were removed by centrifugation.The pH of the clear fraction was adjusted to 2.0 with 6 M HCl and taken to the separating funnel and an equal amount of ethyl acetate was added. The mixture was shaken for several minutes until phase separation occurred. The organic phase was removed and the process was repeated 3 times. The organic fractions were then combined and treated with anhydrous sodium sulfate to remove water. After the water was removed, it was concentrated on a rotary evaporator to obtain biosurfactant extract [5].

2.4. *Oil Spreading Technique*

Presence of biosurfactant produced determination by oil spreading technique. 25 mL of distilled water was added to petri dishes (9 cm in diameter) and 10 µL of crude oil was dropped into the middle of the water with a plastic pipette then, 10 µL supernatant was dropped in the middle of the dispersed oil and formed zone diameter was measured [6,7].

2.4. *Surface Tension*

Surface tension were determined using Optical Contact Angle / Surface Tension Meter (TD1C LAUDA) by Du Nouy ring method. [8].

3. RESULTS AND DISCUSSION

3.1. Hemolytic Activity

Hemolysis activity of *bacillus* strain selected for using in the study is given in figure 1.

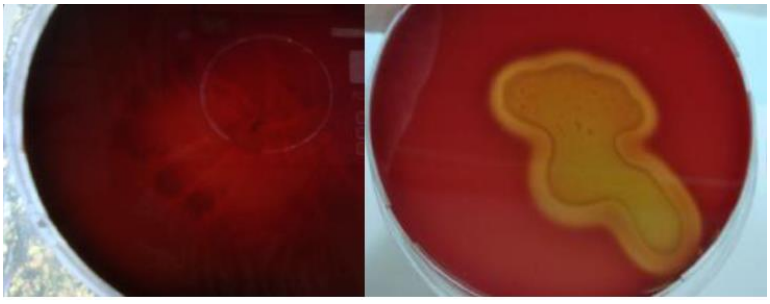

Figure 3.a) uninoculated agar b) hemolysis zone of *bacillus culture*

3.2. Oil Spreading Technique

The results of the determination of the presence of biosurfactant produced by oil spreading technique are shown in Table 1

Table 1. Zone diameters of biosurfactants according to Oil Spreading Technique

	Corn Steep Liquor		Waste Oil	
Incubation time	48 h	72 h	48 h	72 h
Bacillus sp	3 cm	2.5 cm	5 cm	8.6 cm
P. aeruginosa	1 cm	2.5 cm	0.5 cm	5.5 cm
Escherichia coli	1 cm	2.3 cm	3.5 cm	5 cm

Zone diameters formed by tween 80 and tween20 were measured as 8 cm and 7 cm respectively

At the end of 72 h, biosurfactant from *bacillus* sp. that incubated in the oil waste has showed 8.6 cm zone diameter which is even higher than tween 80 and tween 20 used as a control.

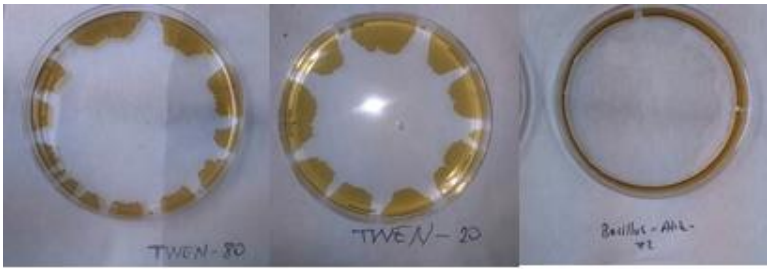

Figure 2. Compariosn of chemical surfactant with biosurfactant from bacillus according to oil spreading capacity

3.3. Surface Tension

The surface tension results measured according to the Du Nouy ring method are shown in table 2. It has been determined that the biosurfactants obtained can reduce the surface tension range %23.6 to %44.8 for vegetable oil waste and range to %3 to 18% for corn steep liquor.

Table 2. Surface tension measurements of biosurfactants

	Waste Oil (mN/m)			Corn Steep Liquor (mN/m)		
	24 h	36 h	72 h	24 h	36 h	72 h
Distile Water	69	69	69	69	69	69
CSL	-	-	-	46,8	46,8	46,8
LB	50,4	50,4	50.4	-	-	-
Bacillus sp.	34,4	29,02	27.8	14,8	41,3	41,7
P. aeruginosa	34,9	37,2	40	45,6	45,7	38,6
E. coli	36,6	38,5	35.4	41,3	46,4	40,6

4. CONCLUSIONS

In today's society, great importance is given to issues such as recycling of wastes, especially recycling them into valuable products.

In this study it is shown that industrial wastes are appropriate growth mediums as inducer for biosurfactant production from bacteria. The synthesis of biosurfactants using microorganisms is a developing field. Microorganisms have been preferred due to easy extraction processes, ability growth on wastes as well as simple production conditions.

In the future studies, it is recommended to investigate the production capabilities of other microorganism species and to make optimization studies of biosurfactant production.

More studies on surface tension reducing properties of produced biosurfactants should be performed.it is also considered that the determination of the chemical structures of the obtained biosurfactants is important for better detection of their usage field.

ACKNOWLEDGMENT

The authors acknowledge to the BAP Unit of Cukurova University for the financial support. The project code is FLY-2017-8708.

REFERENCES

[1]. M. Sumengen, S. Dincer, "Bacillus subtilis kullanilarak atik ekmeklerden alkali proteaz ve biyosurfektan uretimi, " C.U. Fen ve Muhendislik Bilimleri Dergisi ,2016 Cilt:34-6. p:70-79.
[2]. J. Breckling, Ed.,. Kaczorek, E., Pacholak, A., Zdarta, A., & Smułek, W, The impact of biosurfactants on microbial cell properties leading to hydrocarbon bioavailability increase. Colloids and Interfaces, 2018, 2(3), 35.
[3]. M.E. Mercadé, M.A. Manresa, M. Robert M.J. Espuny, C.De. Andrés, J. Guinea, Olive Oil Mill Effluent (OOME). " New Substrate for Biosurfactant Production". Bioresource Technology, 1993, 43, pp. 1-6.
[4]. G.D. Noudeh, M.H. Moshafi, P. Khazaeli, , F. Akef, "Studies on Bioemulsifier Production by Bacillus licheniformis PTCC 1595 " African Journal of Biotechnology, 2010, Vol. 9(3), pp. 352-356
[5]. H. Yin, J. Qiang, Y. Jia, J. Ye, H. Peng, H. Qin, N. Zhang, , B. He, "Characteristics of biosurfactant produced by Pseudomonas Aeruginosa S6 isolated from oil-containing wastewater". Process Biochemistry, 2009, 44, pp.302-308.
[6]. N.H. Youssef, K.E. Duncan, D.P. Nagle, K.N. Savage, R.M. Knapp, M.J. Mcinerney, "Comparison of Methods to Detect Biosurfactant Production by Diverse Microorganisms ". Journal of Microbiological Methods, 2004, 56, 339-347.
[7]. L. Karthik, G. Kumar, K.V.B. Rao, "Comparison of methods and screning of biosurfactant producing marine actinobacteria isolated from nicobar marine sediment " . The IIOAB Journal, 2010, Vol. 1; Issue 2, 34-38.
[8]. F.R. Accorsini, M.J.R. Muttan, E.G.M. Lemas, M. Benincasa, " Biosurfactant production by yeasts using soybean oil and glycerol as low cost substrate ", Brazillian Journal of Microbiology, 2012, 116-125.

ICOEST SARAJEVO
5TH INTERNATIONAL CONFERENCE ON ENVIRONMENTAL SCIENCE AND TECHNOLOGY
October 09-13 2019

Determination of PGPR Properties of Rhizospheric*Pseudomonas* Strains

FatmaAzgin[1], Fatima Masume Uslu[1], IsilUntac Olgun[1], Sadik Dincer[1,2]

Abstract

Plant growth-promoting rhizobacteria (PGPR) are belong to wide range of bacteria species that can enhance plant growth by several mechanisms like phosphate solubilization, siderophore production, pytohormone production etc. In this study, a total of 48 Pseudomonas strains were obtained from rhizosphere layer of agricultural soils. These strains were evaluated for their plant growth promoting traits, including siderophore production and phosphate solubilization. 8 Pseudomonas strains were selected by their performance on the performance of PVK (Pikovskaya) and CAS (Chrome Azurol S) Agar plate. Then, to evaluate the IAA activity, the selected Pseudomonas strains inoculated to LB broth which contains L-Tryptophan (0,5 g L^{-1}) and incubated at 28 ºC for 3 days. The quantitation of IAA production was determined by using Salkowski reagent. The optical density was taken at 530 nm with a spectrophotometer. The results of quantitative analysis were range from 8,48 to 36,88 µg/mL.Pseudomonas sp. 18 was found to be the highest efficient IAA producer.

Keywords: *Indole Acetic Acid, PGPR, Pseudomonas sp., Siderophore*

1. INTRODUCTION

Agricultural systems that use excess input for high yields cause environmental problems and depletion of natural resources. As a result, it is a threat to human health. It is also seen that the rapid increase in production resulting from these chemical applications is gradually decreasing. All these reasons make it necessary to work on sustainable agricultural applications. One of theseapplications rely on microorganisms such as PGPR "Plant Growth promoting Rhizobacteria" is considered a promising strategy to ensure the maintenance and regularity of production without health risk and with less dependence on chemical fertilizers [5].

Plants are always interaction with soil microorganisms (bacteria and fungus) during germination, growth and development. The free-living soil microorganisms live in the rhizosphere of many plant species and have various beneficial effects on the host plant through different mechanisms such as phytohormoneproduction and phosphate solubilization are generally referred to as Plant Growth Promoting Rhizobacteria (PGPR). The PGPRs are contain different genera such as *Azotobacter*, *Acetobacter*, *Serratia*, *Azospirillum*, *Bacillus*, *Chromobacterium*, *Agrobacterium*, *Erwinia*, *Flavobacterium*, *Arthrobacter*, *Micrococcous*, *Paenibacillus*, *Pseudomonas* and*Burkholderia*. The PGPRs enhance plant growth through direct and indirect mechanisms. Direct mechanisms: Phytohormone production, phosphate solubilization, siderophore production, N fixation. Indirect mechanisms:ACC Deaminase activity, antibiotic and antifungal production, Volatile Organic Compounds (VOCs) production, lytic enzymes production, competition[7].

2. MATERIALS AND METHODS

2.1. Isolation of Pseudomonas strains

Rhizospheric soil for bacterial isolation obtained from Cukurova UniversityAgricultural area. Pseudomonas Isolation Agar and GSP Agar were used isolation of *Pseudomonas* sp. strains. Selected *Pseudomonas* ssp. characteristic colony morphology from on the media were tested for PGPR properties: P solubilization and Siderphore production.

2.2. Siderophore Production

[1] *Cukurova University, Science and Letter Faculty, Biology Department, Balcalı/ADANA, Turkey*

[2]*Corresponding author: sdincer@cu.edu.tr*

Siderophore production was shown by the modified of method described by Schwyn and Neilands[1].Preparation of CAS reagent; Sol 1: Dissolve 0.06 g of CAS (Chrome Azurol S) in 50 ml ddH_2O, Sol 2: Dissolve 0.0027 g of $FeCl_3.6H_2O$ in 10 ml of 10 mMHCl, Sol 3: Dissolve 0.073 g of HDTMA (hexadecyltrimethylammonium bromide) in 40 ml of ddH_2O. Sol 1 and Sol 2 are mixed, then mixed Sol 3. 100 ml CAS Reagent and 900 ml Nutrient Agar, which prepare for 1000 ml, was autoclaved in different bottle. Then CAS Reagent and Nutrient Agar was mixed at 50 ºC in sterile cabinet. Siderophore removes iron from the CAS dye, the color changes from blue to yellow/orange.48 *Pseudomonas* strains incubated 48 h at 30 °C.

2.3. Phosphate Solubilization

Qualitative determination of phosphate solubilization was shown on PikovskayaAgar [2].Pikovskaya agar; Glucose10 g/L. $Ca_3(PO_4)_25$ g/L, $(NH_4)_2SO_4$0.5 g/L, NaCl0.2 g/L, $MgSO_4.7H_2O$ 0.1 g/L, KCl0.2 g/L, Yeast extract0.5 g/L, $MnSO_4 \cdot H_2O$ 0.002 g/L, $FeSO_4 \cdot 7H_2O$ 0.002 g/L, Agar 15 g/L. P-solubilization ability was shownby the formation of a halo zone around the colony. 48 *Pseudomonas* strains incubated at 30 °Cfor 5 days.

2.4. IAA Production

The selected 8 *Pseudomonas* strains (10^8 cells/mL) were grown in 100 mL flasks containing 50 mL Nutrient Broth supplemented with L- Tryptophan(0,5 g L^{-1}) and incubated at 28 ºC for 3 days on 150 rpm rotary shaker. The quantitation of IAA production was determined by using Salkowski reagent (1 mL of 0.5 M $FeCl_3$ in 50 mL of 35% $HClO_4$). 2 ml Salkowski reagent and 1 ml supernatant was mixed and incubated at room temperature 30 min in dark. The optical density was taken at 530 nm with a spectrophotometer. Standard curve was prepared with 5-100 µg/ml of IAA for quantification[3].

2.5. Bacterial identification

Identifying has been conducted with molecular sequence-based identification, for this purpose isolated microorganisms' 16S rRNA genes were amplified with PCR technique using universal primers 27f(5′-AGAGTTTGATCMTGGCTCAG-3′), 519r (5′-GWATTACCGCGGCKGCTG-3′) and DNA sequences have been submitted to an online database (NCBI DNA sequence database) for comparison with known sequences.

3. RESULTS AND DISCUSSION

Siderophore production and phosphate solubilization capabilities were used to select from 48 *Pseudomonas* strains. According to these capabilities, 8 strains were selected for evaluation in terms of IAA production. As shown in the Table 1, siderophore production and phosphate solubilization properties were evaluated at strong (++++) and weak (+) ranges. IAA production of selected 8 *Pseudomonas* strains was determined quantitatively.

Table 1. Results of PGPR properties of Pseudomonas strains

Strain	IAA (µg/ml)	Siderophore Production	P Solubilization
Pseudomonas lactis (5)	19,8	++++	++
Pseudomonas putida (10)	8,48	++	+++
Pseudomonas lactis (14)	9,28	+++	+
Pseudomonas cerasi (15)	21,28	+++	+++
Pseudomonas syringae (16)	16,88	+	+++
Pseudomonas lactis (18)	36,9	+++	++
Pseudomonas paralactis (20)	34,08	++	++++
Pseudomonas lactis (24)	31,29	++++	++

Comparison of *Pseudomonas* strains: (++++) strong and (+) weak

All isolates were capable of producing IAA at different extents with a range of 8,48–36,88 µg/mL.*Pseudomonas lactis* (18) was found to be the highest efficient IAA producer. So, the strain should be optimized to see if commercial production is possible. The strain should be applied to agricultural seeds such as wheat, corn etc. and its efficiency should be analyzed.

4. CONCLUSION

A single strain cannot be expected to exhibit all PGPR feature.Researchers are working to determination of strains that best show at least one PGPR feature [4]. It is expected that by obtaining strains, it will be beneficial

for sustainable agriculture. However, increasing accessibility, reducing costs and educating farmers should be included in the agricultural policies of the countries.

ACKNOWLEDGMENT

The authors acknowledge to the BAP Unit of Cukurova University for the financial support. Project code is FBA-2018-10914

REFERENCES

[1]. Schwyn, B., Neilands, J.B., Universal chemical assay for the detection and determination of siderophores. Anal. Biochem. 160, 47–56. 1987.
[2]. Pikovskaya, R.I., Mobilization of phosphorus in soil in connection with vital activity of some microbial species. Mikrobiologiya 17, 362–370. 1948.
[3]. Malik D.K. and Sindhu S.S., Production of indole acetic acid by *Pseudomonas* sp.: effect of coinoculation with *Mesorhizobium* sp. *Cicer* on nodulation and plant growth of chickpea (*Cicer arietinum*). PhysiolMolBiol Plants. 17(1): 25–32. 2011
[4]. Etesami H. And Maheshwari D.K., Use of plant growth promoting rhizobacteria (PGPRs) with multiple plant growth promoting traits in stress agriculture: Action mechanisms and future prospects. Ecotoxicology and Environmental Safety 156, 225–246. 2018
[5]. Ansari F.A., Ahmad I., Fluorescent *Pseudomonas* -FAP2 and *Bacillus licheniformis* interact positively in biofilm mode enhancing plant growth and photosynthetic attributes, Scientific reports, 2019
[6]. Chandra S., Askari K, Kumari M., Optimization of indole acetic acid production by isolated bacteria from *Stevia rebaudiana* rhizosphere and its effects on plant growth Journal of Genetic Engineering and Biotechnology 16, 581–586. 2018
[7]. Patten C.L. and Glick B.R., Role of *Pseudomonas putida* Indoleacetic Acid in Development of the Host Plant Root System, Applied And Environmental Microbiology, Aug. 2002, p. 3795–3801

ICOEST SARAJEVO
5TH INTERNATIONAL CONFERENCE ON ENVIRONMENTAL SCIENCE AND TECHNOLOGY
October 09-13 2019

Evaluation of an Industrial Park Wastewater Treatment Plant Environmental Performance by Using Life Cycle Analysis

Aysegul Pala[1], Gunes Kursun[2], Mesut Mutlu[1]

Abstract

The irregular usage of natural resources leads to environmental problems and a decrease in natural resources. In order to prevent this situation, various studies have been carried out. One of the techniques developed for this purpose is Life Cycle Analysis (LCA) method. LCA is a method that allows us to evaluate all environmental impacts from the procurement of raw materials to the disposal of a product. In this study, the environmental performance of an Industrial Park Wastewater Treatment Plant (IPWWTP) was determined by using LCA method. In the life cycle analysis and inventory analysis, the data of the facility's internal report were analysed by using GaBi 8.7 Education Software.

Keywords: Life Cycle Analysis, GaBi, Wastewater Treatment, Industrial Park, Environment

1. INTRODUCTION

Although waste management systems help us protect the environment, they can damage the environment with energy consumption, greenhouse gas emissions, chemical use, and some toxic material outcomes as opposed to their main purpose. There has been an increase in environmental awareness in wastewater treatment sector. It has been necessary to include tools for evaluating of the processes.

Overmuch producing and consuming society structure became dominated to developed and developing countries. Therefore, overconsumption has caused so many problems. At the beginning of these problems, the increase of raw material needing. Increasing of natural resources consumption and excessive production causes negative environmental conditions because of the occurred liquid, solid and gaseous waste. With the global growing economy, both of environmental pollution and owning cost need to optimize. In this way, the idea of review process which is examined from extraction of raw material to returns to the nature of the raw material was emerged. Then, assessment systems were developed for it [1].

Life cycle assessment is a technique used to assess all possible environmental impacts of all activities. Turkish Standards Institute (TSE) published "Environmental Management – Life Cycle Assessment – Principles and Frame" Standard in 19.06.2007. According to this, Life Cycle Assessment goods and services obtained from a particular material and energy. As UNEP explains it "the aim of LCA is to suggest more sustainable forms of production and consumption". LCA is science-based, quantitative and integrative [2].

The prime and quite likely most important step of a LCA is the Goal and Scope definition. Present part is defined the reason to make the assessment [3]. The system boundaries of a system are identified by an input and output flow diagram. All operations that promote to the life cycle of the product, process, or activity fall within the system boundaries [4].

[1] *Corresponding author: Dokuz Eylul University, Department of Environmental Engineering, 35160, Buca/Izmir, Turkey.* *aysegul.pala@deu.edu.tr*

[1] *Dokuz Eylul University, Natural and Applied Sciences, 35160, Buca/Izmir, Turkey.,* *gunes.kursun1@gmail.com*

It has been developed to be used various softwares SimaPro, CML 2001, EDIP 96, EPS, EarthSmart, Ecopoints 97, Sustainable Mind, Umberto, GaBi and etc.

Softwares must be commercially available. But some free software is also available. GaBi allows you to design your ideas when it comes to interworking. By using the process recording property of GaBi, data saved across the entire design process and clearly determined where efficiencies occur. [5].

2. MATERIALS AND METHODS

In order to perform LCA, these steps were carried out, respectively. Creating a flow diagram of the process under consideration, development of data collection plan, data collection, evaluation and reporting. Life cycle analysis studies were carried out by using GaBi 8.7 LCA software. The required data for the operating of the software was obtained from the IPWWTP. When the scenario is created in program, the plans were created with subdivided their plans. Then, the scenario was obtained by combining them. The treatment process have coarse screen, fine screen, grit chamber, balancing pond, chemical treatment with $FeCl_3$ and polyelectrolyte addition, biological treatment and discharge into the river.

IPWWTP's data were evaluated in many environmental impact categories in the LCA studies. The environmental impact categories of the results were described. CML 2001 (Institute of Environmental Sciences, Leiden University) impact assessment method was used to determine the environmental impacts. 11 environmental impact categories were taken into consideration. Global warming potential (GWP), Acidification potential (AP), Eutrophication potential (EP), Ozone Layer Depletion Potential (ODP), Abiotic element depletion potential (ADP), Abiotic depletion potential (ADP), Freshwater Ecotoxicity Potential (FAETP), Marine Aquatic ecotoxicity potential (MAETP), Terrestric ecotoxicity potential (TETP), Human toxicity potential (HTP), Photochemical ozone creation potential (POCP). In this study, Global Warming Potential (GWP), Eutrophication Potential (EP), Freshwater Ecotoxicity Potential (FAETP), Human Toxicity Potential (HTP), Marine Aquatic Ecotoxicity Potential (MAETP), Terrestrial Ecotoxicity Potential (CETP) impact categories were determined. Processes and substances, energy inputs-outputs depending on the system boundary of the IPWWTP were investigated.

3. RESULTS AND DISCUSSION

The components of the IPWWTP were given in Figure 1.

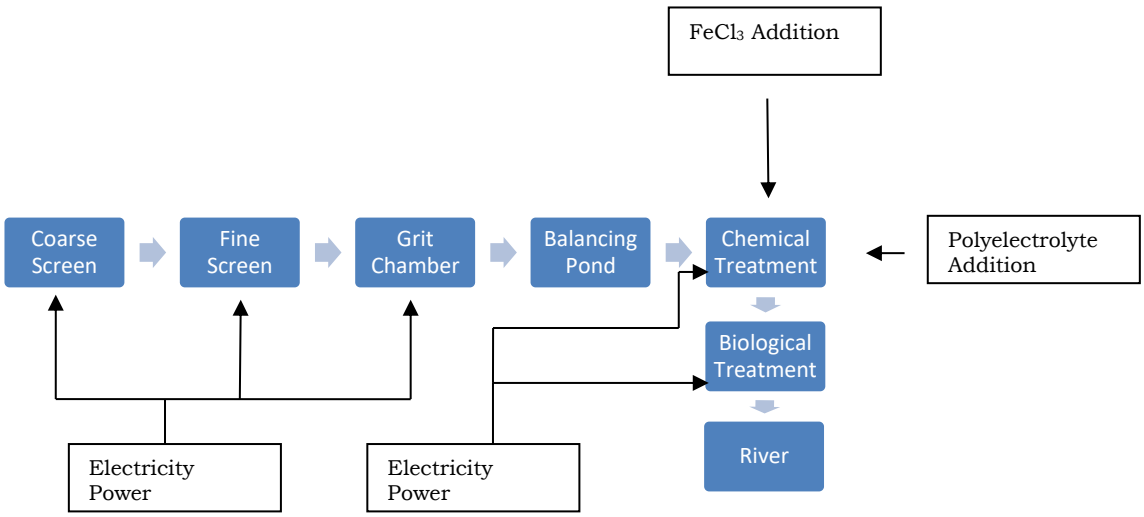

Figure 1. The components of the system

The annual average influent and effluent water quality parameters of IPWWTP is shown in Table 1. The regulation values to the discharge of the IPWWTP wastewater into the river in Turkey is given in Table 2.

Table 1. IPWWTP's annual average influent and effluent water quality parameters.

Parameter	Influent	Effluent
pH	7,33	7,57
SSM (mg/L)	634,70	24,76
COD (mg/L)	1683,90	120,8
Color (Pt-Co)	206,1	98,56
TN (mg/L)	40,30	9,83
NH4-N (mg/L)	6,64	4,65
TP (mg/L)	3,01	0,71
Cd (mg/L)	0,87	0,03
Fe (mg/L)	3,05	1,33
$T.Cr^{-}$ (mg/L)	2,45	0,61
Cr^{+6} (mg/L)	0,55	0,19
CN- (mg/L)	0,29	0,11
F^{-} (mg/L)	4,11	2,07
Cu (mg/L)	1,67	0,92
Zn (mg/L)	3,39	1,28
Oil-Grease (mg/L)	171,57	8
°C	23,81	24,6

Table 2. Requirements for the discharge of IPWWTP into the river in Turkey (SKKY, Table 19).

PARAMETER	UNIT	Sample 2 hours	Sample 24 hours
Chemical oxygen demand (cod)	(mg/L)	400	300
Suspended solid matter (ssm)	(mg/L)	200	100
Oil and grease	(mg/L)	20	10
Total phosphorous	(mg/L)	2	1
Total chromium	(mg/L)	2	1
Chromium (cr^{+6})	(mg/L)	0.5	0.5
Lead (pb)	(mg/L)	2	1
Total cyanide (cn^{-})	(mg/L)	1	0.5
Cadmiyum (cd)	(mg/L)	0.1	-
Iron (fe)	(mg/L)	10	-
Floride (f^{-})	(mg/L)	15	-
Copper (cu)	(mg/L)	3	-
Zinc (zn)	(mg/L)	5	-
Mercury (hg)	(mg/L)	-	0.05
Sulfate (so_4)	(mg/L)	1500	1500
Total kjehdahl nitrogen(*)	(mg/L)	20	15
Fish bioexperiment (zsf)	-	10	10
pH	-	6-9	6-9
(Add:RG-24/4/2011-27914) Color	(Pt-Co)	280	260

The results of Global Warming Potential (GWP), Eutrophication Potential (EP), Freshwater Ecotoxicity Potential (FAETP), Human Toxicity Potential (HTP), Marine Aquatic Ecotoxicity Potential (MAETP), Terrestrial Ecotoxicity Potential (CETP) were shown in Figure 2-9.

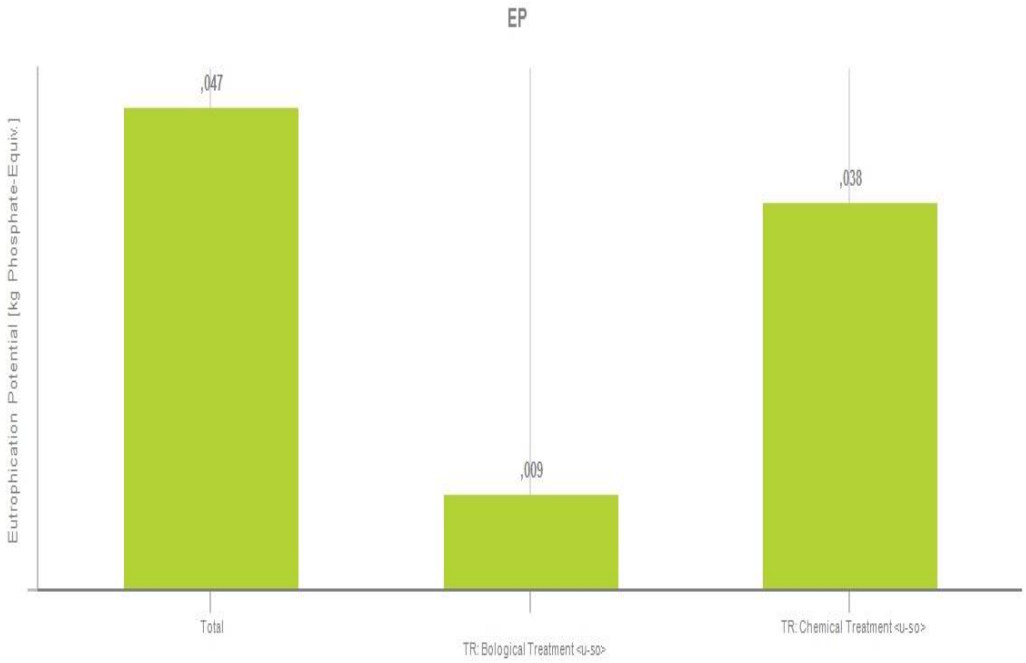

Figure 2. Eutrophication Potential

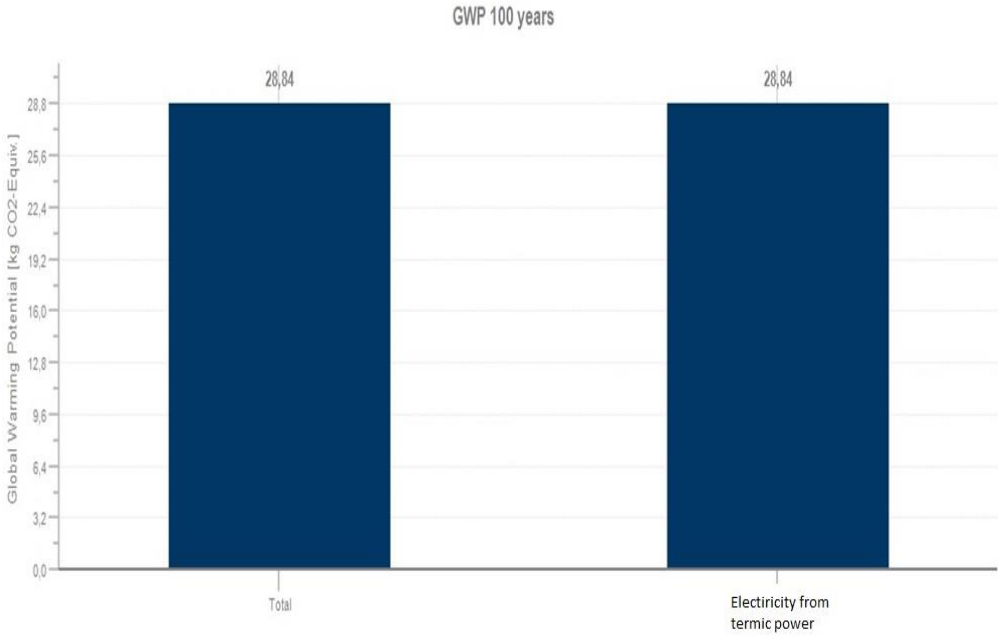

Figure 3. Global Warming Potential

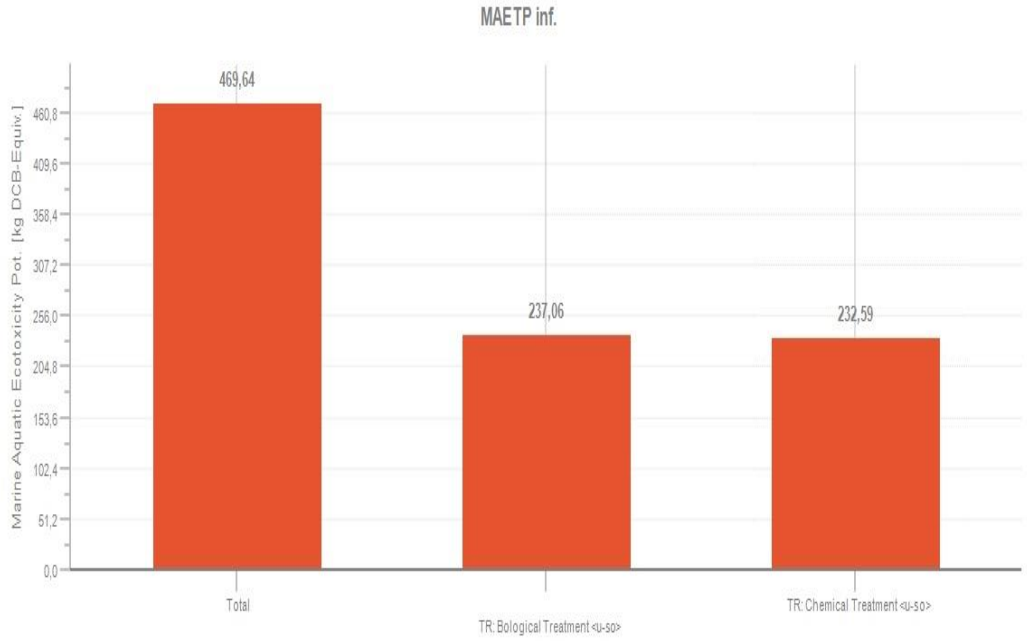

Figure 4. Marine Aquatic Ecotoxicity Potential

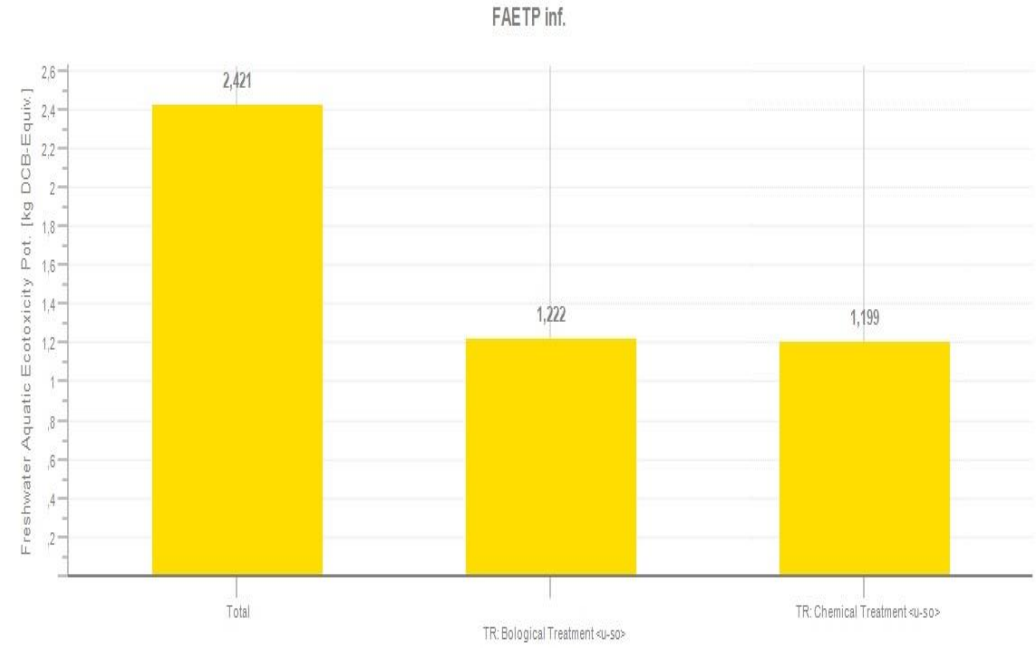

Figure 5. Freshwater Aquatic Ecotoxicity Potential

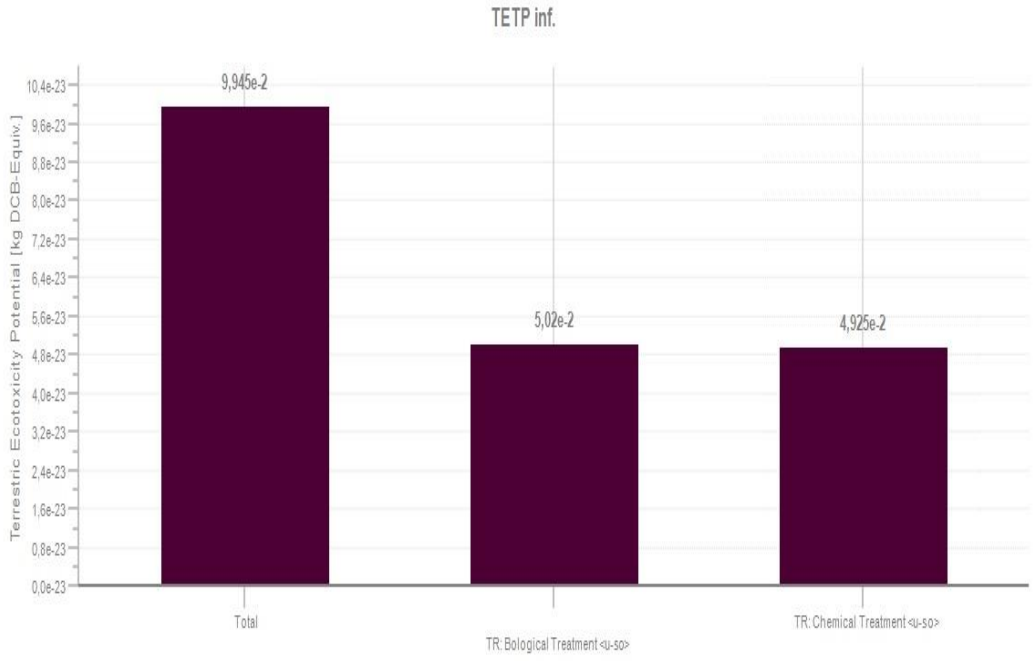

Figure 6. Terrestric Ecotoxicity Potential

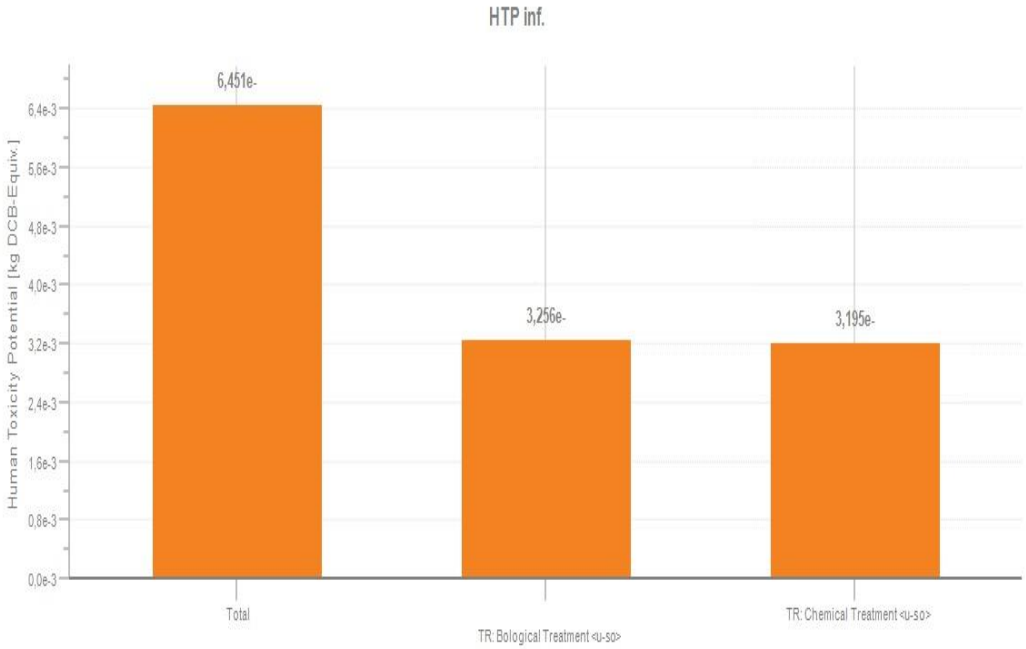

Figure 7. Human Toxicity Potential

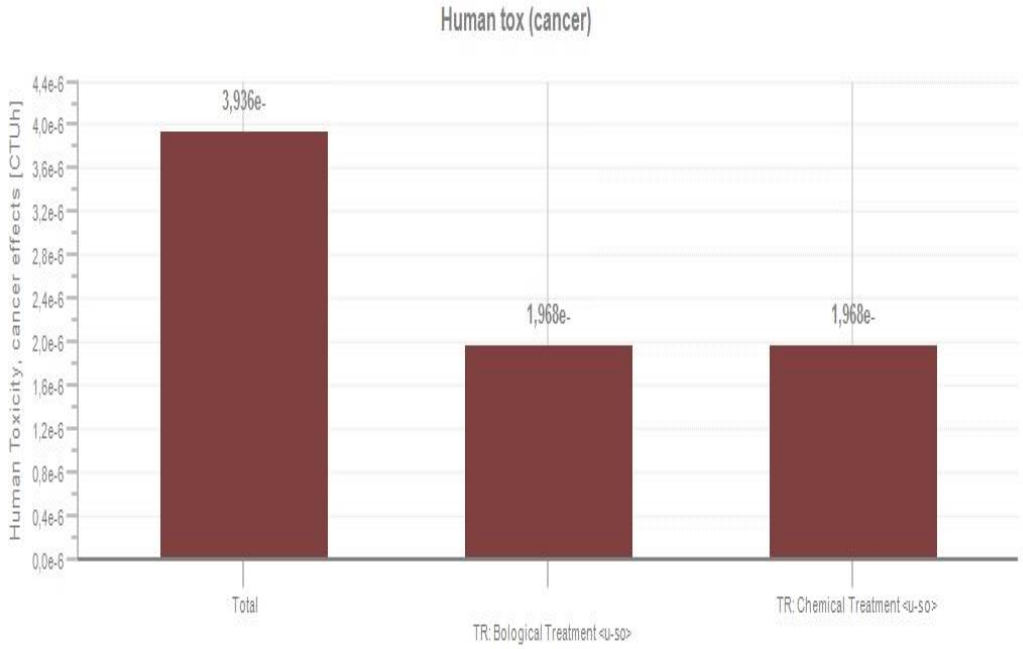

Figure 8. Human Toxicity, Cancer Effects

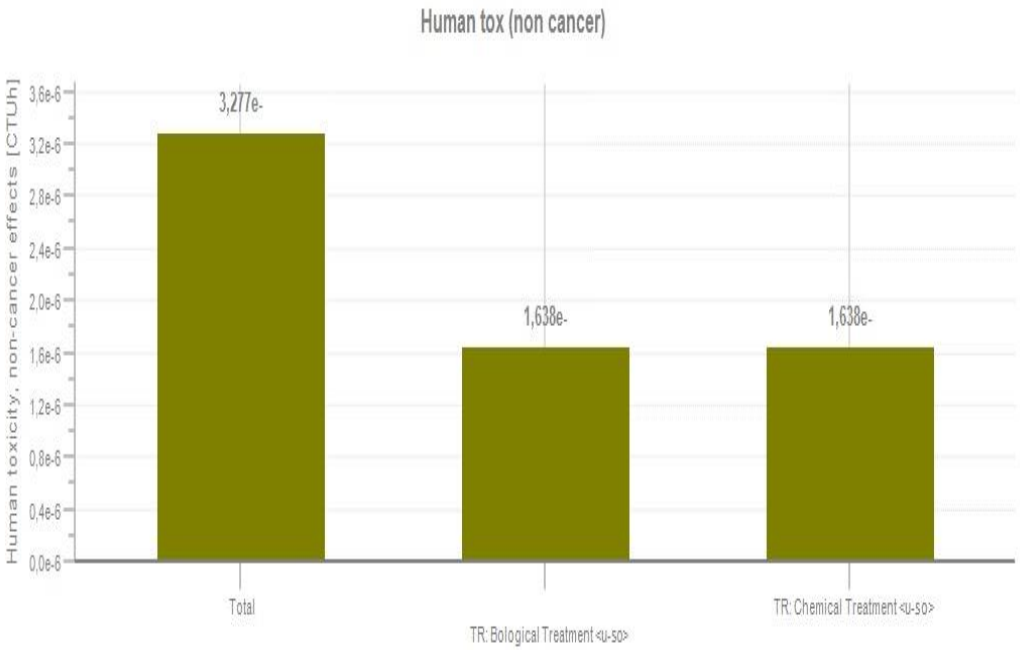

Figure 9. Human Toxicity, Non-Cancer Effects

4. CONCLUSIONS

In this study, the environmental performance of the IPWWTP was determined by using LCA method. The results summarized in below;

- Energy use was significant parameter for WWTP. The energy consumption was found to be 0.607 kwh /m^3. Adam Maslon were reported that the energy consumption of the treatment plant of the Rzeszow, Poland was 0.865 kwh /m^3 [6].
- Global Warming Potential, Eutrophication Potential, Freshwater Aquatic Ecotoxicity Potential, Human Toxicity Potential, Marine Aquatic Ecotoxicity results have been summarized in Table 3.

Table 3. The environmental impacts

Environmental Impact Category	***Unit***	***Value***
Global Warming Potential (100 years)	kg CO_2 eq.	28,84
Eutrophication Potential	kg PO_4^{-2} eq.	0,0009
Freshwater Aquatic Ecotoxicity Potential	kg DCB eq.	1,222

Human Toxicity Potential	kg DCB eq.	0,0326
Marine Aquatic Ecotoxicitiy Potential	kg DCB eq.	237,06
Terrestrial Ecotoxicity Potential	kg DCB eq.	0,00502

REFERENCES

[1]. Findikci, "Life cycle assessment of treatment options for an industrial wastewater," M. Eng. thesis, Dokuz Eylul University, Izmir, Turkey, Feb. 2016.

[2]. Schuurmans-Stehmanna, M. S. A. M, Environmental life cycle analysis of construction products with and without recycling. *Environmental Aspects of Construction with Waste Materials*, 60, pp. 709-718, 1994.

[3]. Ramirez, "Life cycle assessment for wastewater treatment in the chemical industry," M. thesis, Cologne University, Koln, Germany.

[4]. Roy, P., Nei, D., Orikasa, T., Xu, Q., Okadome, H., Nakamura, N., et al., A review of life cycle assessment (LCA) on some food products. *Journal of Food Engineering*, 90, pp. 1-10, January 2009.

[5]. A. Loijos. (2012) LCA webpage on Linkcycle. [Online]. Available: http://www.linkcycle.com/comparison-of-bestlife-cycle-assessment-software/

[6]. M. Adam, "Analysis of energy consumption at the Rzeszów Wastewater Treatment Plant" *E3S Web of Conferences*. 22., 2017.

ICOEST SARAJEVO
5TH INTERNATIONAL CONFERENCE ON ENVIRONMENTAL SCIENCE AND TECHNOLOGY
October 09-13 2019

Impact of Static Compression Loads on Foam Glass Aggregate

Waleed Sulaiman Mustafa[1], Szendefy János [2]

Abstract

Foam glass aggregate is a man made light weight material manufactured by depending on waste glass as a main basic material. It can be used in various geotechnical applications such as such as bridge abutments, retaining wall back fill, road embankments and bedding layers of isolated floors. Therefore, good understanding of the material behaviour is an essential. In this study, foam glass aggregate samples has been subjected to static compression loads by using big size of oedometer apparatus. The static compression test with continuous loads (50, 100, 150 and 200) kPa were applied on foam glass aggregate samples which were compacted in three different compaction percentages (10%, 20%, and 30%). A change in the amount of deformation with time has been revealed in the loading steps of low compaction percentage (10%), while approximately same amount of deformation with time has been observed for all loading steps of each individual compaction percentages (20% and 30%). Maximaum amount of deformation which obtained at the end of each compaction ratio decreased by increasing compaction percentages due to an increasing in the stiffness of foam glass aggregate samples. The oedometric module (E_{oed}) has been calculated for foam glass aggregate samples under all loading steps and for all compactionpercentages.

Keywords: *foam glass aggregate, static load, deformation, oedometric module*

1. INTRODUCTION

Utilizing traditional materials with high densities to execute civil engineering applications which depend on using high amounts of materials lead to adapt huge vertical loads and subsequently result to get some geotechnical problems. The short and long term of geotechnical problems which appeared may lead to structure instability. Therefore, the request behind finding out proper lightweight backfill materials with acceptable geotechnical properties in all around worlds increased specially after results in decreasing the design and executing costs.

Many types of lightweight materials have been studded by numerous researchers such as lightweight cellular cemented clays [1] and lightweight concrete [2],[3]. Foam glass aggregate also has been produced and used as a new lightweight material with appropriate engineering properties for executing geotechnical projects [4]. It consists of two main parts, gas part which fill the pores of the material and glass part which represents the solid part of the material [5]. The porosity of foam glass materials reaches about 60% of the total volume. The pore size and distribution nature select many properties of the material such as density, thermal conductivity, high surface area, permeability, chemical and thermal stability [6]. Some of foam glass materials have the resistance against insects and bacterial acts[7].

The importance of foam glass can be seen due to its usage in a variety of engineering applications such as insulation blocks to resist the energy consumption (e.g., from roofs, walls, floors and ceilings), lightweight filler material during slope stability and retaining wall structure applications, as light weight aggregate material (during constructing road embankments, retaining walls and bridge abutment, for producing light weight concretes [8], and also as scaffolds for bone tissue engineering [9].

[1] *Corresponding author: PhD student, Budapest University of Technology and Economics, Budapest Hungary and Lecturer at Duhok Polytechnic University Kurdistan Region, Iraq.* waleed.sulaiman@epito.bme.hu, waleed.sulaiman@dpu.edu.krd

[2] *Szendefy János: Budapest University of Technology and Economics, Budapest Hungary,* szendefy@mail.bme.hu

Although, foam glass aggregate considered as a very good light weight filling material [4], while the compressive strength of this brilliant material is relatively considered low. Therefore, many investigations have been executed to enhance the mechanical strength of the foamed glass by adding different types of admixture materials. A group of researcher [10] prepared foam glass by adding 89% of coal fly ash and 6% CaCo3 at sintering temperature 1150 ºC and they got a bending strength reached 80.3 MPa with relatively high bulk density. Another group of researcher [11] made the foam glass by adding (5-25) % of glass fibers to the glass powder admixture at a sintering temperature ranged between (790–815) °C. They observed an increasing in bending strength of (10.45–22.26 MPa/(g cm^{-3}), and the specific compressive strength of 30.45– 34.34 MPa/(g cm^{-3}).

Due to leak of researchers about foam glass aggregate and because it's newly manufactured in Hungary, therefore investigating the mechanical properties of this material in very important. The focus of this research will be on the effect of static compression loads on foam glass aggregate behaviour. Different amounts of static loads was applied on foam glass aggregate samples starting from (50) kPa to (200) kPa with (50) kPa interval. To show the effect of compaction ratios on foam glass aggregate behaviour, three different compaction ratios were investigated which were (10%, 20% and 30). At the end of this study, the amount of deformation within time and the oedometric modulus (E_{oed}) of foam glass aggregate samples were calculated which led us to a better understanding from material behaviour and help us during design process.

2. MATERIALS AND METHODS

Foam glass aggregates produced with various particle sizes as shown in figure (1, a). Particle size distribution curves, figure. (1), show that the material mainly contained gravel and sand sized particles. From particle size distribution curves of all conditions (as received & 10% compaction, 20% compaction and 30% compaction), the coefficient of uniformity (Cu=1.01, 1.12 and 1.51) and coefficient of curvature (Cc=1.58, 1.58 and 2.24) show that the material is classified as poorly graded, with one major grain size range (16-64) mm. It can be observed from figure (1) that the particle size distribution of 10% compaction of foam glass aggregate approximately has same particle size distribution due to low compaction ration.

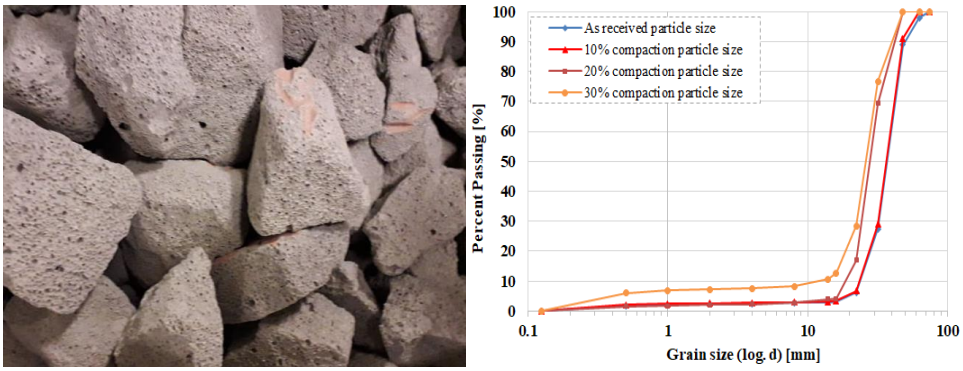

Figure 4. *left to right: foam glass aggregate*, grain size distribution curves

For static compressional tests of this material a conventional geotechnical apparatus is impractical as the single particle could exceed the normal sample size (ranged between 16 to 64 mm in diameter). Therefore, a special test frame was constructed with 300 mm in diameter and 250 mm in high, which fulfilled the suggested 5D (largest particle diameter) size rule.

To achieve (10% and 20%) compaction percentages in the lab, a heavy load plate was used for compacting foam glass aggregate as done on-site compaction. While to reach (30%) compaction percent in the lab, the sample was prepared by compacting the material in to the same mold size by two layers. Due to the size of the individual particles, a perfectly flat surface couldn't obtain. This in turn caused the load plate to transfer loads on distinct points, rather than uniformly significantly altering test results. To decrease the effect of the rough surface, a gravel and sand was used as a load distribution layer on top (Figure 2). First 4/8 mm gravel was used to “wedge” the foam glass particles’ surface and create a more flat face. This is turn was then covered with 0/1 mm sand to create the smooth surface on which the load plate can uniformly transfer loads.

Figure 2. Foam glass aggregate laboratory sample preparation (left to right: foam glass aggregate, with gravel layer, sand load distribution layer)

3. RESULTS AND DISCUSSIONS

3.1. Static Compressional Load

Time versus deformation curves, as shown in figure (3), revealed that the stiffness of foam glass aggregate decreased as the amount of applied load is increased during the selected loading interval. Figure (3) show also that by increasing the percent of compaction from (10%) to (30%), the stiffness of foam glass aggregate increased. Also from same figure appeared that by increasing the amount of applied load more than (100) kPa at (10%) compaction, sudden increasing in the amount of deformation was observed. This may be related to the availability of big amount of voids between particles due to low compaction percentage. On the other side, the change in the amount of deformations for each loading step at both compaction percentages (20% and 30%) and after increasing the amount of applied load were approximately the same.

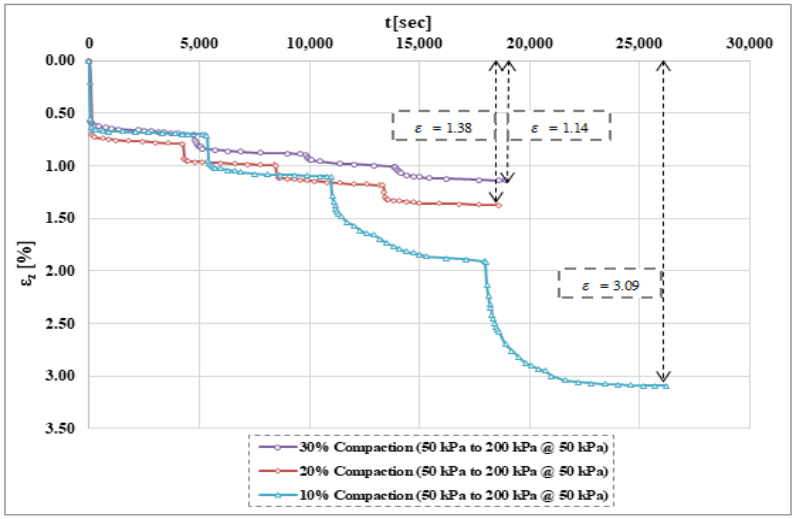

Figure 3. Time deformation curves of foam glass aggregate.

The oedometric modulus (E_{oed}) values of all loading steps (50, 100, 150 and 200) kPa and for all compaction percentages (10%, 20% and 30%) were calculated by depending on the amount of deformations which were obtained at approximately (5000) sec. From figure (4) can be observed that the amount of oedometric modulus (E_{oed}) for both compaction percentages (20% and 30%) increased with increasing the loading steps due to higher stiffness of foam glass aggregate samples. While at (10%) compaction and especially after applying more that

(100) kPa the amount of oedometric modulus (E_{oed}) decreased which may related to low stiffness of foam glass samples due to low compaction ratio and high amount of applied load.

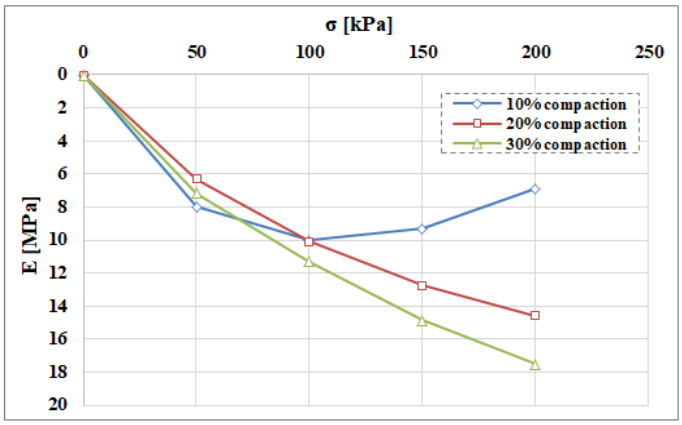

Figure 4. Compression modulus of foam glass aggregate for different amount of loads.

4. CONCLUSIONS

From static compression tests on foam glass aggregate samples which were prepared by three different compaction percentages (10%, 20% and 30%) the following points were concluded:

1- The maximum amount of deformation which obtained at the end of each compaction ratio decreased by increasing compaction percentages due to an increasing in the stiffness of foam glass aggregate samples.

2- A change in the amount of deformation with time has been revealed in the loading steps of low compaction percentage (10%), while approximately same amount of deformations with time were observed for all loading steps for each individual compaction percentages (20% and 30%) due to an increasing in the stiffness of foam glass aggregate samples.

3- For both compaction percentages (20% and 30%) the amount of oedometric modulus (Eoed) were increased with increasing the amount of applied loads. While, at low compaction percentages (10%) and after applying loads more than (100) kPa the amount of oedometric modulus (Eoed) decreased with increasing the amount of applied load.

4- To be away from big amount of deformation, it's better to compact foam glass aggregate more than (10%) compaction and it's better to not apply more than (100) kPa at low compaction percentages (10%).

REFERENCES:

[1] S. Horpibulsuk, A. Wijitchot, A. Nerimitknornburee, S. L. Shen, and C. Suksiripattanapong, "Factors influencing unit weight and strength of lightweight cemented clay," Q. J. Eng. Geol. Hydrogeol., vol. 47, no. 1, pp. 101–109, 2014.

[2] P. Chindaprasirt and U. Rattanasak, "Shrinkage behavior of structural foam lightweight concrete containing glycol compounds and fly ash," Mater. Des., vol. 32, no. 2, pp. 723–727, 2011.

[3] Y. W. Wang and B. X. Tang, "Experimental Study of the Foam Agent in Lightweight Aggregate Concrete," Appl. Mech. Mater., vol. 226–228, pp. 1776–1779, 2012.

[4] A. Arulrajah et al., "Engineering and environmental properties of foamed recycled glass as a lightweight engineering material," J. Clean. Prod., vol. 94, pp. 369–375, 2015.

[5] N. Sasmal, M. Garai, and B. Karmakar, "Preparation and characterization of novel foamed porous glass-ceramics," Mater. Charact., vol. 103, pp. 90–100, 2015.

[6] P. Scheffler, M., Colombo, "Cellular Ceramics: Structure, manufacturing, properties and applications," Wiley-VCH Verlag GmbH Co. KGaA, Weinheim, p. 669, 2005.

[7] S. Midha, T. B. Kim, W. Van Den Bergh, P. D. Lee, J. R. Jones, and C. A. Mitchell, "Preconditioned 70S30C bioactive glass foams promote osteogenesis in vivo," Acta Biomater., vol. 9, no. 11, pp. 9169–9182, 2013.
[8] Lu, J., Onitsuka, K., "Construction utilization of foamed waste glass," J. Environ. Sci., vol. 16, no. 2, pp. 302–307, 2004.
[9] Q. Z. Chen, I. D. Thompson, and A. R. Boccaccini, "45S5 Bioglass®-derived glass-ceramic scaffolds for bone tissue engineering," Biomaterials, vol. 27, no. 11, pp. 2414–2425, 2006.
[10] M. Qian, Q. Wang, L. Luo, and C. Fan, "Preparation of high strength and low-cost glass ceramic foams with extremely high coal fly ash content," IOP Conf. Ser. Mater. Sci. Eng., vol. 397, no. 1, 2018.
[11] Guo, H. W. et al. 2010. "Improved Mechanical Property of Foam Glass Composites Toughened by Glass Fiber." Materials Letters 64(24): 2725–27. http://dx.doi.org/10.1016/j.matlet.2010.09.012.

ICOEST SARAJEVO
5TH INTERNATIONAL CONFERENCE ON ENVIRONMENTAL SCIENCE AND TECHNOLOGY
October 09-13 2019

University Campus Air Quality Monitoring Platform

Radosveta Sokullu[1], Onem Yildiz[2], Abdullah Balci[3]

Abstract

This paper describes an ongoing work for creating a mobile platform for air quality monitoring in Ege University, Izmir-Turkey. The goal is to measure temperature and humidity levels as well as some basic air pollution components using mobile devices and interfaces. Data, collected through mobile platforms mounted on users' phones, bicycles or cars moving around the campus, is analyzed to allow observing the quality of the surrounding air on user mobile devices. This paper describes the system architecture and interfaces as well as the sensor's selection and operation. Two separate system architectures were determined. In the first architecture, collected sensor data is sent to a smartphone application via a Bluetooth module. Arduino Nano MCU is used for data transfers from the sensors. The user is able to initiate data collection and observe current sensor values on his smartphone screen. In the second proposed system architecture, the goal is to transmit the collected data from the sensors to a control center using a GSM module (Adafruit FONA 808). Data exchange is done using the publish-subscribe application layer protocol - MQTT, which is simple, low power protocol, specifically used in IoT applications. The data from the sensors is read and then transmitted to the MQTT broker using a predetermined topic. For the Subscriber, a website in Java Script was designed, allowing users to connect to the MQTT broker, subscribe to the data published on the selected topic and receive messages (sensor data) published in a certain period.

Keywords: GSM module, humidity levels, MQTT broker

1. INTRODUCTION

Together with global warming air pollution has been one of the major environmental issues in the last decade. However, while global warming is an environmental issue which requires large scale international actions, solution of air pollution has been targeted at different levels, starting from small scale (cities and areas) to larger scale government initiatives. It is the most direct cause related to human health deterioration and according to the World Health Organization (WHO) studies 9 out of 10 people in the world breathe highly polluted air, a thread to their health. Only in 2016 7 million deaths were reported from contaminated air including a large number of children under the age of 5 [1]. Central and local government organizations in many countries have implemented fixed air monitoring systems, especially in larger cities and actions are taken to tackle the main

[1] *Corresponding author: Ege University, Department of Electrical and Electronics Engineering, 35100, Bornova/Izmır, Turkey. radosveta.sokullu@ege.edu.tr*

[2] *Adnan Menderes University, Aydın, Turkey, onem.yildiz@adu.edu.tr*

[3] *Yalova University, Dept. of Electrical and Electronics Engineering,77200, Yalova, Turkey, abdullah.balci@yalova.edu.tr*

reasons for air pollution – industrial and traffic gas emissions. On the other hand, a variety of small, stationary, individually owned devices have appeared in the market which can give an idea about the air quality in personally selected surroundings. These systems, even though not very accurate, allow individuals and groups of people in a given location to quickly respond and take proper actions in order to reduce the immediate negative effects air pollution has on their health. Furthermore, very recently, availability and low cost of digital electronics, accompanied by increased networking functionality has made mobile air monitoring platforms a viable solution. Thanks to them people are becoming more aware of and more interested in the air quality around them.

In this project we are addressing the issue of air pollution on the campus of Ege University in Izmir, Turkey. The campus covers a large open area in the eastern part of the city and is bordering on the one side a highly populated quarter of Bornova, while on the other three sides it is surrounded by industrial and high-traffic concertation zones. The project addresses not only the air pollution issue but also the dangerous UV radiation since Izmir has a subtropical climate with quite high sun exposure during a large part of the year. Its goal is the design of a mobile platform for monitoring the air quality in various locations on campus. Data related to air quality, temperature, humidity and radiation is collected by mobile platforms mounted on users' phones, bicycles or cars around the campus. Later on, it is analyzed and results are transmitted to users in the form of SMS, mail or interactive mobile interfaces. This paper describes the system architecture and interfaces as well as the sensor's selection and operation.

From here on the paper is organized as follows: Section 2 presents an overview of related works, followed by description of the proposed system architecture and main components in Section 3. In Section 4 the user interfaces are described in detail; finally in Section 6 the current progress and results are summarized.

2. RELATED WORK

While in the previous decade centralized air pollution measurement and monitoring stations were most popular, the recent years have seen a lot of research on smaller more adaptive air monitoring systems. Reference [2] describes a study carried out in Lima, Peru. It addresses the evaluation of air quality considering especially pedestrians in the capital city, who are exposed to high emissions of polluting gases such as carbon monoxide, carbon dioxide, methane and other leading to respiratory and cardiovascular problems and diseases. The authors propose an air evaluation system using electrochemical sensors (MQ4, MQ9, and MQ135) which collect raw data from the surrounding environment. It is the transmitted to a cloud-server through the IoT platform based (NodeMCUESP8266), where a more detailed assessment of gas concentration is carried out. The system can be used along public transport routes where it is believed that toxic gas discharges are above acceptable levels. A bicycle mounted air monitoring system is described in [3]. The authors develop a device for measuring both the exhaust gas of motorized vehicles and particulates over roadways. The device can be mounted on the public use bicycles as a simple sensor node, thus creating a mobile sensor network is built to monitor the air quality along various paths in the city of Changzhou. The system is composed of a low-cost particulate matter sensor, an exhaust gas sensor, a Bluetooth interface, and a GPS receiver that provides both a spatial localization and time to the data collection process. While the bicycle is in motion raw data is collected and save d to a microSD card. When the bicycle is returned to the docking station collected data is of-laded over Bluetooth to the Dock

station unit. An affordable portable optical aerosol sensor, Shinyei PPD42NS, is used to measure particulate matter and TGS 2201 is used to measure exhaust gases such as CO2, N2, NOX, CO. Preliminary results for the city and surrounding areas were visualized using Baidu heat map.

A pilot project for environmental monitoring using an integrated sensors-based hardware-software system is discussed in [4]. Parked cars are used as sensor platforms to provide data for environmental monitoring. The prototype is composed of LinkIt Smart 7688 Duo with two processors. The main processor runs the OpenWrt Linux distribution and handles communication and location data from the GPS receiver. The second processor is compatible with Arduino, and handles air quality, temperature, humidity, barometric pressure and dust particle sensors. Arduino collects the environmental data from sensors and brings to the other processor running Linux. Then, Linux application sends the all sensors data, with the attached location and time information which are collected from the GPS, to the server.

AirSense platform is introduced in [5]. The platform consists of three key components, a portable Air Quality Monitoring Device (AQMD), mobile application and the cloud service. AQMD includes MQ-135 air quality sensor, MQ-7 CO gas sensor and Bluetooth module HC-05 which are connected to the Arduino Pro Mini board. AQMD is as an interface between mobile phones and the cloud. The environmental data is collected through volunteer users equipped with AQMD and is transferred to smart phone via Bluetooth module. The collected data, stamped with location information is transferred to the cloud server through the Internet. Then, AQImap of the city or given area is generated from the aggregate data so other users of the mobile application can see the Air Quality Index (AQI) from the map and select a healthy route.

A system for real-time monitoring developed in Sibiu, Romania is described in [6]. The platform consists of LinkedIt Smart Duo 7688 an open development board with two processors, a combined GPS/GSM unit for location and communication, SainSmart MQ135 air quality sensor and hazardous gas detection module for measuring CO2 and NOx, PM10 grove dust particle concentration detection sensor, DS18B20 temperature sensor and BMP085 digital barometric pressure measurement sensor. This prototype has two sides: client and server. On the client side, the environmental data is collected from the parked cars and stamped with time and location information taken from the GPS receiver, then send to a server using a GSM module. The server stores the location of relevant cars and the data in a database for further analysis.

3. PROPOSED SYSTEM ARCHITECTURE AND MAJOT COMPONENTS

3.1. System Architecture

The goal of the project is to develop an IoT based mobile air monitoring system to be tested on the campus of Ege University, Izmir, Turkey. Both data collection and data dissemination are done through mobile devices. Besides the engineering side, the project has an additional goal to increase the involvement and awareness of young people in environmental issues.

Two separate system architectures are considered. In the first architecture, data collected by selected sensors is wirelessly transmitted through an Arduino Nano over a Bluetooth Low Energy module (BLE HM-11) to an Android device. This simple architecture allows the user to directly observe the sensor values (i.e. gas concentration of CO2) in the air on his smartphone screen. An Android application needs to be specifically

developed for this case. The functional diagram and the picture of the actual setup for this architecture are given respectively in Fig.1 (a) and Fig. 1 (b) below.

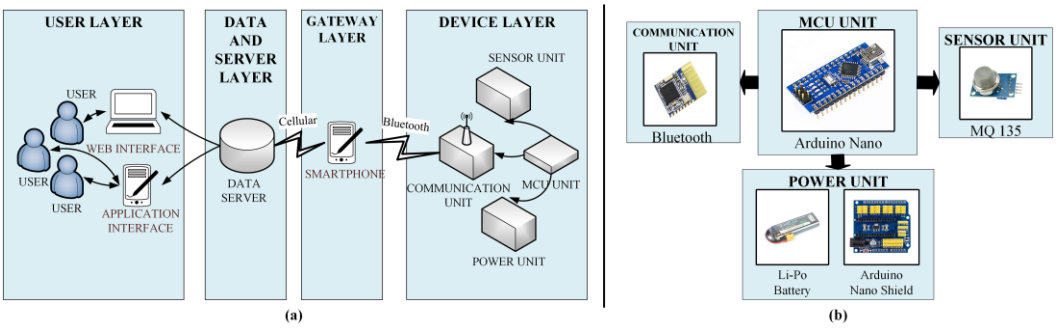

Figure 1. (a) System Architecture *(b) System Components and Setup*

In the second system architecture, the aim is to transmit the data read from the sensors to a central unit by using a GSM/GPRS module. (Fig.2) Adafruit FONA 808 is used as GSM module. Since FONA 808 GSM /GPS module can communicate using TCP/IP protocol, MQTT (Message Queuing Telemetry Transport) is preferred as application layer protocol for data exchange. Unlike the HTTP protocol based on the request-response structure, the MQTT protocol uses simple and low power publish-subscribe structure. For this reason, it is a preferred choice for many IoT applications. As a key element of the MQTT protocol, MQTT broker is used as a server installed on the internet. Arduino Nano MCU card and FONA 808 GSM module to which sensors are connected are used as Publisher. The data from the sensors is read by the Arduino Nano MCU and transmitted to the MQTT broker via a predetermined topic using the FONA 808 GSM module. The Subscriber is a website prepared in Java Script language. Through the created website, the user can connect to the MQTT broker and subscribe to the data published on a subject and receive specific messages published in a certain period.

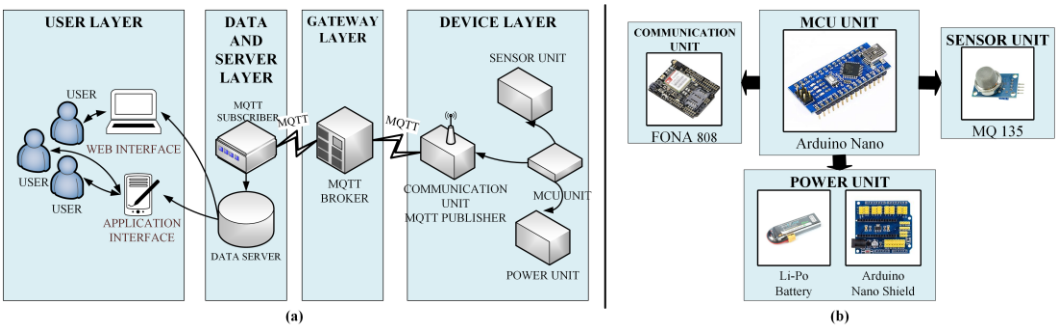

Figure 2. (a) System Architecture *(b) System Components and Setup*

3.2. Major Components

The major components in these proposed architectures are the DHT-11 sensor, the MQ-135 sensor, BLE HM-11, the Arduino Nano and Adafruit FONA 808.

The DHT-11 sensor is a simple off-the-shelf sensor used for measuring the temperature and humidity in the environment and transferring it to the Arduino via a digital pin. It is able to perform temperature measurements in the range of 0-50 ° C with ± 2 ° C sensitivity and humidity measurements between 20-90% with 5% RH (Relative Humidity) margin of error [7]. It is widely preferred in such applications because of its acceptable margin of error, its ability to maintain a balanced performance in long-term studies and its cost-effectiveness.

MQ-135 is a gas sensor that detects and measures the amount of air components such as NH3, alcohol, benzene, smoke and CO2 in the environment. It is preferred in terms of being a good price/performance product in measuring air quality. As with any gas sensor, the MQ135 sensor must be calibrated in accordance with the gas to be measured so that the data received with this sensor is as close as possible to the actual data. The reference atmospheric CO2 value is taken as 411 ppm [8]. The MQ135 gas sensor was operated for 24-48 hours, as indicated in the sensor catalog, to ensure accurate measurements. After this time, the sensor was placed outside (with preferably 20°C temperature and 35% humidity) and the R_{zero} resistance value of the sensor continued to be read until a stable value was obtained. R_{zero} resistance value is obtained using the R_s parameter obtained by converting the voltage value taken from the analog input of the sensor to the resistance value using the equation and the CO2 value of 411 ppm used for calibration [8]. After determining the resistance value of Rzero, the CO2 in terms of ppm can be measured for the desired environment according to the equation obtained CO2 gas curve (equation 1) from MQ135 sensitivity characteristic graph indicated in [9]. The term "a" specified in the equation is a scaling factor of 116.6020682 and the term "b" is an exponent of 2.769034857. In addition to that, if another gas quantity, such as NH3, is to be measured, the curve for this gas should be looked up and the a-b values should be changed accordingly.

$$CO_2(\text{ppm}) = a * (R_s/R_{zero})^{-b} \qquad (1)$$

Adafruit FONA 808 is a GMS module operating in the Quad-band (850,900,1800,1900 MHz) spectrum, with integrated GPS. In addition to the ability to send and receive SMS data, the module can send and receive GPRS data by supporting TCP/IP and HTTP. GSM/Cellular Quad-Band Antenna with 3 dBi gain and thin sticker type uFL connector is used as GSM antenna, Passive GPS antenna with uFL connector and 1 dBi gain is used as GPS antenna. In addition to the latitude and longitude information taken from GPS antenna, the altitude, direction and speed metrics of location are also expressed [10]. To supply the FONA module, a 3.7V and 1400 mA LiPo battery is required because of its high power during operation. The FONA module needs to be initially tested by operating in a fixed position, before it can be used to provide mobile data from around the campus.

An important feature of the FONA 808 GSM/GPS module is that it can communicate using TCP/IP like protocol. For the project MQTT (Message Queuing Telemetry Transport) is used as application layer protocol for data exchange. However, unlike the HTTP protocol based on the request-response structure, the MQTT protocol uses simple and low power with publish-subscribe structure [11]. For this reason, MQTT is frequently used in Internet of Things (IoT) applications. As a key element of the MQTT protocol, a server installed on the Internet was used as the MQTT broker. Arduino Nano MCU card which is connected to sensors and FONA 808 GSM module are used as Publisher. The data from the sensors is read by the Arduino Nano MCU and

transmitted to the MQTT broker via a predetermined topic using the FONA 808 GSM module. As a Subscriber, a website prepared in Java Script language was used. In the created website, the user can connect to the MQTT broker and subscribe to the data published on a subject and receive messages published in a certain period.

4. USER INTERFACE DESIGN

An important part of the design is the user interface. The two different system architectures explained in the previous section have led to the consideration of two different user interfaces.

The first one allows directly informing the user about the data collected from the sensors. Preliminary designs have been developed based on the following simple fictional scenarios.

Scenario 1: Sensor data from the environment is collected at time instants specified by the user. He can connect, scan and disconnect for transferring each sensor reading. Each time the data is processed through the Arduino Uno and sent in a BLE packet to the user. While this scenario can provide nearly real-time information it consumes a lot of energy for transmission because each data reading is transmitted as a separate packet. An example of the smartphone interface is given in Fig. 3 (a) below.

Scenario 2: In this scenario sensor readings are taken at predefined intervals (i.e. 2000 ms) and are transferred to the Arduino Uno to be concatenated with other data. As it is well known data aggregation allows high energy savings. If the goal is nearly real-time data exchange, then the interval can be kept small. However, considering the nature of environmental parameters and the fact that data is collected through mobile users moving at low speed (pedestrians, bicycles or at the most slow moving vehicles through the campus) nearly real-time performance can be achieved with considerably large sampling intervals. Sampling period and transmission time are negligible relative to the changing of environmental parameters like temperature, humidity and even gas concentrations. Thus, the second scenario, with a aggregated BLE payload is considered more suitable. Fig. 5 (b) shows a sample smartphone screen developed with MIT App Inventor 2.

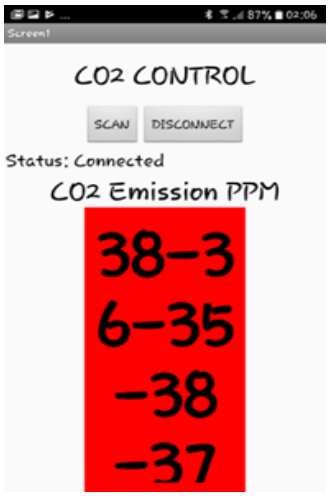

Figure 3. (a) User Interface for Scenario 1 *(b) User Interface for Scenario 2*

The second proposed architecture leads to a very different presentation of the collected sensor data. It allows us to track and map the sensor reading for a given period of time. Using the FONA module collected sensor readings are sent to the IoT cloud using Ubidots. Ubidots is a free, easy-to-use platform for educational purposes. It is easily integrated with Arduino Nano and the addition of the desired dashboards and displays in various formats such as graphics and maps is quite straight forward. It also allows to transfer the collected data for more detailed processing, if required, through the MQTT protocol. This architecture allows both centralized and de-centralized (mobile) display of the collected environmental data. An example of the user interface related to this architecture is given in Fig. 4. The graphs of temperature and humidity metrics are plotted depending on the measurement time and the location information obtained from the GPS. Each measurement can be allocated a different color and the mapping frequency can be adjusted to a desired value.

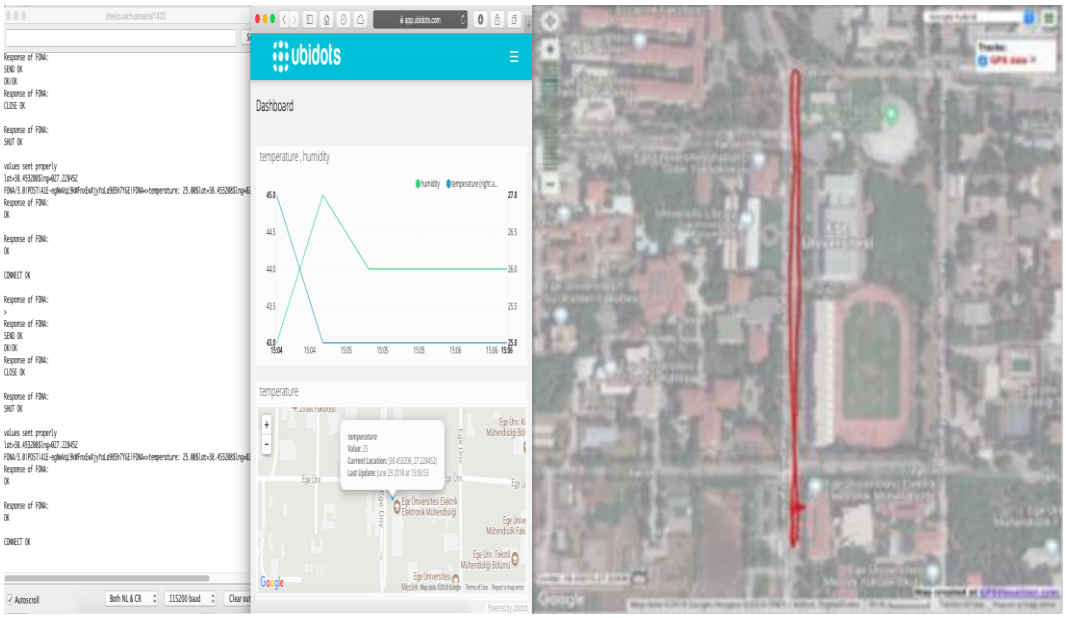

Figure 4. (A) Ubidots Interface Example *(B) Mobile Unit Route Shown On Campus Map*

5. PRELIMINARY RESULTS AND DISCUSSION

The work described in this paper covers a current project sponsored by the Research Fund of Ege University, Izmir, Turkey. At this stage different system architectures and components were examined. The possible solutions were evaluated both based on their technical characteristics and also based on the public opinion. A questionnaire was distributed among students from the university and the results show that there is a near balance between the ones that prefer a centralized display of air quality information and those that prefer individualized (i.e. text message) information delivery. Two systems architectures were selected: one a totally distributed system, one with a centralized option. Furthermore the details of the user interfaces related to these architectures were examined and simple examples were discussed. Considering the social involvement side of the project, the questionnaires reveal high interest from the students and also that more than 85% of them think that such an air monitoring system is a necessity for the campus.

6. CONCLUSION

In this paper we have discussed the proposed system architecture and main components for an IoT based air quality monitoring system. It is a current project sponsored by the Research Fund of Ege University, Izmir, Turkey. The project aims to collect data from mobile units carried by volunteer users, mounted on bikes or cars moving inside the campus. Besides the engineering side the project has also a community involvement goal. Questionnaires were designed and distributed among university students to increase their environmental awareness, help determine the most desirable user interface designs and functions, and determine volunteers that will take part in the testing phase of the project.

ACKNOWLEDGMENT

This project is sponsored by the research fund of Ege University under grant No. 17-MÜH-059, 2017

REFERENCES

[1]. (2018) Organización Mundial de la Salud. [Online]. Available: http://www.who.int/topics/environmental_health/es/
[2]. M. Medina-De-La-Cruz, A. Mujaico-Mariano and M. M. Soto-Cordova, "Implementation of an evaluation system to measure air quality on public transport routes using the Internet of Things," in: Congreso Argentino de Ciencias de la Informática y Desarrollos de Investigación (CACIDI), IEEE, 2018, p. 1-4.
[3]. X. Liu, B. Li, A. Jiang, S. Qi, C. Xiang, and N. Xu, "A bicycle-borne sensor for monitoring air pollution near roadways," in: IEEE International Conference on Consumer Electronics-Taiwan, 2015, p. 166-167.
[4]. L. Berntzen, M. R. Johannessen, and A. Florea, "Smart Cities: Challenges and a Sensor-based Solution," International Journal on Advances in Intelligent Systems., vol. 9, pp. 579-588, 2016.
[5]. J. Dutta, C. Chowdhury, S. Roy, A. I. Middya, and F. Gazi, "Towards smart city: sensing air quality in city based on opportunistic crowd-sensing," in Proceedings of the 18th International Conference on Distributed Computing and Networking, p. 42, 2017.
[6]. A. Florea, L. Berntzen, M. R. Johannessen, D. Stoica, I. S. Naicu, and V. Cazan, "Low Cost Mobile Embedded System for Air Quality Monitoring," in Proceedings of the Sixth International Conference on Smart Cities, Systems, Devices and Technologies (SMART), pp. 25-29.
[7]. "DHT11 Datasheet," Aosong (Guangzhou) Electronics Co.,Ltd.
[8]. CO2 Earth website. [Online]. Available: https://www.co2.earth/
[9]. "MQ-135 datasheet," Olimex, Plovdiv, Bulgaria.
[10]. Adafruit website. [Online]. Available: https://www.adafruit.com/product/2542
[11]. MQTT website. [Omline]. Available: http://mqtt.org/

ICOEST SARAJEVO
5TH INTERNATIONAL CONFERENCE ON ENVIRONMENTAL SCIENCE AND TECHNOLOGY
October 09-13 2019

Mineralogical speciation as a tool in polluted soils assessment: a case study

Jéssica Álvarez-Quintana[1], Almudena Ordoñez[1], Jorge Loredo[1] and Rodrigo Álvarez[1]

Abstract

During the last decades, soil contamination derived from mining and industrial activities has been a matter of special environmental concern. Risk assessment studies are usually carried out following USEPA procedures, in which the concentration of contaminants in the soil and the toxicity are considered key factors. The toxicity of a given element depends on its chemical form, so chemical speciation (sequential extraction procedures) is a widely applied method in most of the environmental studies that include the soil pollution characterization. Mineralogical speciation has some advantages when compared to chemical speciation and provides a better understanding of the samples geochemistry. In this paper, the case of a soil polluted by As compounds is presented and discussed.

Keywords: Mineralogical speciation, Soil contamination, Arsenic

1. INTRODUCTION

Although it is in the 1960s when the first systematic works on environmental affections arising from extractive and industrial activities appear, it is during the last two decades when the number of studies in this discipline grows exponentially, mostly promoted by public environmental agencies. Simultaneously, a great effort has been carried out in the research and quantification of toxic effects of certain chemical compounds considered as frequent soil pollutants. The environmental studies of polluted sites allow defining contamination values, and taking into account pollutants toxicity (dose/response assessment) and some parameters of the potential human sensitive receptor (exposure, body weight…), a risk assessment can be undertaken. The US Environmental Protection Agency (EPA) has developed methodologies that allow us to calculate the risk that a specific polluted site involves for human health and ecosystems. These risk assessment methodologies can also be used to establish the maximum concentration of a given pollutant that causes an acceptable risk level (depending on soil future use). These maximum concentration values has usually been transferred to several legal requirements in many countries.

As mentioned above, the contaminant level (generally expressed as a mean or a percentile of a set of samples) in a polluted soil does not constitute by itself an optimal criterion to assess the associated risk, as it is also highly dependent on the contaminant toxicity. Inevitably, this led to take into consideration the contaminant chemical form (or, at least, the contaminant oxidation state), introducing complexity in the procedure. During the last years, in the vast majority of the cases, this "chemical speciation" has been accomplished following sequential extraction schemes (Tessier *et al*., 1979; Ure *et al*., 1993 (BCR),…). These protocols use different extractants (of increasing leaching strength) and assign each fraction to a non-formal group ("exchangeable", "acid-soluble", "easily reducible", "oxidizable"…). These methodologies, although can be considered as useful approximations, have also been object of criticism in the specialized bibliography (Filgueiras *et al*., 2002; Tlustos *et al*., 2005 and Zimmerman and Weindorf, 2010, among others) mainly due to the significant burden of subjectivity concerning the results interpretation. In this work, we will try to evaluate the suitability of the mineralogical techniques to carry out a "mineralogical speciation" of the As species present in a soil polluted by old mining operations. Specific objectives for this work are summarized as follows:

[1] *Corresponding author: Rodrigo Álvarez. University of Oviedo, Mining exploration and prospecting Department, 33004, Oviedo, Asturias (Spain)* alvarezrodrigo@uniovi.es

a) To determine the advantages and limitations of classical mineralogical techniques (optical and electronic microscopy and X-ray based analyses) in the study of polluted soils.

b) To deepen the knowledge and understanding of mineral transformations involved in the As mobilization from spoil heaps rock fragments to soil.

c) Establish a qualitative comparison of the results obtained by means of chemical and mineralogical techniques.

2. MATERIALS AND METHODS

2.1. Study Area

The area of study is constituted by an ancient As mine and its surroundings. “Rita” mine is located north of the village of Compludo, in a natural area known as "Los Salgueiros" (Ponferrada, Spain, X_{UTM} = 708,420; Y_{UTM} = 4,706,074, UTM Zone 29). In this mine, a set of arsenopyrite-rich quartz veins (N140E trend) was exploited by ditches and galleries (directly over the veins), between 1940 and 1954. The host rock is a thick sequence of quartzites and slates of Cambro-Ordovician age locally known as “Serie Los Cabos”. From a geological point of view, this area is located within the so-called “West-Asturian Leonese Zone”, following the classical division of the Iberian Massif proposed by Lotze (1945). Extracted low-grade ore and gangues were directly disposed over the hillside in the form of spoil heaps (see figure 1). Main mineral As species found in mine wastes are arsenopyrite and scorodite, accompanied by small quantities of other sulphides.

Mine wastes were randomly sampled in the spoil heaps in order to know the characteristics (mineral phases, texture, grain size…) of the As pollution source. Regarding to soils, a total of 6 samples were taken at a depth of 20 cm. Selected sampling points were the areas in which a higher As concentration could be expected (immediately downstream of the spoil heaps) and an extra sampling point (number 6, figure 1) to check the effect of As dispersion in soils.

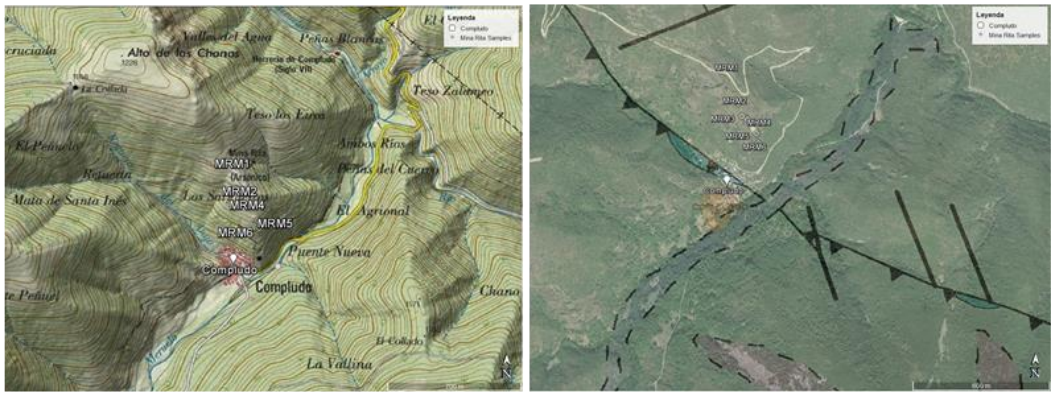

Figure 1. Area of study: a) topographic map; b) geological map.

2.2. Instrumental techniques employed

In the present work, the following techniques have been used: Polarizing-light microscopy (PLM), X-ray diffraction (XRD), X-ray fluorescence (XRF), Scanning-electron microscopy (SEM) and Transmission-electron microscopy (TEM). Scientific equipment details and measurement conditions are summarized below.

PLM studies were performed with a conventional Leica DMLP petrographic microscope at the School of Mining Engineering of the University of Oviedo. XRF analyses were carried out by means of a Niton XL3t X-ray portable analyzer operating at 50 kV, 100 µA, capable of detecting and quantifying chemical elements from S to U. SEM, XRD and TEM tests were undertaken at the common scientific facilities of the University of Oviedo. A JEOL JSM 5600 unit was used for the SEM studies; this equipment operates at 30 kV, with a maximum resolution of 3.5 nm at a 300,000X magnification and incorporates backscattered and secondary ion detectors. The XRD analyzer is a multipurpose diffractometer Bruker D8 Discover, optimized for phase identification and structural analysis. Regarding the TEM instrument, it is a JEM JEOL-2100 that operates at 200 kV with a maximum resolution of 2 Å and an EDX microanalyzer.

3. RESULTS AND DISCUSSIONS

PLM

After studying the rock (mine wastes) samples by PLM, it can be concluded that the primary mineralization consists essentially on disperse arsenopyrite (Aspy) which is often replaced by secondary scorodite (Sc) in different grades. Arsenopyrite appears as millimeter-sized euhedral crystals (see figure 2a), often with pyrite (Py) inclusions. Inter- and transgranular fractures are the typical sites in which scorodite neoformation begins: this mineral replacement is sometimes clearly revealed by the formation of characteristic corrosion gulfs in arsenopyrite. Primary original sulphides that appears (in low quantities) with the arsenopyrite include (from early to late): pyrite (small inclusions, 10-15μm), sphalerite (Sph) and galena (Gn, see figure 2b). The case of a complete replacement is shown in figure 2c, where an arsenopyrite idiomorphic crystal is almost completely weathered (remains a small arsenopyrite residue in the central part).

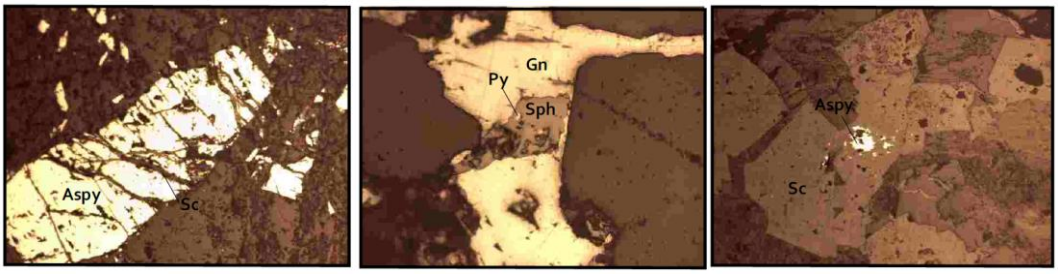

Figure 2. a) Subhedral arsenopyrite (Aspy) crystal affected by dense transgranular fracturation; b) Intercrystal space filled with pyrite (Py), sphalerite (Sph) and galena (Gn); c) Pseudomorphic growth of scorodite (Sc) over previous arsenopyrite (Aspy).

XRF

XRF results have revealed an environmental affection in soils: high As contents (up to 5,182 mg/kg) have been detected in some samples, indicating that this metalloid is being leached from the mine wastes and partially retained in the soil particles. Current reference levels in the region establish a maximum As content of 40 mg/kg for unpolluted soils. Despite of the presence of sphalerite and galena in the mineral paragenesis of the mineralization, Zn and Pb levels in soils are not worrisome. Reference legal values are also exceeded for Co in some samples (no Co-bearing minerals have been detected in mine wastes samples).

Table 3. Contents of soil samples in selected elements, determined by XRF (<LOD: below limit of detection).

SAMPLE	MRM1	MRM2	MRM3	MRM4	MRM5	MRM6
Mo	<LOD	2.78	3.9	<LOD	8.56	<LOD
Zr	482.84	170.73	685.86	641.3	136.88	527.66
Sr	35.34	42.94	56.27	76.42	40.69	51.07
Th	13.41	7.23	15.81	15.46	<LOD	13.7
Pb	<LOD	138.39	<LOD	<LOD	87.19	12.65
As	45.9	1676.65	172.73	179.49	5182.38	101.48
Hg	<LOD	<LOD	<LOD	<LOD	9.85	<LOD
Zn	69.53	150.38	77.56	67.49	198.87	71.61
Cu	21.61	66.79	26.28	32.29	73.95	41.63
Ni	45.4	75.88	28.11	27.14	<LOD	50.96
Co	120.72	154.94	77.51	54.85	<LOD	75.18
Fe	21348.94	40671.79	20776.04	19066.87	32094.72	28335.61
Mn	489.98	1156.99	906.62	779.62	1993.52	618.81
Ti	3317.9	3802.85	3867.37	3940.5	1645.74	4350.69
Ca	229.09	<LOD	219.59	550.12	3281.59	<LOD
K	20005.97	25386.38	16154.97	16721.73	8149.36	20016.51
S	<LOD	<LOD	<LOD	<LOD	607.19	<LOD
Ba	319.52	535.94	203.41	187.18	<LOD	424.41

XRD

As-rich soil samples (MRM2 and MRM5) were also analyzed by XRD in order to identify the main crystalline soil mineral matter constituents. None As-specific phase has been detected, given the relative low resolution of the technique. As shown in figure 3, soil mineral matter includes quartz (Q), muscovite (M) and albite (A).

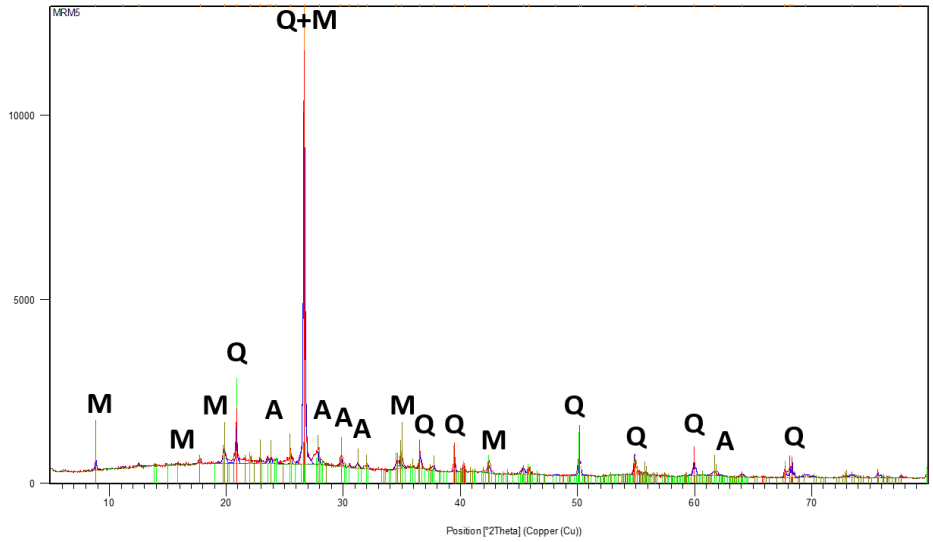

Figure 3. XRD diagram for soil sample MRM5 (comments in the text).

SEM

EDX determinations carried out with the SEM over mine waste samples have allowed to confirm the presence of pyrite, Cd-rich sphalerite and galena, in addition to arsenopyrite and scorodite. Microanalysis of bright, small and commonly zoned particles that appear as mineral inclusions in arsenopyrite and scorodite are unidentified Pb-Al-As and Pb-Fe-As phosphates (figure 4a). It can also be pointed out the presence of small crystals (<10 µm) of species of the xenotime (YPO_4)-chernovite ($YAsO_4$) solid solution series (figure 4b). As it was suspected from PLM observations, the transformation arsenopyrite-scorodite is developed in slate-hosted samples more than in quartz-hosted samples.

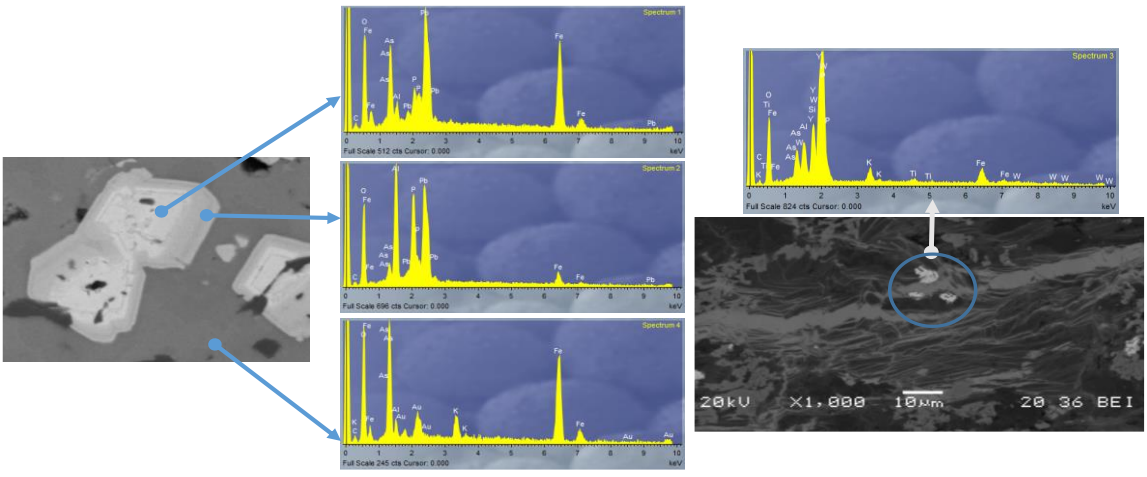

Figure 4. SEM backscattered-electron images (BEI): a)(left) unidentified zoned Pb-As phosphates (horizontal framing: 20 µm); b) (right) mineral species of the xenotime-chernovite s.s. series.

Polished sections were prepared from soil samples and studied by SEM. A great part of the As present in the soil is in the form of weathered and sub-angular scorodite particles (figure 5) of 10-40 μm of diameter. Minor quantities of As have also been detected associated to Fe oxides and K-Fe or Mg-Fe phyllosilicates. On the contrary, no As has been detected in relation to Mn oxides and organic matter.

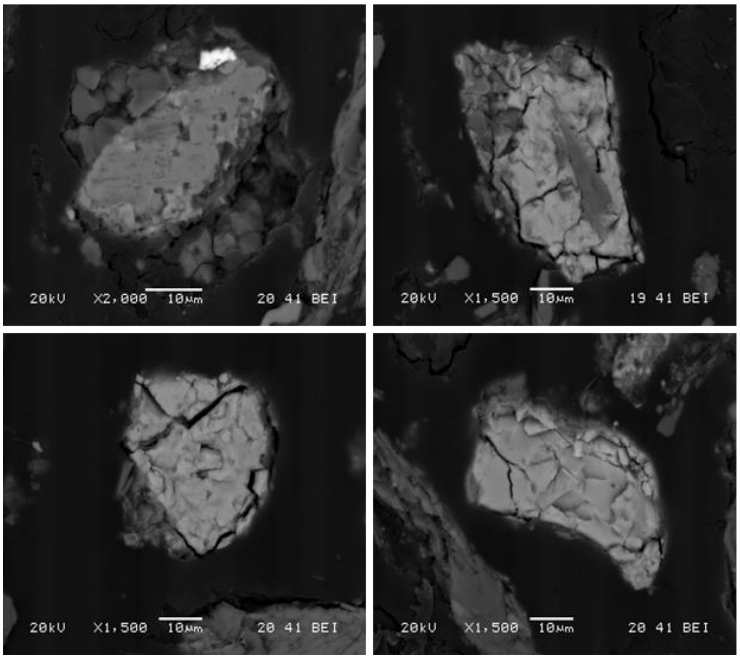

Figure 5. SEM backscattered-electron images showing typical scorodite grains within soil mineral matter fraction

TEM

Among the tools available for the study of very small soil particles, TEM instruments enable detailed analysis in the clay-sized soil fraction. These particles are mainly phyllosilicates, and the specialized literature considers them as the main responsible compounds for the fixation of ions by adsorption and ion exchange. In fact, As concentrations up to 5.61% have been measured over Fe-Mg phyllosilicates. In these particles (figure 6), As seems to be homogeneously distributed along the whole surface, presenting similar patterns to those of Mg and not in accordance with Fe distribution.

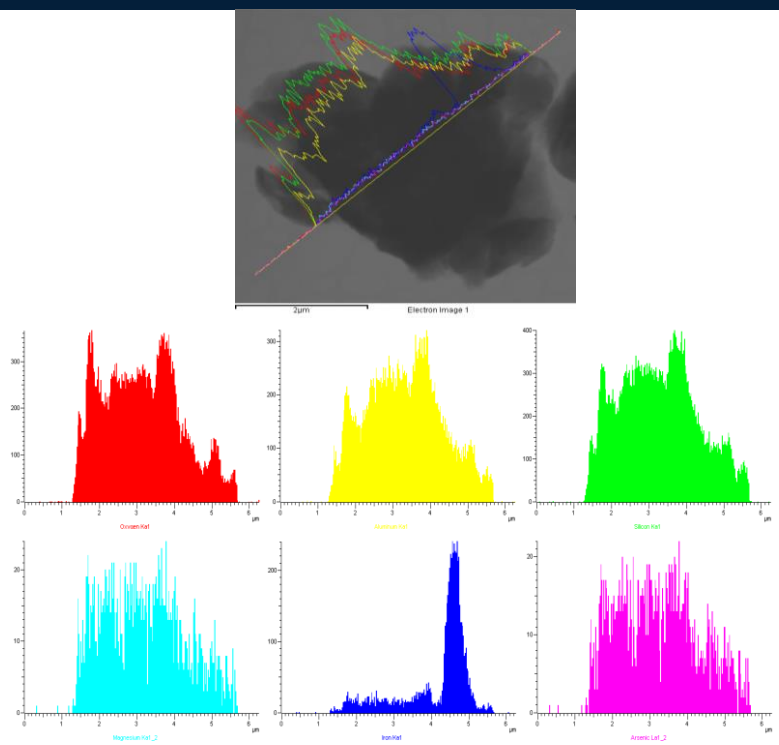

Figure 5. Fe-rich phyllosilicate (1.61% As) in a TEM image, with the distribution of elements along a diametric section (red: O; yellow: Al; green. Si; light blue: Mg; dark blue: Fe and pink: As. $K_{\alpha 1}$ line was used in all cases, excepting for As, determined by its $L_{\alpha 1}$ line).

4. CONCLUSIONS

Spoil heap materials (mine wastes) at Rita mine are constituted by slate and quartzite fragments mineralized with a primary paragenesis of arsenopyrite with minor quantities of pyrite, Cd-rich sphalerite and galena. Secondary scorodite is common in slaty samples (not so much in quartz/quartzite hosted). These materials are the responsible of As dispersion to the surrounding soils.

Optical (LPM) and electronic (SEM, TEM) microscopy techniques have been applied to soil and mineral samples in order to obtain As mineralogical speciation. As in soils is mainly present in the form of: i) weathered scorodite and minor arsenopyrite (little bioavailable) particles; ii) linked to Fe oxides (not to Mn oxides) and iii) linked to Fe-rich phyllosilicates (moderately bioavailabe). It has not been found (although it was carefully examined) associated to organic matter. From a quantitative point of view, scorodite is the main As compound in soils, suggesting that mechanical dispersion is the dominant mechanism.

Mineralogical techniques provide objective and useful information in geochemical assessment in environmental studies, avoiding some disadvantages of common sequential extraction procedures. Not only pollutant concentration, but the shape, grain size and mineralogy of As-bearing particles are important aspects to take in consideration in a risk assessment project.

ACKNOWLEDGMENTS

The authors express their gratitude to the Scientific and Technical Services (STSs) of the University of Oviedo for their help in the analytical part of this research.

REFERENCES

[1]. A. V. Filgueiras, I. Lavilla and C. Bendicho. Chemical sequential extraction for metal partitioning in environmental solid samples. *Journal of Enviromental Monitoring*, pp. 823-857, 2002.
[2]. I. Gómez-Parrales, N. Bellinfante and M. Tejada. Study of mineralogical speciation of arsenic in soils using X ray microfluorescence and scanning electronic microscopy. Talanta, vol 84, Issue 3, pp. 853-858, May. 2011.
[3]. F. Lotze. Zur Gliederung der Varisziden der Iberischen Meseta, *Geotektonische Forschungen*, vol. 6, pp. 78-92, 1945.
[4]. A. Tessier, P.G.C. Campbell and M. Bisson. Sequential extraction procedure for the speciation of particulate trace metals. *Analytical Chemistry*, vol, 51, pp. 844-851, 1979.
[5]. P. Tlustos, J. Szakova, A. Starkova, D. Pavlikova. A comparison of sequential extraction procedures for fractionation of arsenic, cadmium, lead and zinc in soils. Central European Journal of Chemistry 3(4), pp. 830-851, 2005.
[6]. A. M. Ure, Ph. Quevauviller, H. Muntau and B. Griepinck, Int. J. Environ. Anal. Chem., pp. 51-135, 1993.
[7]. A.J. Zimmerman, D.C. Weindorf. Heavy metal and trace metal analysis in soils by sequential extraction: a review of procedures. *International Journal of Analytical Chemistry*, vol. 2010, paper 387803, 2010.

ICOEST

SARAJEVO

5TH INTERNATIONAL CONFERENCE ON ENVIRONMENTAL SCIENCE AND TECHNOLOGY